A COMPARATIVE STUDY OF TRAVELLING FIRE IN LARGE SPACES WITH MULTI-ZONE FIRE MODEL AND FDS

Paolo Bertoli

Fire Safety Engineering
Lund University
Sweden

Report 5643, Lund 2021

Master Thesis in Fire Safety Engineering

A Comparative Study of Travelling Fire in Large Spaces with Multi-Zone Fire Model and FDS

Paolo Bertoli

Report 5643
ISRN: LUTVDG/TVBB—5643--SE

Number of pages: 119
Illustrations: 56

Keywords
Multi-Zone fire model, FDS, Large enclosures, Travelling fire.

Abstract

A knowledge of far field temperatures is valuable for Performance-Based Design structural analysis and life safety analysis, where a parametric study is needed. A fire model using multiple zones – called a multi zone (MZ) fire model – has in previous studies shown good potential as an analytical tool for predicting far field temperatures in large compartments. This thesis aims to build upon the existing state of knowledge for application of MZ fire model, as a predictive tool for far field temperatures. The research approach primarily involves designing and testing several large-scale travelling fire scenarios in MZ fire model and comparing these results to Fire Dynamic Simulator (FDS). As a further step, a comparison is made between MZ fire model predictions for two well documented large-scale travelling fire experiments: the Tisova full-scale fire test and the Edinburgh Tall building Fire Test using MZ fire model. Results of this thesis are mixed. Comparison of far field temperature values show reasonably good agreement between MZ fire model and FDS computational fluid dynamics (CFD) models (on average 11-22% differences). However, comparison of MZ fire model temperatures to the measured temperatures of the two travelling fire experiments yielded significant differences (on average 7-35 % between the models, and 37-101% between MZ fire model and the experiments). The substantial difference between analytical and experimental results indicates that MZ fire model and FDS were not successful at predicting far field temperatures for the actual experimental fires. This can be caused by a combination of parameter and model uncertainties, and a lack of reliable data from the experiments. This research effort shows that MZ fire model has the potential to be a useful tool for predicting far field temperatures in large compartment fires; however, further research and experimentation are needed to refine modelling methods and techniques before MZ fire model is a viable engineering tool for fire safety analysis.

Fire Safety Engineering
Lund University
P.O. Box 118
SE-221 00 Lund
Sweden

http://www.brand.lth.se

Telephone: +46 46 222 73 60

HOST UNIVERSITY: Lund University

FACULTY: Faculty of Engineering

DEPARTMENT: Fire Safety Engineering

Academic Year 2020-2021

A COMPARATIVE STUDY OF TRAVELLING FIRE IN LARGE SPACES WITH MULTI-ZONE FIRE MODEL AND FDS

Paolo Bertoli

Promoter: Dr. Nils Johansson

Master thesis submitted in the Erasmus+ Study Programme

International Master of Science in Fire Safety Engineering

DISCLAIMER

This thesis is submitted in partial fulfilment of the requirements for the degree of *The International Master of Science in Fire Safety Engineering (IMFSE)*. This thesis has never been submitted for any degree or examination to any other University/programme. The author(s) declare(s) that this thesis is original work except where stated. This declaration constitutes an assertion that full and accurate references and citations have been included for all material, directly included and indirectly contributing to the thesis. The author(s) gives (give) permission to make this master thesis available for consultation and to copy parts of this master thesis for personal use. In the case of any other use, the limitations of the copyright have to be respected, in particular with regard to the obligation to state expressly the source when quoting results from this master thesis. The thesis supervisor must be informed when data or results are used.

Read and approved,

Paolo Bertoli
(May 11, 2021)

Acknowledgements

I would like to thank my thesis supervisor, Nils Johansson, for the interesting and challenging topic. Nils have helped me with an advice on MZ fire model's set up, took time to meet me to answer my questions and replied to my numerous e-mails. His constant support and advise throughout this research project are greatly appreciated.

I would like to also thank Daniel Funk for the help with proofreading my thesis.

Table of contents

List of symbols and acronyms

BRE	Building Research Establishment
BSI	British Standards Institution
CFL	Courant–Friedrichs–Lewy number
CFD	Computational Fluid Dynamics
ETFM	Extended Travelling Fire Model
FDS	Fire Dynamic Simulator
GER	Global Equivalent Ratio
HRR	Heat Release Rate
HRRPUA	Heat Release Rate Per Unit Area
HoC	Heat of Combustion
LES	Large Eddy Simulation
MZ	Multi Zone model
MLZ	Multi Layer Zones model
MPI	Message Passing Interface
MC	Moisture Content
NIST	National Institute Standards and Technology
PBD	Performance-Based Design
PP	Polypropylene
RISE	Research Institute of Sweden
SLCF	Slice file
SP	Swedish Technical Research Institute
SFPE	Society of Fire Protection Engineers
VTT	Technical Research Centre of Finland

c	specific heat [kJ/kgK]
g	grams [g]
h_p	height of fuel bed [m]
k	conductivity [W/mK]
m	mass [kg]
m	meters
$\dot{m}$	mass flow rate [kg/s]
min	minutes [m]
M	moisture content [%]
q	heat flux [W/m2]
$\dot{Q}$	heat release rate [kW]
R	thermal resistance [m^2K/W]
s	seconds [s]
t	thickness [m]
t	time [s]
T	temperature [°C]
U	transmittance [W/m^2K]
V	flame spread [mm/s]
χ	burning efficiency [%]
χ_r	radiation energy [%]
ρ	density [kg/m3]
ΔHc	Heat of Combustion [MJ/kg]
α	growth rate [kW/s^2]

Abstract

A knowledge of far field temperatures is valuable for Performance-Based Design life safety analysis, where a parametric study is useful. A fire model using multiple zones – called a multi zone (MZ) fire model – has in previous studies shown good potential as an analytical tool for predicting far field temperatures in large compartments. This thesis aims to build upon the existing state of knowledge for application of MZ fire model, as a predictive tool for far field temperatures. The research approach primarily involves designing and testing several large-scale travelling fire scenarios in MZ fire model and comparing these results to Fire Dynamic Simulator (FDS). As a further step, a comparison is made between MZ fire model predictions for two large-scale travelling fire experiments. Comparison of far field temperature values show reasonably good agreement between MZ fire model and FDS computational fluid dynamics (CFD) models (on average 11-22% differences). However, comparison of MZ fire model temperatures to the measured temperatures of the two travelling fire experiments yielded significant differences (on average 7-35 % between the models, and 37-101% between MZ fire model and the experiments). This research effort shows that MZ fire model has the potential to be a useful tool for predicting far field temperatures in large compartment fires; however, further research and experimentation are needed to refine modelling methods and techniques before MZ fire model is a viable engineering tool for fire safety analysis.

Keywords: Multi-zone fire model, FDS, Large enclosures, Travelling fire.

Word Count: 17410 words.

Introduzione

Conoscere la temperatura lontano dalla zona dell'incendio è di particolare importanza quando il metodo prestazionale (PBD) viene utilizzato per analisi termiche strutturali e modelli d'esodo. Il modello d'incendio che divide il volume interessato in zone multiple, conosciuto con il nome di "Multi-Zone fire model" ha mostrato in precedenti studi di essere un buon metodo per valutare le temperature lontane dall'area dell'incendio in grandi compartimenti. Lo scopo della presente tesi è lo sviluppo del lavoro svolto precedentemente utilizzando il concetto di incendio mobile (travelling fire). L'approccio utilizzato nella presente tesi è diviso in due parti. La prima dove alcuni scenari d'incendio sono stati modellati utilizzando il modello Multi-Zone e i cui risultati confrontati con i risultati ottenuti con il codice fluidodinamico FDS. La seconda dove i dati ottenuti da due esperimenti di travelling fire in scala reale vengono confrontati con i risultati degli stessi scenari d'incendio modellati utilizzando il modello Multi-Zone.

I risultati della presente tesi sono multipli. Il confronto delle temperature lontane dall'area interessata dall'incendio mostrano un buon livello di similarità tra il modello a Multi-Zone e FDS (in media 11% e 22% di differenza). Tuttavia, il confronto delle temperature restituite dal modello Multi-Zone e quelle misurate durante i test presentano sostanziali differenze (in media 7-35% tra i modelli e 37-101% tra il modello multizone e i test).

Questa tesi mostra come il modello Multi-Zone abbia il potenziale per essere utile nella valutazione delle temperature lontane dall'incendio in grandi compartimenti, tenendo conto che ulteriori studi e validazioni sono necessari per implementare il modello e le tecniche di utilizzo dello stesso prima che questo diventi un utile mezzo da utilizzare durante le analisi in ambito di sicurezza antincendio.

1 Introduction

This chapter identifies the objectives and research goals of this thesis, including limitations. Multi-zone (MZ) fire model and its relevance to fire safety engineering are introduced. It is intended that the reader gains an appreciation for the potential capability of MZ fire model as a predictive tool of far field temperatures for travelling fires in large compartments.

1.1 Context and problem description

Nowadays, fire simulations are used in fire safety engineering and research to predict the fire behaviour and study different phenomenon. To predict the fire behaviour accurately is a complex task that includes modelling of turbulence, combustion, and radiation. The higher the complexity of models that are used in simulations, the higher is the computational cost. Multiple simulation packages that are available on the market offer different possibilities and are more or less capable to represent the complexity of fire dynamics. These models can be divided into two types: two-zone models, and field models (Karlsson & Quintiere, 2000, p. 3).

Two-zone models, despite its simplification, are very useful in certain situations, for example when a first crude estimate of fire behaviour is needed to be done fast prior to full scale Computational Fluid Dynamics (CFD) modelling, i.e., in comparative studies. The two-zone models assume that a homogenous stratified smoke layer has formed in a pre-flashover compartment or for a post-flashover compartment, treated as a single zone. These models perform well in small and medium-sized compartments (Bong, 2011), but the difficulty arise when it comes to using such models in larger spaces.

In large compartments no uniform smoke layer is formed, instead the fire can travel and is often considered to be fuel controlled (Torero, et al., 2014) due to abundance of oxygen. In such compartments the performance of CFD packages such as FDS provides better results compared to the two-zone models. The problem is that CFD is computationally expensive and thus not well-suited for comparative studies. A solution to this can be to use multi-zone (MZ) fire model based on a multi-zone concept, that subdivides the domain into multiple smaller zones in a similar way as meshing is done in CFD. This model has a low computational cost (basically in order of minutes to hours), but no validated commercial model is available so far (Johansson, 2021). The model can potentially be used to make fast estimates of near and far field temperatures, prior to running a complex and computational demanding CFD simulations. Such fast estimates are valuable for Performance-Based Design, in particular, structural analysis of large buildings where the engineer might need to look at many different fire scenarios and life safety during evacuations.

1.2 Objective

The purpose of this thesis is to build upon previous work for using MZ fire model to predict far field temperatures of travelling fires in large compartments (Johansson, 2021), (Anderson, et al., 2020). The specific objective of this research is to:

> **Further the state of knowledge for using MZ fire model as a predictive tool of far field temperatures for travelling fires in large spaces.**

This objective will be accomplished through two comparative analyses:

- Benchmark MZ fire model results for two travelling fire scenarios in large spaces against the results predicted by CFD modelling using Fire Dynamic Simulator (FDS).
- Evaluate the far field temperatures predicted by MZ fire model and FDS analysis to actual experimental results, obtained by previously conducted full-scale fire tests involving travelling fires.

In short, the main focus of this thesis is to see how well MZ fire model estimates temperatures in the far field regions of travelling fires in large compartments, thereby providing further insights into the use of MZ fire modelling as a reliable tool for fire safety analysis. Additionally, the capability of MZ fire model to predicting the obscuration will be investigated.

1.3 Limitations

Two important limitations exist for this thesis:

- Firstly, time constraints preclude consideration of all possible travelling fire scenarios and the analysed cases should not be considered bounding. Only two fictive scenarios are modelled (a typical office and supermarket). For both the office and supermarket scenarios, a large, open floor plan is used. This approach is intended to represent the configuration of a typical modern high-rise building (open cubicle concept) and supermarket (including aisles of food storage shelves).
- Secondly, there are few well-documented fire scenarios for travelling fires in large spaces. Hence, comparative evaluations for a broad range of realistic scenarios are not feasible. Consequently, results should not be extrapolated to other scenarios.

2 Theoretical background

The literature review focuses on MZ fire model capabilities, limitations and the research that was done in support of this thesis. A short section is dedicated to travelling fires, which are an integral part of the modelling concepts used in this study.

2.1.1 Historical background

The two-zone models are well accepted within the fire safety engineering community. These models assume that a homogenous stratified smoke layer has formed in a pre-flashover compartment and that a post-flashover compartment can be treated as a single zone. The classical two-zone model divides the compartment into two-zones: a zone with hot gases and a zone where the temperature is assumed to remain at ambient. These models are based on many assumptions and thus their range of applicability is limited. The two-zone models can give reasonable results for some studies, but they can also be used when a comparison study is needed.

There has been attempts to extend the application of two-zone models to multi-cell models, which are models that divide the compartment into cells in the vertical direction (Chow, 1996), with the goal of achieving improved accuracy for large compartments. Other research efforts have attempted to combine CFD models (used in the room of fire origin) with two-zone model (used for locations outside the room of fire origin) to model more efficiently fires in multi-story buildings (Hua, et al., 2005).

In 2004, Suzuki K. et al. (Suzuki, et al., 2004) published an article on development of a so-called Multi-Layer Zone (MLZ) model, which is essentially based on the same principles as a two-zone model. The difference being that a user is allowed to divide a compartment into an arbitrary number of layers instead of only two layers, as shown in Figure 1. A MLZ model uses the same concept for solving equations of mass and enthalpy for each layer as that used by a two-zone model, which results in predicted temperatures and species mass fractions. However, due to the many layers representing multiple control volumes, the fire plume does not immediately mix with the upper layer; instead, it propagates layer-by-layer upwards until it reaches the ceiling and spreads horizontally. An important difference between two-zone models and MLZ model is that the latter uses fixed control volumes, while two-zone models allow control volumes to vary over time.

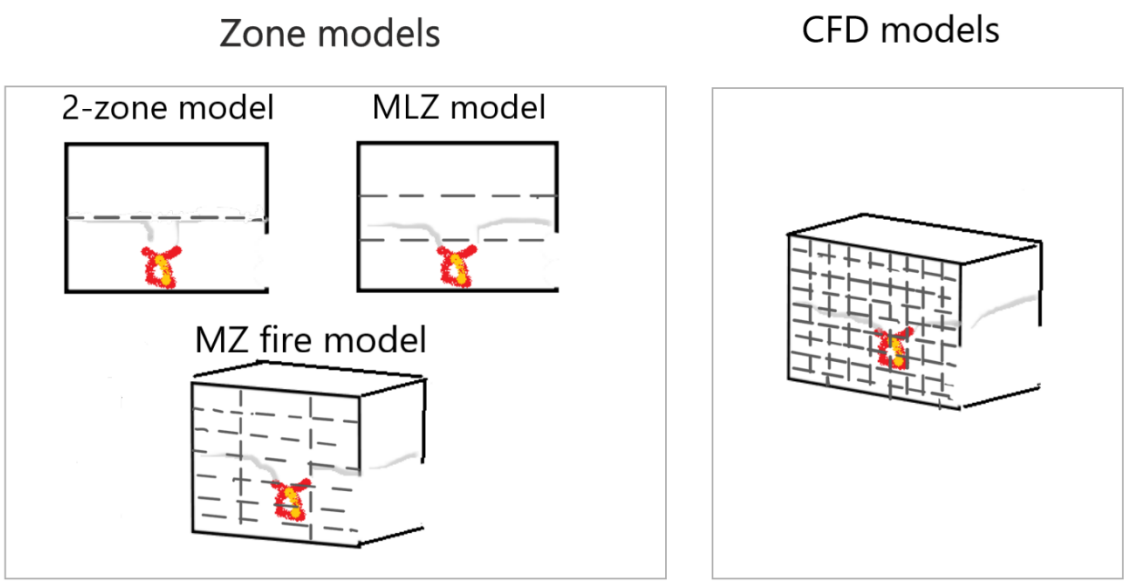

Figure 1 Fire model concepts in a general framework of zone and field (CFD) models. (The figure shows how the different zone models divide the domain into control volumes for 2-zone, MLZ and MZ fire model compared to CFD. The control volumes in MZ fire model are three dimensional, as in CFD models).

During the same year, the authors applied the MLZ model to a tunnel fire to see whether it is more accurate in predicting the vertical temperature profile, as compared to a two-zone model. These efforts showed some promising results (Suzuki, et al., 2004). Subsequently, in 2005 the model was extended to a multi-room compartment, which had improved physics modelling that was validated by experiment (Suzuki, et al., 2005).

Also in 2005, a group of researchers in China made improvements to MLZ modelling by updating sub-models for energy and heat transfer and applying an integration solution method for the zone equations. This model was successfully tested on a small compartment and on a multi-compartment setup. The simulation results showed good agreement with experimental results (Xiaojun, et al., 2005). No literature was identified relating to extension of MLZ model techniques to large compartments. The next mentioning of MLZ modelling was in 2019, where Nishino and Kagiya (Nishino & Kagiya, 2019) applied the MLZ model to compartments with combustible linings and then combined the model with a wall and ceiling flame spread model.

The code developed for MLZ model is not an open-source code, but the principles are described by Suzuki (Suzuki, et al., 2004), (Suzuki, et al., 2005). However, MZ fire model has been developed based on key principles identified by the MLZ literature. MZ fire model is the focus of this thesis; it is best characterised as a "work in progress" and is still under development by the head supervisor of this thesis, Nils Johansson, Associate Senior Lecturer at the Department of Fire Safety Engineering, Lund University (Sweden).

2.1.2 Multi Zone fire model

This chapter examines MZ fire model's capabilities and limitations as documented by research conducted to date. MZ fire model is a C++ based model, which has a command list very similar to FDS. The model is freely downloadable at www.mzfiremodel.com (Johansson, 2020). It aims to extend the two-zone model using multiple cells in three dimensions to larger compartments,

where temperature profiles are no longer uniformly distributed – similar to CFD modelling concepts (see Figure 1). Otherwise, the modelling approach is, in general, similar to the two-zone model concept. The size and number of the "zones" or cells is prescribed by the user.

The principle of conservation of mass and energy for MZ fire modelling is similar to Suzuki's MLZ model (Suzuki, et al., 2004) (Suzuki, et al., 2005). This is schematically shown in Figure 2 below.

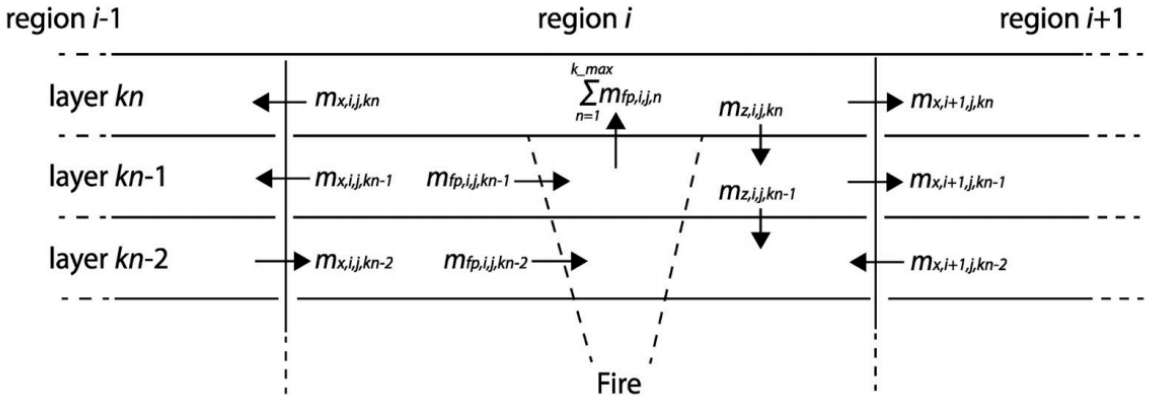

Figure 2 Conservation of mass principle for MZ fire model based on description developed by Suzuki K. (Suzuki, et al., 2004) [taken with permission from (Johansson, 2021)].

The full description of mass and energy equations used to model vertical flow between the cells in MZ fire model can be found in MZ fire model user's manual (Johansson, 2020), and thus only a short description is provided in this report. Figure 2 shows that the mass balance will differ depending on the location with respect to the fire source, i.e., cells in region *i*-1 do not have the term for the mass flow from the plume. The conservation equation for energy takes into account heat transfer to the boundaries (convection to the walls) and includes the net radiation term (Johansson, 2021). As in a two-zone model, the calculated properties are uniform in each zone. Within obstructions, one dimensional heat conduction is used.

Figure 2 is a two-dimensional representation of the three-dimensional MZ fire model, where the enclosure is divided into layers and, in turn, layers are divided into the cells that depict 3D results in volumes. For example, if a fire source is placed in region *i*, defined with a heat release rate per unit area, then the convective part of this heat will be transferred to the cells above using the mass and energy balance until the plume reaches the upper cell. The temperature difference is driving flow from the fire source to the upper layer. The horizontal mass flow, as in two-zone models, is represented using hydrostatic pressure differences. The plume is modelled using Heskestad's empirical plume model with the concept of virtual origin; thus, no representation of turbulence is available. (Johansson, 2020)

As for guidance on the cell size for MZ fire model, there is a recommendation to make sure that the raising plume is captured in a one cell-column (Johansson, 2021), as shown in the Figure 2 above. This approach makes sure the plume also fits into the third dimension of the cells. Per the author's knowledge, no cell sensitivity study has been performed, nor have the impacts on the properties of interest has previously been studied. Nevertheless, the work performed earlier gives an indication of cell sizes used previously. A cell size of 4 x 4 x 0.5 m^3 is recommended

and the minimum recommended number of cells in each direction of the domain is three (Johansson, 2020).

MZ fire modelling allows the placement of devices (temperature measurement and obscuration) anywhere inside the cell because the temperature inside the cell is uniform. Consequently, if the fire is within a cell the temperature measurement device will show a uniform gas temperature throughout the cell. MZ fire model calculates gas temperature, whereas the fire and flames are not directly modelled. This simplification results in temperatures and radiation close to the fire being under-estimated.

2.1.3 Travelling Fire

Rein G. et al. (Rein, et al., 2007) studied travelling fires in multi-storey compartments for the purpose of structural element response to fire. In this article (Rein, et al., 2007) it is suggested to divide the compartment into two main areas, near and far field regions. The near field region represents the area where the fire is burning, and the heat is most intense. While the far field is the zone further away from the fire source, where the heat comes from the smoke layer (Degler & Eliasson, 2015). Later, the same group of researchers have studied the concept of travelling fire (Stern-Gottfried, et al., 2010). They confirmed that the temperature distribution in a large post flashover compartment is not homogenous. This is because in larger spaces, as experiments have shown (Kirby, et al., 1999) (Hidalgo, et al., 2017), the fire spreads or "travels" rather than flashes over and therefore being fuel controlled and not ventilation controlled.

Modelling far field temperatures is computationally expensive, which has led to efforts to develop simplified theoretical models for travelling fires. These efforts are well described in literature reviews (Stern-Gottfried & Rein, 2012) and (Dai, et al., 2017). Thus, only a short summary of modelling attempts for travelling fires is presented here. One such model suggested by Clifton G.C. (Clifton, 1996) is intended for ventilation-controlled fires. This concept is based on the idea of dividing a compartment into a series of cells and assigning a parametric fire curve to each of these cells, specifying fuel with the fuel load density. Another model, suggested by Rein et al. (Rein, et al., 2007), is based on a series of fire curves for estimation of far field temperature for fuel-controlled fires. In this model, the far field temperature is determined using Alpert's correlation. An additional model – extended travelling fire model (ETFM) (Dai, et al., 2018) – estimates both near field and far field temperatures using a two-zone model. The path of the fire for this model is predefined and it can be used for both fuel and ventilation-controlled scenarios.

Another study (Johansson, 2018) was made to investigate application of MZ fire model to larger compartments that include a fictive travelling fire. This study compared estimation of far field temperatures using MZ fire model to Alpert's correlation and FDS simulations for two fictive scenarios. The first scenario was comprised of a compartment of 640 m^2 with 36 m^2 openings placed opposite to the ignition side, with fire spread between four 2 x 2 m^2 fuel packages. The second scenario included a fire progressing between nine fuel packages similar to the previous scenario. This case uses a predefined fire path and arbitrarily selected ignition time. The results of this study indicate that Alpert's correlation underpredicted the far field temperature, whereas MZ fire model produced results similar to FDS simulations for both horizontal and vertical

temperatures. No near field temperature comparison using MZ fire model was possible at the time of this study.

3 Methodology

This chapter describes the general methodology and the choices made for simulation setups in both MZ fire model and FDS for the postulated fire scenarios (office and supermarket) and for experimental cases (The Tisova fire test and The Edinburgh tall building fire test).

3.1 General methodology

The general methodology applied in this thesis for both theoretical and experimental fire scenario cases is summarized in the flowchart (see Figure 3). Once a decision on fire scenario is made, either by creating a theoretical design fire scenario or by choosing the experimental case, the information needed for heat release rate (HRR) and fire spread is collected. The travelling fire movement is then modelled with a user-defined time of ignition in both MZ fire and FDS simulations, as prescribed using Modak's heat flux equation (Karlsson & Quintiere, 2000, p. 156). This approximate method to calculate radiation does not take into account the influence of absorbance and emittance of the smoke on radiation, and assumes that radiation comes from the point source. Fire spread modelling using ignition temperature criteria was not possible in MZ fire model since the fire and flames are not accounted for. Nevertheless, a number of tests were performed to see if the ignition temperature criteria is applicable to MZ fire model. Some results of this effort are included in the discussion.

Further on in the process (Figure 3), the layout and thermal properties of materials are defined. This process is straight forward for the theoretical scenarios, where engineering judgement and applicable references are used. But, for the models of the experimental cases, this process becomes complicated due to the lack of information. Also, some effort is needed to fit the experimental layout into MZ fire model cells. The fitting of geometry is performed first for MZ fire model and then the identical domain is modelled in FDS. The FDS model is designed to be as similar as possible to the corresponding MZ fire model, including the same geometry, same positioning of the fuel package and same temperature measurement devices.

When the results are ready, the choice on averaging periods is made. After that, temperature results are averaged and compared. An engineering judgement is used to determine whether the output is reasonable. For this, prescribed total HRR is compared to the output HRR from MZ fire model and FDS. If the curves are similar, as shown in Appendix I, then the further analysis of results is performed. Additionally, temperature results can indicate errors in the model's settings. Therefore, the results are deemed reasonable if the profiles are not drastically different. Otherwise, the input is double-checked. In some cases, the procedure was repeated because of differences in HRR or errors in the code. All inputs were double-checked prior to conducting reruns.

A cell sensitivity study is performed in FDS for the office scenario only and is presented in Appendix A. The sensitivity study is limited to one scenario due to the time constraint (as a point of reference the fine mesh simulation (5 cm) took seven (7) weeks to reach 1102 s). For future studies, if possible, it is recommended to perform a sensitivity study for each fire scenario separately. Ideally, the cell sensitivity and parameter sensitivity analysis should also be performed for MZ fire model, but this aspect of analysis is not within the scope of this research project. Running the programs can takes months, depending on the mesh size chosen in FDS for large spaces and hours or minutes in MZ fire model.

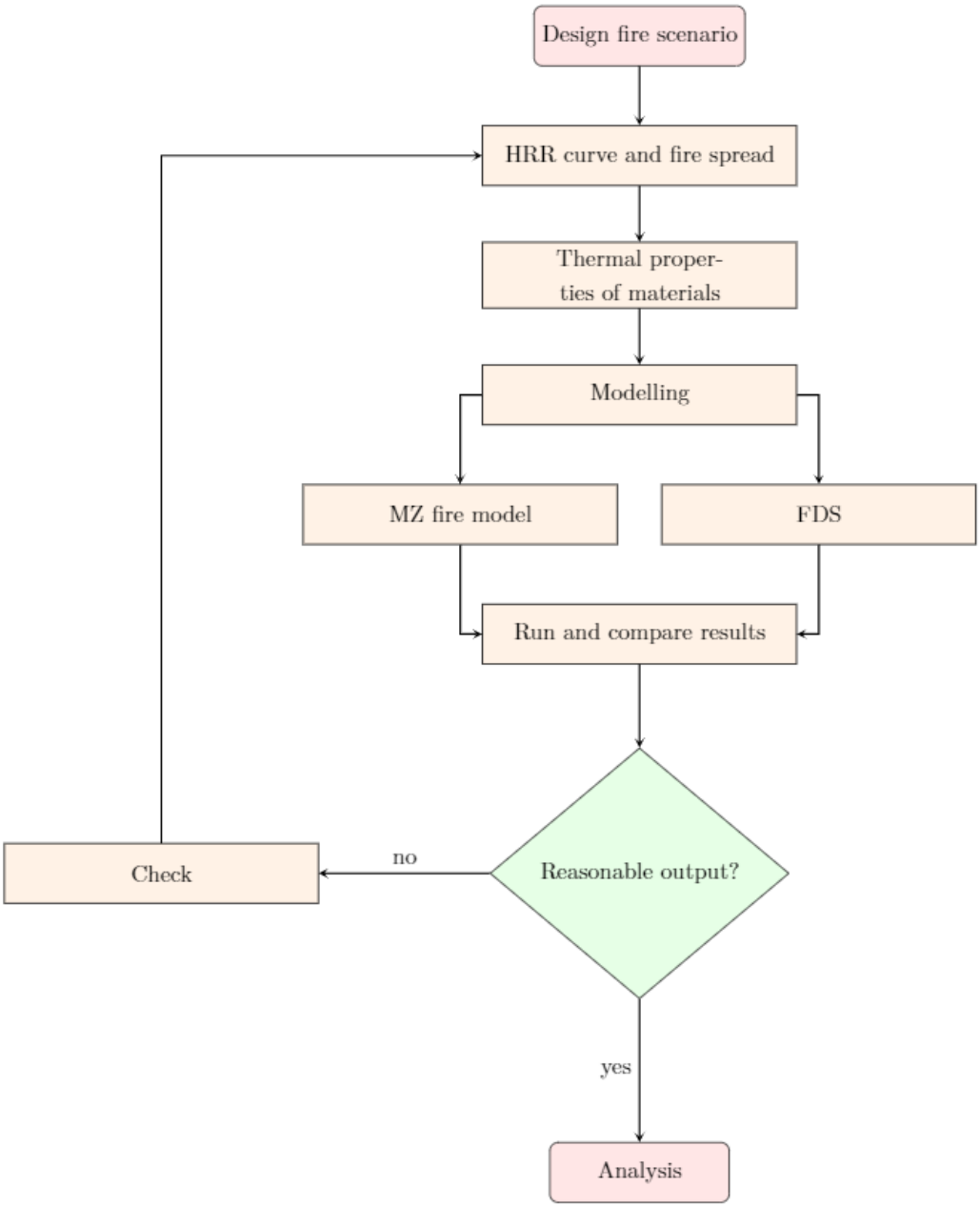

Figure 3 General methodology process flow chart.

3.2 Office scenario

The chapter describes how the office scenario was set up and modelled in MZ fire model and FDS. This scenario is based on the literature research for large fires in offices; no experimental data is available for comparison.

3.2.1 Enclosure layout and openings

Figure 4 shows office enclosure layout and the positions of the openings. The enclosure is 24 x 40 x 3 m^3, with a concrete core in the middle. Continuous fuel bed with travelling fire has been previously modelled (Dai, et al., 2017) using discrete fuel packages. This study used similar concept, by placing fuel packages evenly throughout the compartment, to simulate continuously spreading fire, see Figure 4. To obtain the maximum space optimization for a similar open space layout, workstations are more likely to be located closer to each other and to the concrete core rather than as showed in Figure 4. For the fire scenario to be fuel controlled, sufficient openings are needed. Therefore, a calculation of the Global Equivalence Ratio (G.E.R.) is performed (see Appendix B-2 for details). Figure 4shows the location of the windows. Note that these openings are modelled in the open position from the start of the analysis and therefore might not represent realistic windows. The windows are positioned at the floor level up to 1.0 m height to allow smoke layer build-up. The possibility to "break" the windows, i.e., remove an obstruction at a predefined temperature, is not available in the current MZ fire model code version. The total surface area of the openings in the office scenario is 96 m^2. This area was chosen after running several simulations with different opening areas that resulted in HRR changes due to the insufficient openings surface.

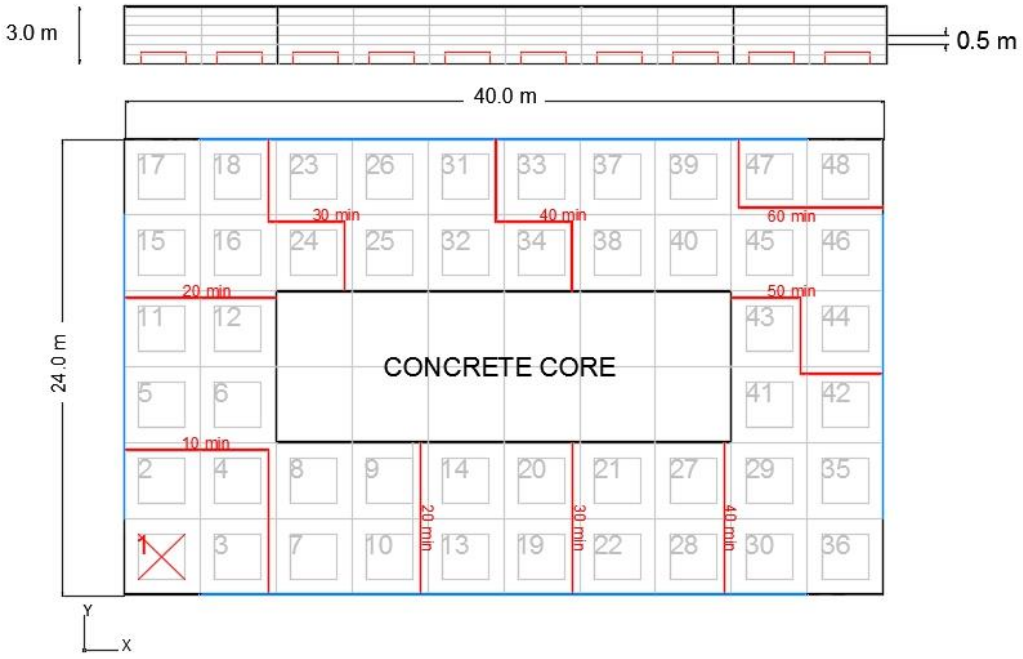

Figure 4 Schematic top view of the office scenario with idealized working stations (2.4 x 2.4 m^2) with the total surface area of 40 x 24 m^2. (In total, 48 working stations are located around the concrete core. The ignition starts at station number 1 and then moves throughout all of the fuel packages around the core, as showed with the red lines marked with different times. Openings are marked with blue).

3.2.2 Thermal and fire properties of materials

The walls, the floor and the ceiling are assumed to be made of a normal concrete with thermal properties given in Table 1. The burner obstructions represent idealized workstations, and the generalized material is arbitrarily chosen to a particle board, assuming it is a prevailing material in a common office furniture set.

Table 1 Thermal and fire related properties of materials used in office scenario modelling (Karlsson & Quintiere, 2000, p. 122).

	Thermal properties			Fire related properties		
Material	***k*** **[W/m*K]**	***ρ*** **[kg/m3]**	***c*** **[kJ/kg*K]**	**HoC [MJ/kg]**	**Soot yield [ ]**	**Ignition T [C]**
Concrete	1.1	2100	0.88			
Particle board	0.1081	637	1.424	18	0.015	250
Fiber insulating board	0.041	229	2.09			

Table 1 shows that the heat of combustion was assumed as 18 MJ/kg, which is on the high side for the particle board values reported in (McGrattan, et al., 2005). This choice is made because an office may contain other fuels, for example: plastic, electronics, waste, wood, and paper. Using the same reasoning, a higher value for soot yield (0.015) is used compared to 0.008 found in (Sun-Yeo, et al., 2019) for particle board. The radiative fraction is set to 0.35 in both FDS and MZ fire models.

3.2.3 HRR and fire spread

A literature study was necessary to construct the HRR curve for a single burning working station. Several different office cubicle and workstation HRR values were found in literature (Hurley, 2016, pp. 854-857) (Ohllemiller, et al., 2005). One of the studies (McGrattan, et al., 2005) reports a high peak HRR, up to 8 MW, due to a high ignition energy (replicating the World Trade Center (WTC) disaster. The choice of peak HRR was instead based on the Figure 26.71 (Hurley, 2016, p. 857) to 1.6 MW. The ignition source is arbitrarily placed in a corner of the model to generate a longer travelling path.

The fire growth is approximated using the α-t^2 fire growth concept, where a growth rate of 0.012 kW/s^2 is taken from PD 7974-1:2003 (BSI, 2003) to represent a medium growth rate reported for offices. Comparison with the applicable Eurocode (CEN, 2004) values for offices gives a similar fire growth rate. The HRR curve was constructed using the total energy estimated at 1306.2 MJ from the Figure 26.71 SFPE Handbook (Hurley, 2016, p. 857). The HRR curve that was used as an input to MZ fire model and FDS model is shown in Figure 5. The resulting HRR per unit area (HRRPUA) is 277 kW/m^2. The current version of MZ fire model does not allow multiple ramps to represent the decay phase. The decay phase is assumed to be fast because in a large enclosure space the thermal inertia from the walls of the building is of a less importance (Stern-Gottfried, et al., 2016).

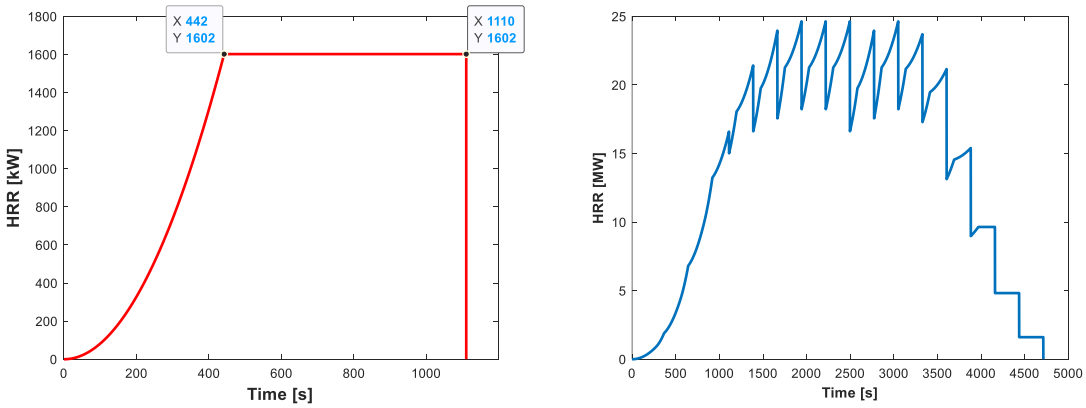

Figure 5 HRR curve for a single workstation (left) and a total HRR curve for the office scenario (right).

A travelling fire in MZ fire model and FDS office scenario is prescribed based on the user-defined ignition time. The HRR curve for a single fuel package is used to create a total HRR curve for the whole office space (Figure 5). This is done using Modak's equation (Karlsson & Quintiere, 2000, p. 156) for estimation of the radiant heat. See Appendix B-1 for the ignition time calculation.

The fraction of total radiation energy, X_r, depends on fuel type, size and location of the fire (Hurley, 2016). In this case, the fuel package area is set at 2.4 x 2.4 m^2 (Figure 6) and the fuel is assumed to be mainly comprised of the office furniture. The radiative fraction is assumed to 0.35 based on engineering judgement and (Iqbal & Salley, 2004, p. 207). The distance between the fuel packages is 1.6 meters, as shown on Figure 6. This value is higher compared to 0.9 m reported in (Hamins, et al., 2005). However, it is also chosen to allow the ignition of the next fuel package within a reasonable time compared to similar experiments (Ohllemiller, et al., 2005). The critical heat flux for ignition of particle board is assumed to be 10 kW/m^2 (Babrauskas, 1986, p. 265), a value that is representative for the fuel in this scenario. This heat flux is then used together with Modak's equation to determine the time to ignition of the next fuel package, see Appendix B-1.

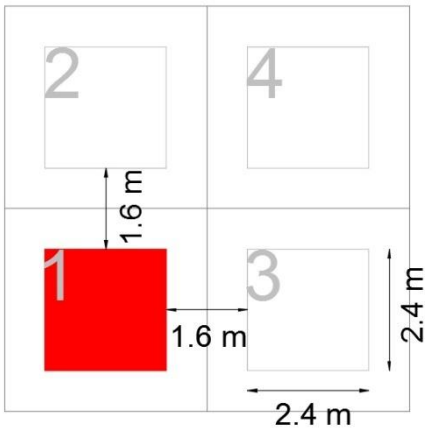

Figure 6 Close-up figure of the office layout, showing the ignition fuel package in red and the distance to the nearest fuel packages 2 and 3.

Ignition is assumed to start at fuel package 1 and, at first, spread to the neighbouring fuel

packages 2 and 3. The calculated ignition time for fuel packages 2 and 3 is 277 s after fuel package 1 is ignited. Even though fuel package 4 is placed slightly further away from fuel package 1, it is assumed to be ignited simultaneously with fuel packages 2 and 3. Using this principle, a travelling fire is mapped to the rest of the fuel packages throughout the entire office space, as shown in the Figure 4. The resulting total HRR curve is shown in Figure 5.

In general, similar codes were used in both MZ fire and FDS models. The next two sections report on the settings that are specific to MZ fire model and FDS, highlighting the differences where applicable. The code of MZ fire model can be found in Appendix H and the corresponding FDS code in the Appendix G.

3.2.4 Scenario configuration in MZ fire model

The limitations of MZ fire model dictate certain simplifications that must be made in order to simulate a fire scenario in an office. A workstation (a fuel package) is modelled as an area at the height of 0.6 m above floor level. This simplified modelling is used because MZ fire model currently is not capable of modelling burning on all sides of an obstruction. The height of 0.6 m is selected based on engineering judgment and does not fully correspond to reality. Some office partitions between different workstations, called "privacy walls," might be a level higher compared to the surface of a working desk, as the experiments show (Ohllemiller, et al., 2005). Nevertheless, the selected height is deemed sufficient to represent the current scenario, given the number of other simplifications that must also be made.

In MZ fire model, workstations are placed according to Figure 4. To obtain the maximum space optimization for a similar open space layout, workstations are more likely to be located closer to each other and to the concrete core rather than as showed in the Figure 4. A fire can be placed in any position inside a cell in MZ fire model. Nevertheless, it is recommended to place a fire in a cell in such a way that it fits the plume diameter (Johansson, 2020). A rough estimate (see Appendix B-3) shows that the plume reaches a diameter of 4.47 m at ceiling height, which is slightly bigger than the cell size used in the model (4 x 4 x 0.5 m^3).

Continuous fuel packages have been used in some tests for the travelling fire concept (Hidalgo, et al., 2017), (Dai, et al., 2017). This test setup has been modelled using discrete fuel packages placed evenly throughout the compartment to simulate continuously spreading fire. Figure 4 shows how 4 x 4 x 0.5 m3 cells in MZ fire model divides the office space. The arrangement results in 10 cells in the x-direction, 6 cells in the y-direction and 6 cells in z-direction. The model was run on a personal computer.

3.2.5 Scenario configuration in FDS

FDS model for the office scenario uses 20 cm cells, which results in 527340 cells in total. The domain is extended 2 m outside the openings, to properly model the smoke dynamics at the openings. The domain was divided into 10 meshes, and each mesh was assigned to an MPI (Message Passing Interface) process on a computer cluster.

The geometry of FDS office is identical to MZ fire model, see Figure 7 for a 3D representation of the office geometry. Figure 7, shows positions of the temperature measurement devices in yellow colour. The temperature devices are placed in the middle of the cells in the same positions, or as close as possible to the corresponding positions in MZ fire model. Devices for

measuring obscuration (PATH OBSCURATION) are placed near virtual exits in the same positions as the obscuration measurement points in MZ fire model (black lines in Figure 7). In order to perform a measurement that is comparable to MZ fire model, the obscuration in FDS is measured over the length of 4 m (length of one cell in MZ fire model).

In FDS, burner obstruction material was assumed to have particle board material properties, which was not possible in MZ fire model. A sensitivity test was run with FDS having no material property assigned to the obstruction and the result have shown negligibly small temperature differences (not reported here).

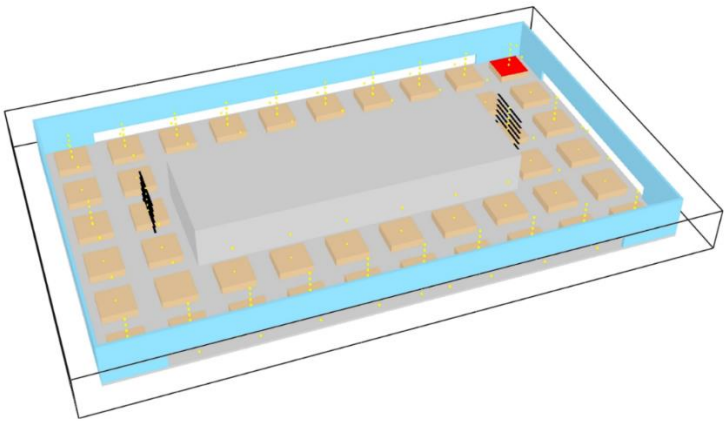

Figure 7 SmokeView office scenario geometry, showing overall fuel packages placement, ignition package in red, obscuration devices in black and temperature measurement devices in yellow, positioned similarly to MZ fire model.

3.3 Supermarket scenario

This chapter describes how the supermarket case was set up and modelled in MZ fire model and FDS. This scenario, like the office scenario, is based on the literature research and has no experimental data available. The chapter provides information on assumptions and design choices for the enclosure layout and openings, thermal and fire related properties of materials, design of HRR and fire spread design.

3.3.1 Enclosure layout and openings

Figure 8 shows a simplified supermarket 60 x 42 x 6 m^3 (Length x Width x Height) where the goods are stored on the shelves of 4.0 x 1.6 m^2 (Length x Width), placed in rows with a separation distances of 4.4 m and 2 m between two fuel packages (see Figure 9). The supermarket in this scenario has 8 windows in the x-direction and 5 windows in the y-direction, all with the same dimensions, 4 x 3 m^2 (Width x Height) (Figure 8).

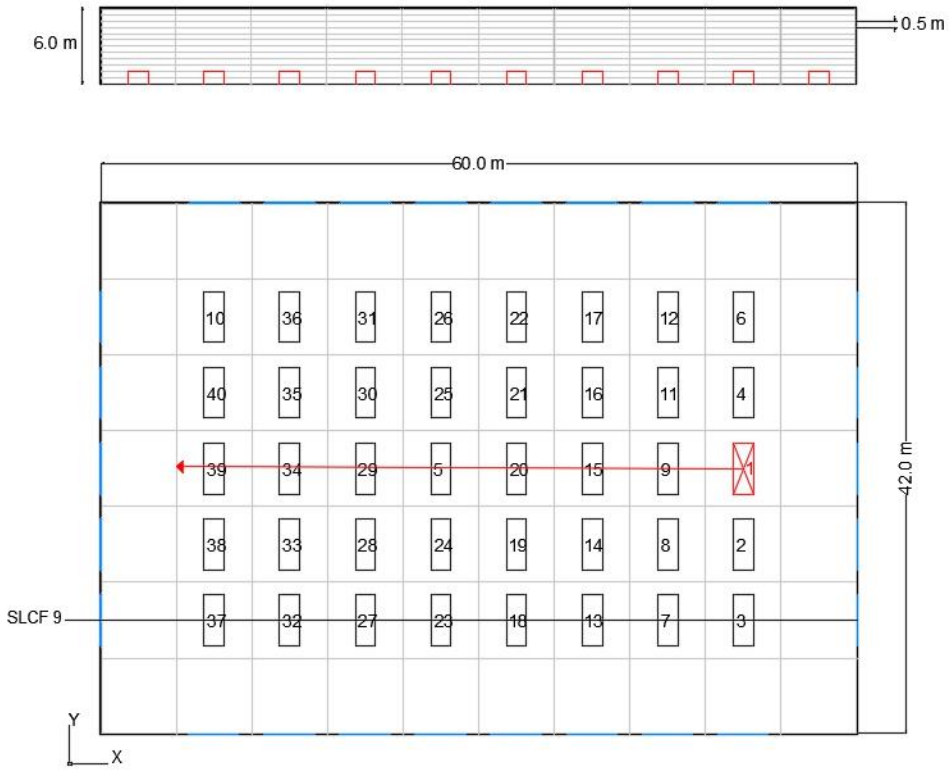

Figure 8 Layout of the supermarket fire scenario, where 5 fuel packages are placed in 8 rows (40 fuel packages in total). The ignition package (1) is marked with red cross, and the fire spreads from right to left. Openings are marked with blue colour.

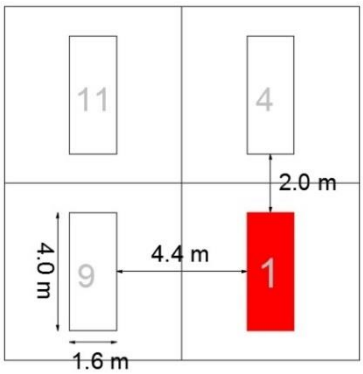

Figure 9 A close-up of the supermarket case with four fuel packages representing shelves. A fuel package represents a supermarket shelf with dimension of 4.0 x 1.6 m^2. Distance between the adjacent fuel packages is 2 and 4.4 m.

3.3.2 Thermal and fire properties of materials

Thermal properties and fire related properties for fuels in typical supermarkets differ significantly. A supermarket may contain a range of food products packed in plastic or carton-board baskets/bags, materials used for cleaning, cooking, and different commodities. Due to the persistent presence of polypropylene (PP) as packaging material, it is used as a fuel in the current simulations, with a soot yield of 0.059 g/g as reported in Table 3-4.14 (DiNenno, 2002, pp. 3-122). Other fire related PP properties, used as input in FDS and MZ fire models are stated in Table 2 (Hietaniemi & Mikkola, 2010).

Table 2 Thermal and fire related properties of materials used as a generalized fuel in the supermarket scenario. (DiNenno, 2002, pp. 3-122), (Hietaniemi & Mikkola, 2010).

	Thermal properties			Fire related properties		
Material	***k* [W/m*K]**	***ρ* [kg/m3]**	***c* [kJ/kg*K]**	**HoC [MJ/kg]**	**Soot yield [ ]**	**Ignition T [C]**
Polypropylene (PP)	0.3	1100	1.6	43.1	0.059	337
Concrete	1.1	2100	0.88			

3.3.3 HRR and fire spread

The data from experiments run by NIST (Madrzykowsky, 2012) and Swedish Technical Research Institute, SP (Arvidson, 2005) are used to develop the HRR curve that represents one supermarket shelf unit. In the NIST tests, potato chips and cheese snacks were tightly packed in three shelf-high and 5.4 m long units. The peak HRR reached in both tests was 6 MW from the Figure 26.45 (Hurley, 2016, p. 836) , and this value is chosen to represent the peak HRR for the supermarket's HRR curve (blue), as shown in Figure 10. A simplified HRR curve for a single shop shelf unit is constructed using the total energy under the HRR curve (blue), estimated to be 4009 MJ. For this curve, a fast fire growth rate of 0.047 kW/s^2 is chosen from PD 7974-1:2003 (BSI, 2003), representing all kinds of shops. Figure 10 shows the resulting HRR curve (red), used as an input for both the MZ fire model and FDS model. The resulting HRRPUA is 936 kW/m^2.

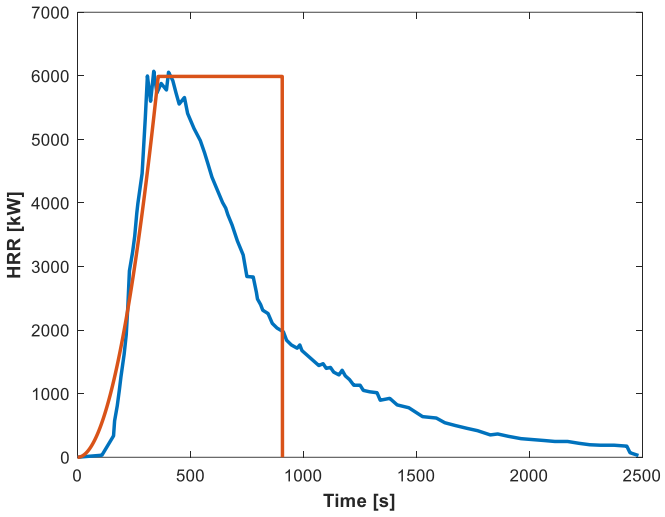

Figure 10 A HRR curve from NIST tests (Hurley, 2016, p. 836) for burning snacks in a shop display unit (blue) and a simplified HRR curve representing one shop shelf unit (red) used in MZ fire model and FDS.

In the supermarket scenario, both MZ fire model and FDS use a prescribed ignition time to model the travelling fire behavior. For this simulation, the ignition times are calculated using Modak's equation, as described in Appendix B-1. In this calculation, the distances between fuel packages (2 m and 4.4 m, see Figure 9) are considered. The heat flux, necessary for ignition is based on the value for polypropylene, 9 kW/m^2 (Babrauskas, 2014, p. 265). The ignition time calculated for all the packages located at the distance of 2 m from each other is 166 s, and for all the packages located at the distance of 4.4 m from each other it is 258 s. The ignition time for packages located at 4.4 m is based on the assumption that the HRR is 1.5 times higher than

the initial value. This is because the fuel packages located at a distance of 2 m ignite earlier.

3.3.4 Scenario configuration in MZ fire model

MZ fire model uses 10 x 7 x 12 cells (840 cells) with dimensions of 6 x 6 x 0.5 m^3, covering the 60 x 42 x 6 m^3 volume (see Figure 8). The model was run on a personal computer.

MZ fire model layout is simplified compared to a real supermarket, where the shelves are normally longer and are placed closer to each other (Lonnermark & Bjorklund, 2008). This simplification is done having in mind MZ fire model's recommendation to position a fire in the center of a cell. The cells around the burning area are placed to represent as realistic layout of a supermarket as possible. The area of the fuel packages has been designed to 4.0 x 1.6 m^2 based on the dimensions reported in the shop shelves tests done by NIST (Hurley, 2016, p. 834), with a fire load density of 936 MJ/m^2. The plume diameter at ceiling height is estimated to be 6.07 m (Appendix B-3), which is close to the cell dimension (6 x 6 x 0.5 m^3). The height of the fuel packages is set to 1.0 m, which is relatively low compared to a height of a shelf. In a supermarket, a fire may start from the bottom of a shelf and spread vertically and horizontally. Such complex fire behavior cannot be modelled using MZ fire model because the fire is prescribed using HRRPUA on the top of a surface. Due to this, an assumption for shelf height had to be made. It is chosen to be lower than the height of a supermarket shelf to represent a possible fire.

3.3.5 Scenario configuration in FDS

The FDS supermarket model uses 20 cm uniform cells, resulting in 300 x 200 x 30 cells (2390528 cells in total), that span the enclosure. The domain is extended for 2 m outside the openings on all sides. The mesh is subdivided into 10 meshes and each mesh is assigned to a process, resulting in 10 MPI on a computer cluster. A SmokeView visualization of the supermarket model is shown in Figure 11. The figure shows enclosure geometry, positions of the fuel packages, temperature measurement devices (yellow) and obscuration devices (black). The obscuration devices are positioned above the height of the openings (3 m) to capture the smoke layer before it exits the building through the windows. In FDS, PP material properties are assigned to the burning obstruction.

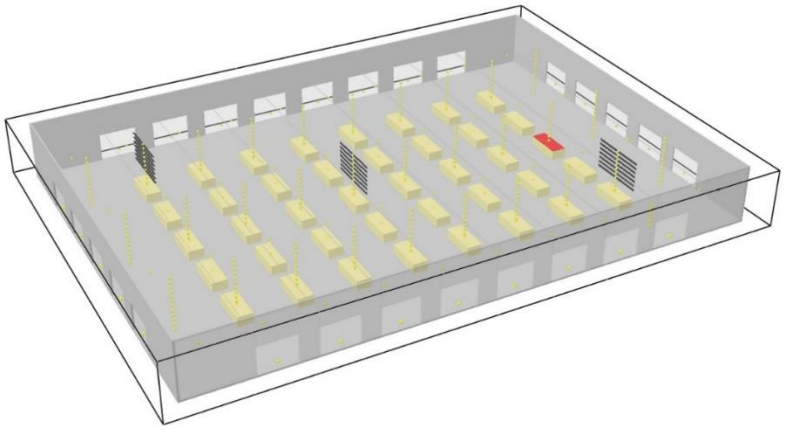

Figure 11 Supermarket layout from SmokeView showing openings, fuel packages placement, ignition package (red), temperature and obscuration measurement devices positioned identically to MZ fire model.

3.4 Tisova experiment

This chapter describes the Tisova fire test, an experiment chosen to validate MZ fire model. A short description of this test provides an overview of information relevant for modelling this scenario. Assumptions and simplifications necessary to model the fire are included in this chapter.

3.4.1 Tisova fire test

The Tisova Fire Test was performed in January 2015 in the Czech Republic. This test was a collaboration of several institutions and universities, including RISE and University of Edinburgh. The purpose of this test was to gather data on travelling fires for model validation, to investigate the influence of such scenarios on structures, composite panels and to perform a post fire investigation. The test was also modeled prior to the experiment in FDS to estimate the severity of the fire (Degler & Eliasson, 2015). The fire compartment was a part of a free-standing building with an approximate total area of 230 m^2, without any nearby constructions. The height to the ceiling varied between 4.21 m and 4.28 m. Four openings were located in the south wall (2.4 x 2.4 m^2), three openings of the same dimensions on the east wall and one larger opening (3.6 x 2.4 m^2) in the north wall, as shown on Figure 12. The fuel bed consisted of spruce wood cribs, uniformly distributed over 170 m^2 of the floor area, placed to the height of 40 cm. A passage, free of cribs, was made near the walls and around the columns. The moisture content of the sticks was 11%, although measurements after the test reported a level of 18-22%. The fuel load in this experiment was estimated at 690 MJ/m^2, based on the heat of combustion for wood (17 MJ/kg). Gas temperature measurements were performed using Type-K Inconel sheathed thermocouples, 1.5 mm diameter of the bead with +/- 2.5°C accuracy. Thermocouple spacing was as follows:

- 56 locations in the horizontal direction with 2.5 m spacing
- 9 positions in the vertical direction between 0.6 m to 4.25 m.

There is no data on visibility available from the test.

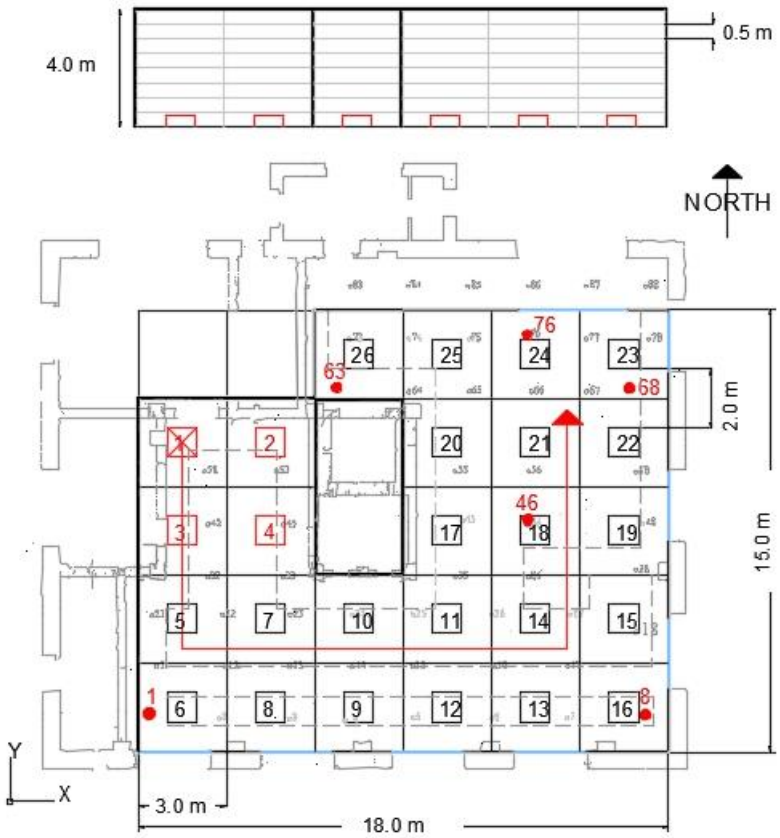

Figure 12 The Tisova fire test enclosure layout, showing the division into MZ fire model's cells and positions of the fuel packages. The ignition package (package 1) is marked with red cross, and the fire spread direction is showed with an arrow.

The total duration of the Tisova test was about six hours (340 minutes). The time maps for fire spread and decay were made based on the thermocouple and webcam recordings. During the growth phase of the test, the fire spread was slow and involved only an area of about 9.0 m^2, with a total duration up to 100 minutes (Rush, et al., 2021). During this phase, the temperatures at the ceiling reached a maximum of 200°C. At 100 minutes, the decision was taken to close the windows and distribute a mixture of gasoline and diesel (10 litres) near the southern wall (from fuel package 6 to 16, see Figure 12). After this change, the fire accelerated and the temperatures in the compartment increased. No further description of the experiment is made here because the scenario is only modelled up to 100 minutes, which covered an approximate area of four fuel packages. The reason for this is twofold. Firstly, because the openings cannot be closed in MZ fire model and, secondly, because the under-ventilated fires are difficult to represent. The gas temperature data was taken from the University of Edinburgh webpage dedicated to the experiment (Rush, et al., 2020).

3.4.2 Enclosure layout and openings

Several assumptions and simplifications are made to model the Tisova fire test. The experimental report (Rush, et al., 2021) provided information on geometry of the building, lay-out of the fuel bed and materials characteristics. The building geometry is discretized into the cells for the purpose of developing MZ fire model. An approximation of geometry is made using 3 x 3 x 0.5 m^3 cells, as shown in Figure 12.

Figure 12 shows the trade-offs made when discretizing: the northern wall is moved 1.7 m inwards, and a small internal western wall is moved 0.63 and 0.3 m out/in to fit the geometry in MZ fire model. The movement of the northern wall may potentially influence the temperatures in this area. Additionally, the elevator shaft is modelled 0.52 m smaller to fit into the chosen cell size. The height of MZ fire model cells is chosen to be 0.5 m which reduced the height of the enclosure from 4.2 m to 4.0 m in both MZ fire model and FDS. The size of the cell (0.5 m) is not an absolute requirement; it can be made smaller if needed.

Figure 12 also shows the choices of temperature measurement positions. Position 1 is located 9.3 m from the ignition source and all the other positions (8, 46, 63, 68, 76) are located 18.6 m and further from the ignition source. In MZ fire model and FDS, the temperature measurements in each position are taken in the center of each cell at 6 different heights (from 0.6 to 3.95 m).

Window sizes and positions have identical settings in FDS and MZ fire model. The simulations are run for 6000 s, which is the time when all the openings are closed. The fire spread between the fuel packages and the fire height (0.4 m) are set up in the same way in both models.

3.4.3 Thermal and fire properties of materials

The external walls are made of 0.6 m thick bricks and the internal walls on the west side are made of breeze blocks with an approximate thickness of 0.3 m. The floor and the elevator shaft are made of 0.2 m thick concrete and the ceiling is made of a 0.3 m thick composite slab. Internal concrete columns and beams are not considered in the models. The thermal and fire related properties of all materials used for both models are reported in Table 3 (Degler & Eliasson, 2015). The ambient temperature used was 1.6 °C. This temperature is an average of all thermocouple readings in the compartment at the start of the experiment.

Table 3 Thermal and fire related properties of materials used for the Tisova fire test modelling from (Degler & Eliasson, 2015).

	Thermal properties			Fire related properties		
Material	k [W/m*K]	ρ [kg/m3]	c [kJ/kg*K]	HoC [MJ/kg]	Soot yield [ ]	Ignition T [C]
Concrete	1.36	2400	1.00			
Masonry	0.69	1600	0.88			
Breeze blocks	0.2	650	1.00			
Wood cribs	0.10	400	1.30	17	0.02	250

3.4.4 HRR and fire spread

The peak HRR is approximated using the equation for non-standard pallets from the SFPE handbook (Hurley, 2016, p. 858):

$$\dot{Q} = 919 \cdot \left(1 + 2.1 \cdot h_p\right) \cdot (1 - 0.03 \cdot M) = 919 \cdot (1 + 2.1 \cdot 0.4) \cdot (1 - 0.03 \cdot 11) \approx 785\ kW$$

where h_p is the height of wood pallets (in this case, wood cribs) is 0.4 m and M is the moisture content of the wood in percent. The wood pallets have a similar arrangement to the wood cribs, but they differ in dimensions (Babrauskas, 1986). The wood pallets (EUR pallets, 1.22 x 1.22 m^2) are not an ideal representation of wood cribs (0.04 x 0.06 x 1 m) because the dimensions of the cribs and the distances between each crib are not the same as in the pallet tests. Nevertheless, the method was used to estimate HRR. Considering the total burning area of one

fuel package of 1 m^2, the HRRPUA is 785 kW/m^2.

Knowing the HRRPUA, and using the fire spread velocity of 0.5 mm/s (Rush, et al., 2021), the growth rate is calculated (Karlsson & Quintiere, 2000, p. 38) as follows:

$$\alpha = HRRPUA \cdot V^2 \cdot \pi = 785 \cdot 0.0005^2 \cdot \pi = 0.0006\ kW/s^2$$

The time to reach the peak HRR is calculated using the t-squared fire equation:

$$t = \sqrt{\frac{Q}{\alpha}} = \sqrt{\frac{785}{0.0006}} = 1144\ s$$

A report from (Lange, et al., 2018) states that the growth phase lasted for 150 minutes. However, the latest reported (Rush, et al., 2021) time of 100 min (6000 s) is used as the total simulation duration time. According to the time maps (Rush, et al., 2021), the first fuel package ignites at 0 s, the second at 3600 s, the third at 1200 s and the fourth at 2400 s. Package positions are shown in Figure 12. Only the first fuel package burns out at 2400 s (before the simulation end time is reached); the other three packages continue burning when the windows are closed. Design HRR for the first fuel package is presented in Figure 13. The rest of the packages (2 – 4) have the same growth rate and peak HRR, but they do not burn out within the simulation time. It would be advantageous to be able to represent a decay phase in this particular scenario for each fuel package. This can be done by assigning a ramp for each fuel package to represent the scenario more closely. However, this capability is not implemented in MZ fire model at this stage.

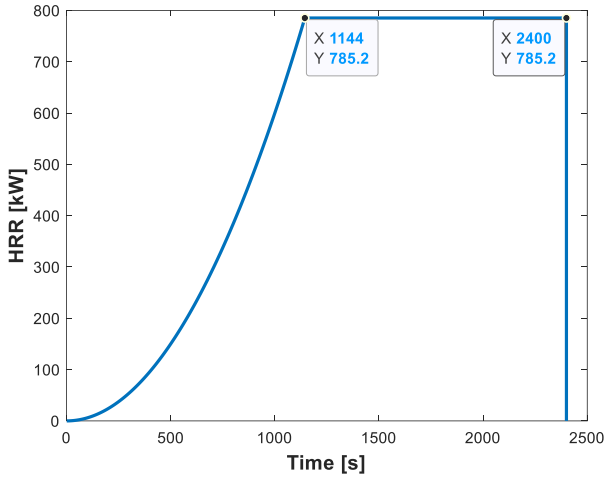

Figure 13 Design HRR for the Tisova fire test used for fuel packages 1, 2, 3 and 4.

3.4.5 Scenario configuration in MZ fire model

In MZ fire model, it is possible to model a fire that takes up part or all of the zone, as in the Tisova fire experiment. This would imply that the burner is flush with the walls of a cell and no tests are yet done on how this can influence the outcome of a simulation. Therefore, the choice was made to represent the continuous fuel bed of wood cribs by discrete fuel packages. The total area of the wood cribs that are ignited in the simulations is 9 m^2. This is represented by discrete fuel packages of 1 x 1 m^2 placed in the center of the cells in order to fit the plume within one cell size. The cells in MZ fire model are 3 x 3 x 0.5 m^3, with a total of 240 cells. The simulation was run on a personal computer.

3.4.6 Scenario configuration in FDS

In FDS, the domain for the Tisova fire scenario is discretized using 20 cm cells, resulting in 211090 cells in total. The domain was subdivided into 7 meshes and run in parallel on a computer cluster.

The SmokeView projection of the Tisova fire model (Figure 14) shows geometry and locations of temperature devices (yellow) and path obscuration devices (black lines). Obscuration is taken as an additional measurement in both MZ fire model and FDS, even though the data is not provided by the test. Three locations for the obscuration measurement are used, as shown in Figure 14. The location of devices for temperature measurements are chosen to be identical to the positions of the temperature measurements reported in the experiment.

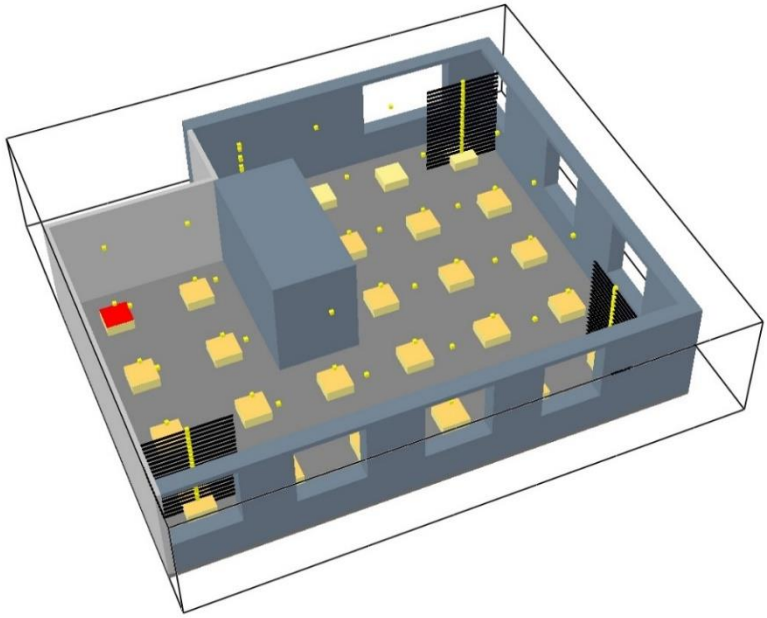

Figure 14 Tisova fire test building layout from FDS model showing openings, fuel packages placement, ignition package (red), temperature devices (yellow) and “path obscuration” measurement devices (black lines), positioned as in MZ fire model.

3.5 Edinburgh Tall Building Fire Test (ETFT)

This chapter describes one of the ETFT fire test series (number 3) chosen to validate MZ fire model. A short description of the ETFT test series is followed by the choice of modelling parameters for MZ fire model and FDS.

3.5.1 Edinburgh Tall Building Fire Test

An experiment used in this thesis (Hidalgo, et al., 2017) is the third test performed by the University of Edinburgh and its partners. A total series of twelve experiments was performed to study and characterise a scaled down fire in a large space. The fire is designed to represent a part of an open-space office building. The area of the openings was changed throughout the tests to model under and well-ventilated fires. For the purpose of this thesis, test number three is chosen because all of the openings were in the open position for the entire duration of the experiment; therefore, the fire was fuel controlled, see Appendix B-2.

3.5.2 Enclosure layout and openings

The ETFT fire test enclosure dimensions are 17.8 x 4.9 x 2.0 m^3 (Length x Width x Height). This enclosure is an attempt to scale down a large open-space floor plan office experiment (Hidalgo, et al., 2017). There are fifteen openings, which are positioned along the south side of the building and separated by 0.1 m metallic profiles protected by BEAMCLAD®, (see Figure 15). These openings are represented in MZ fire model and FDS as six larger openings with the same area. Figure 15 shows both the openings in the experiment (grey) and the openings in FDS and MZ fire model (black). Multiple openings in a single cell of MZ fire model must be avoided.

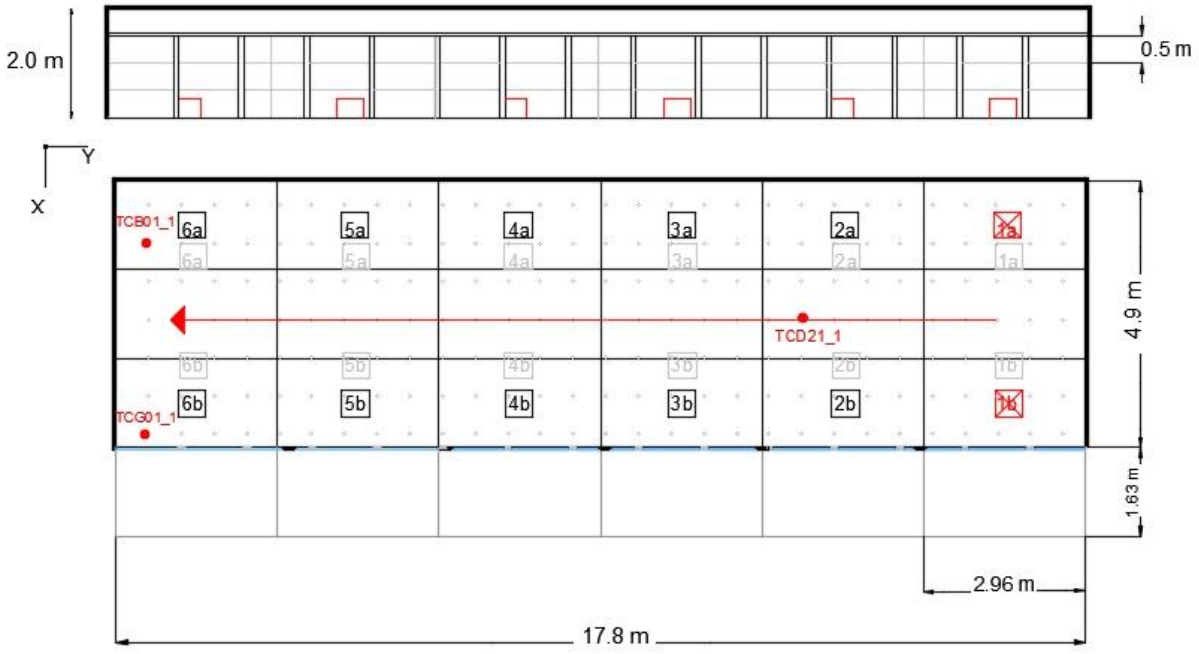

Figure 15 Layout of the enclosure used in the ETFT fire test. Figure shows MZ fire model cells and location of the fuel packages (experimental location is shown in grey, MZ fire model and FDS in black). The ignition packages (1a and 1b) are marked with red crosses, and the fire spread direction is from right to left as the arrow.

3.5.3 Thermal and fire properties of material

The enclosure was custom-built for the tests at the BRE laboratories (Watford, UK), using steel profiles for columns, timber beams and aerated concrete blocks for walls, sandwich panels made of ROCKWOOL® insulation panels and plasterboard for ceiling. Thermal properties of materials are reported in the experiment as resistances (R-values) and transmittances (U-values), refer to Table 4. Thermal insulation materials are used in order to replicate a “nearly zero-energy building” and thermal transmittance values (U-values) following the EU guidelines (EU, 2010).

Table 4 Resistance and transmittance values, reported in the ETFT fire test (Hidalgo, et al., 2017).

Element	Thickness [m]	R-value[m2K/W]	U-value[W/m2K]
Ceiling	0.32	7.42	0.15
Walls	0.255	7	0.18
Floor	0.158	3.79	0.23

Conductivity of materials used in the modelling is calculated based on the experimental data from Table 4, using the following equations:

$$U - value = \frac{1}{\sum R - value}$$ Equation 1

where U-value is the transmittance in W/m^{2}K and R-value is the thermal resistance of materials in m^{2}K/W. It is calculated as:

$$R - value = \frac{thickness}{k}$$ Equation 2

In the test, all of the surfaces are made of different sandwich panels (see Table 5). The floor consists of 0.14 m of mineral wool insulation FLEXI® placed on the top of a 0.018 m plywood panel. The walls are comprised of layers made of 0.05 m aerated concrete blocks, 0.05 m mineral wool insulation FLEXI®, 0.14 m wood structural column with an air gap, and 0.015 m plasterboard as closing side. The ceiling is comprised of 0.025 m of mineral wool panel BEAMCLAD®, 0.5 mm thick steel covered sandwich panel comprised of 0.27 m mineral wool insulation FLEXI® and 0.025 m plasterboard on top. The conductivity values, as well as density and specific heat for all materials, used in the experiment are listed in Table 5. For the calculation of conductivity values used in the simulations see Appendix B-4. To model the ETFT experiment some simplifications were necessary for the thermal properties of materials used and their thicknesses. Table 5 shows the differences between the experimental values and the values used in the models. Some thicknesses differ in order to comply with the cell sizes in the models. The largest difference in thicknesses was made for the walls, where it is assumed that the heat will penetrate past the two first materials only (aerated concrete blocks and FLEXI®) with the total thickness of 0.1 m. As for the thermal properties, the assumption is made that the conductivity of the floor material will have negligible influence on the temperature results, so the values for the normal concrete were used. For the walls, the conductivity of aerated concrete blocks was derived from the U-value using a thickness of 0.1 m. As for the conductivity for the ceiling, the choice was made to model it as close to the experimental value (calculated from U-value) as possible. This decision is based on the importance of the ceiling in the heat transfer, which possibly has the greatest impact on the results.

Table 5 Thermal properties of materials used in the ETFT fire test and the models. References: Plasterboard (de Korte & Brouwers, 2009), FLEXI® and BEAMCLAD® (ROCKWOOL, u.d.), aerated concrete blocks (Chaipanich & Chindaprasirt, 2015), normal concrete (Karlsson & Quintiere, 2000, p. 122) and plywood panels (SYKTYVKAR, s.d.).

	Sandwich materials	QUANTITY	TEST	MZ fire model/FDS
Floor	FLEXI® mineral wool	k [w/mK]	0.036	1.4
	plywood	sandwich thickness [m]	0.158	0.1
		density [kg/m3]	180/550	2300
		specific heat [kJ/kgK]	0.8	0.88
Walls	aerated concrete blocks	k [w/mK]	0.046	0.021
	FLEXI® mineral wool	sandwich thickness [m]	0.255	0.1
	air gap	density [kg/m3]	400	400
	plasterboard	specific heat [kJ/kgK]	1	1.05
Ceiling	BEAMCLAD	k [w/mK]	0.048	0.06
	FLEXI® mineral wool	sandwich thickness [m]	0.32	0.3
	plasterboard	density [kg/m3]	180/180/600	180
		specific heat [kJ/kgK]	0.8/0.8/0.84	1.00

3.5.4 HRR and fire spread

In the experiment, twelve propane gas burners comprised of an open-top metal square with dimensions of 0.5 x 0.5 x 0.35 m^3 were located as shown in Figure 15 (grey colour). After multiple tests in MZ fire model, the burners had to be moved – see new positions in Figure 15 (black colour).

A travelling fire was simulated by switching on two burners at a time and moving along from right to left (starting from burners 1a and 1b and finishing with burners 6a and 6b – see Figure 15). The change of burners was done approximately every 2.5 minutes, until the experiment ended after fifteen minutes. The event log is presented in Table 6.

Table 6 Event log for ETFT test, used as the simulations input (Hidalgo, et al., 2018).

Event	Input Time [s]
Burners 1a and 1b On	0
Burners 1a and 1b Off	152
Burners 2a and 2b On	154
Burners 2a and 2b Off	300
Burners 3a and 3b On	302
Burners 3a and 3b Off	451
Burners 4a and 4b On	454
Burners 4a and 4b Off	600
Burners 5a and 5b On	602
Burners 5a and 5b Off	748
Burners 6a and 6b On	752
Burners 6a and 6b Off	900

HRR is calculated using controlled propane flow of 3.2 kg/min, with a corresponding lower heat of combustion of 46.45 MJ/kg (Drysdale, 2010, p. 21). HRR is estimated as shown below:

$$Q = \dot{m} * \Delta H_c = 3.2\ \left[\frac{kg}{min}\right] \cdot \frac{1}{60}\left[\frac{min}{s}\right] \cdot 46450[\frac{kJ}{kg}] = 2477.3\ kW$$

This represents the energy released by two burners; hence, only half (1238.6 kW) is considered to calculate the HRRPUA. The area of one burner is 0.25 m^2 and the burning efficiency is assumed to be 90% (Tewardson, 1995). The HRRPUA is therefore:

$$HHRPUA = 1238.6 \cdot \chi \cdot \frac{1}{A_f} = 1238.6 \cdot 0.9 \cdot \frac{1}{0.25} = 4458.9\ kW/m^2$$

Using the t^2 equation (Karlsson & Quintiere, 2000, p. 38) and the time to reach the HRR of 10 seconds assumed based on data in (Hidalgo, et al., 2018) the growth factor equals to:

$$\alpha = \frac{Q}{t^2} = \frac{1114.7}{10^2} = 11.1\ \text{kW/s}^2$$

3.5.5 Scenario configuration in MZ fire model

The ETFT fire test scenario in MZ fire model was configured using 2.96 x 1.63 x 0.5 m^3 (Length x Width x Height) 6 x 4 x 6 cells, resulting in 144 cells total. MZ fire model did not allow a higher number of cells in the *z*-direction. The domain was extended outside the openings by adding one cell in front of them. The simulation was run on the personal computer.

3.5.6 Scenario configuration in FDS

The size of the geometry in the ETFT fire test is smaller (87.22 m^2) than other scenarios modelled in this study. Therefore, it was possible to improve the accuracy of FDS simulation by using 10 cm cells (180 x 49 x 20 cells), with the total of 334800 cells. In FDS, the domain was extended outside the openings.

Figure 16 shows a SmokeView visualization of the ETFT fire scenario. The view shows details of the compartment in 3D: ignition packages (red), temperature measurements (yellow) and path obscuration measurement devices (black lines).

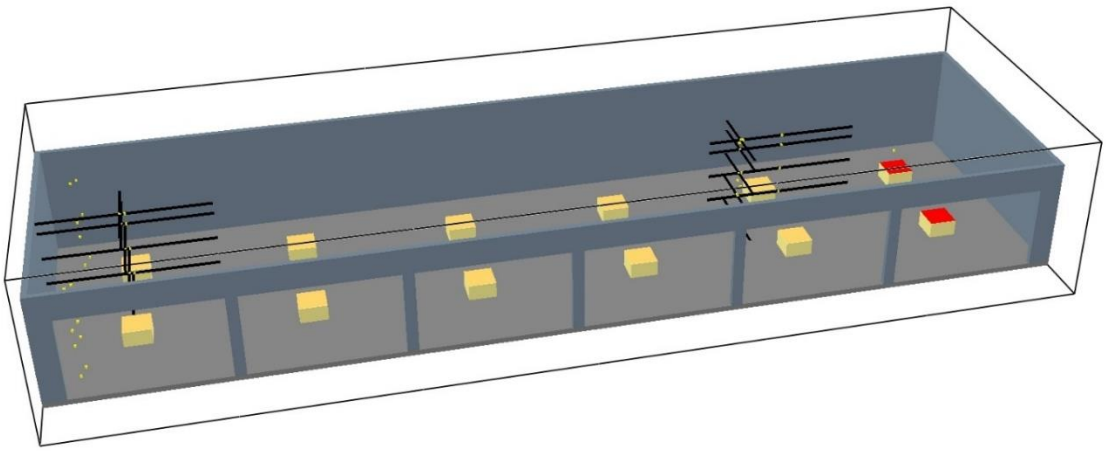

Figure 16 ETFT fire test building layout from FDS model showing openings, fuel packages placement, ignition packages (red), temperature and obscuration measurement devices positioned identically to MZ fire model.

4 Results

This chapter reports the results of different scenarios that were modelled in this study (i.e., office, supermarket, the Tisova fire test and the Edinburgh Tall Building Test). For every scenario, an overview of MZ fire model domain is presented, followed by temperature and obscuration results. The layouts with measurement devices are shown to facilitate understanding.

4.1 Office scenario

Figure 17 shows vertical temperature profiles at 600, 1200, 2400, 3600 and 4712 s for y = 2 m (see red line on the horizontal slice below) as generated by MZ fire model simulation. These temperature maps are generated using a custom-made MATLAB® code and are similar to FDS slices. However, they provide the temperature information in discrete data points with the uniform temperature in each 4 x 4 x 0.5 m^3 cell. Figure 17 shows behaviour of the travelling fire. The temperatures are changing in accordance with predefined ignition, starting from the left corner (0 m) and moving in the forward direction (40 m). Like the two-zone models, MZ fire model does not consider the flame and the results show two distinct temperature layers forming – the hot layer above and the cold layer below. Figure 17 also shows a similar temperature map for a horizontal slice at z = 2.75 m. This figure is shown only for visualisation purposes since the temperatures presented here are not comparable with the FDS model's slices.

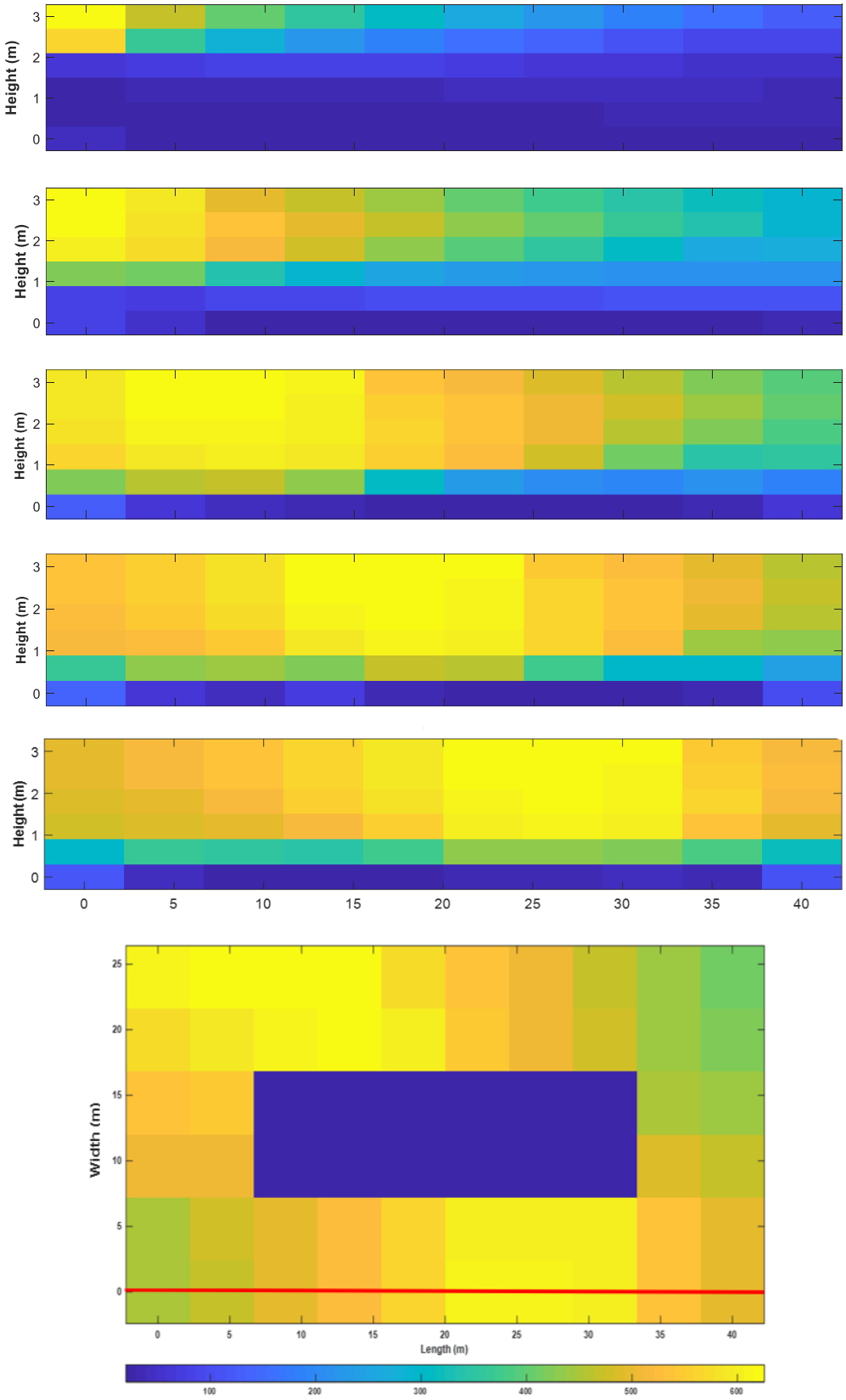

Figure 17 Temperature profiles generated in MATLAB® from MZ fire model for the office output at different times (from top down) vertical profiles at 600 s, 1200 s, 2400 s, 3600 s and 4712 s at y = 2 m, as shown in the horizontal slice below (red line). Horizontal temperature map generated in MATLAB® from MZ fire model output (below) at 4712 s at z = 2.75 m.

The visualization of temperatures for MZ fire model shown in Figure 17 are not comparable to the corresponding slices from FDS. Therefore, a comparison of the output is made instead by choosing several positions for temperature (17, 28, 36, 42 and 48) and obscuration (6 and 41), see Figure 18.

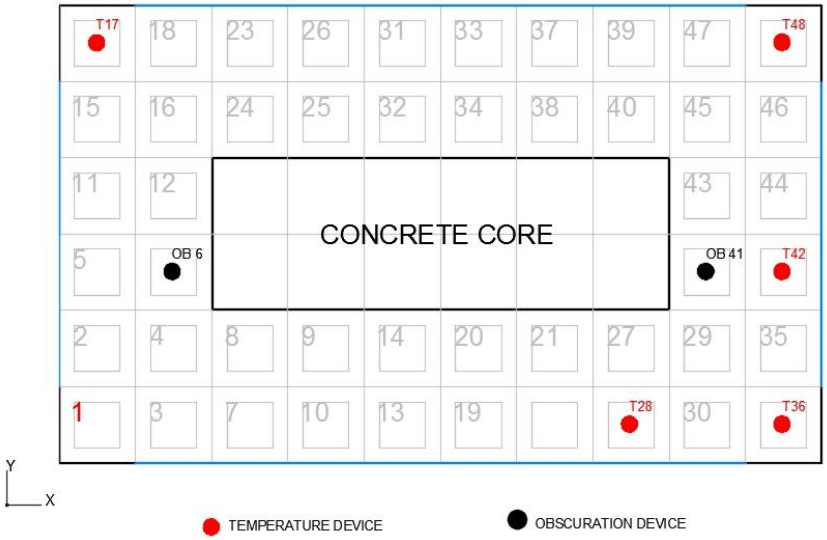

Figure 18 Position of temperature and obscuration devices in the office scenarios.

These positions are chosen to cover the far field range of the enclosure. They are placed at different distances from the ignition source in respect to the openings and the concrete core. Positions 17, 28, 36, 42 and 48 are averaged over the following periods: (1) 1000-1020 s, (2) 1300-1320 s and (3) 1600-1620 s. The locations of the travelling fire for these three averaging periods are shown in Figure 19.

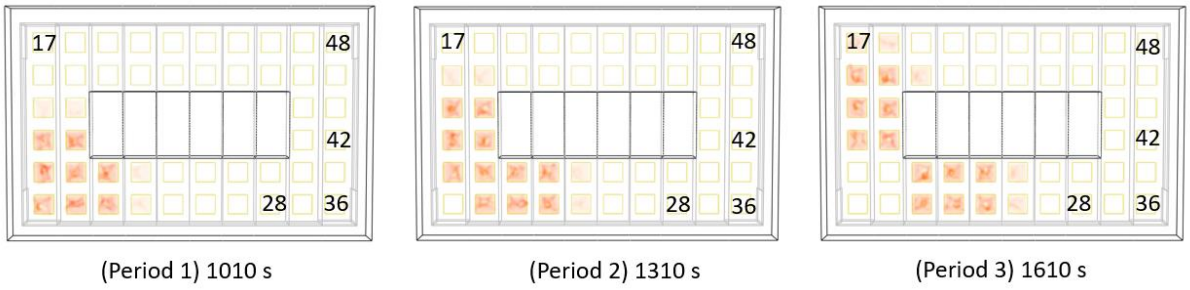

Figure 19 Fire locations in FDS during the averaging periods: (1) 1010 s, (2) 1310 s and (3) 1610 s.

Results of the temperature comparison between MZ fire model and FDS are shown in Figure 20. In position 17, MZ fire model predicts temperatures close to FDS within the averaging period 1. Table 7 facilitates analysis of the temperature curves by averaging the temperatures at the four highest points and estimating the differences in percentage between FDS and MZ fire model. For position 17 in averaging periods 1 and 2, Table 7 shows that the differences on average does not exceed 8.5%. But during averaging period 3 when position 17 is in direct proximity of the fire the predictions show 41.7 % higher temperatures in FDS (see MZ 3 and FDS 3 in Figure 20). Predictions in position 36 (corner of the building) are roughly 16-25 % higher in FDS than in MZ fire model at the hights over 1.5 m. This might be caused by the

corner fire dynamics captured in FDS better than in MZ fire model. In the positions behind the concrete core (Figure 20, position 42 and 48), the predictions at the early stages are good (from 3.3 to 10.9 % differences). However, as the fire travels further (position 48) and involves higher area, the temperatures in FDS are 20 % higher compared to MZ fire model. In position 28 the predictions are good, with FDS predicts being on average 2-5 % higher.

Table 7 Percentage differences in average temperatures between MZ fire model and FDS from the height of 1.25 m up to the ceiling, taken at different times (periods) for each measurement position. Positions 17 during the period 3 is in the near field region.

	Difference FDS - MZ [%]		
Position	**Period 1**	**Period 2**	**Period 3**
17	8.5	-0.2	41.7
36	24.5	17.9	16.4
42	8.6	3.3	2.9
48	7.1	10.9	20
28	4.9	1.6	2.7

MZ fire model simulation results are given in Figure 20 and Figure 21. The simulation was run without extending the domain outside the openings. An additional attempt was made to model the same scenario with an extended domain. The results of this simulation compared to a simulation without extension is provided in Appendix J. No significant differences in temperatures were noted.

An additional test was performed to see if MZ fire model would benefit from more than 6 cells in z-direction using 10 cells. The results in Appendix L have shown an improvement with temperature differences Figure 56. Results agreement between FDS and MZ fire model for positions 36 and 48 were significantly improved (e.g., from 20% to 10% for position 36). This shows that MZ fire model does benefits from higher number of zones (cells) in z-direction, allowing the flow (inflow and outflow) in 3.3 zones instead of 2.

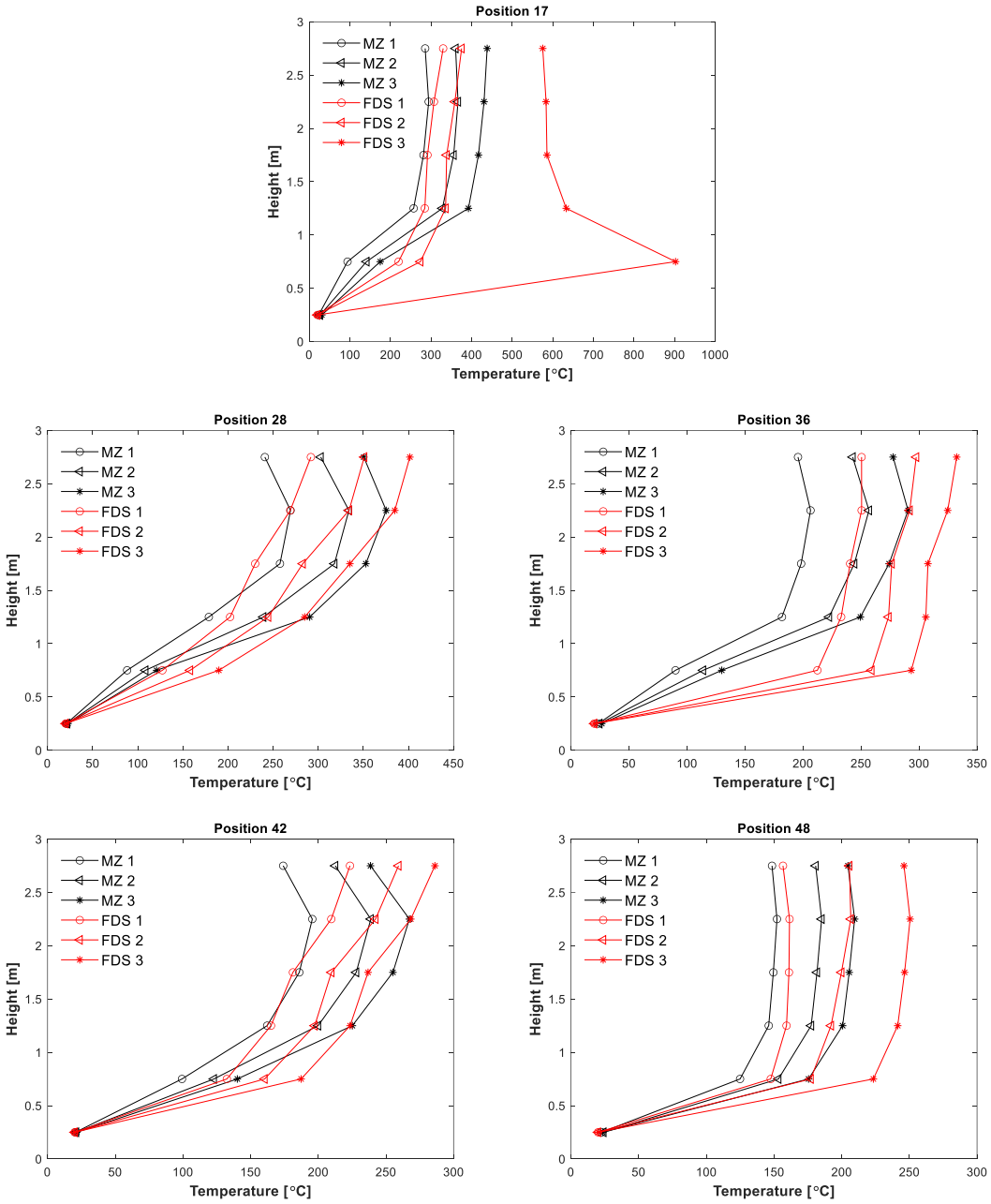

Figure 20 Temperatures profiles of selected positions (17, 28, 36, 42, 48) at the time when the first 1 to 8 packages are burning as shown in Figure 18. The temperatures are averaged over 20 s.

Figure 21 compares obscuration for MZ fire model and FDS at positions 6 and 41 for three different heights (1.75 m, 2.25 m and 2.75 m). The obscuration devices are placed near possible exit locations in the concrete core. The best agreement between MZ fire model and FDS is attained for position 6 at a height of 1.75 m and for position 41 at 2.75 m. Position 6 at 2.25 meters after 200 s FDS shows lower values and reaches 100% obscuration later than MZ fire model. At the same position but higher in the domain, FDS model has lower obscuration from the start of the simulation.

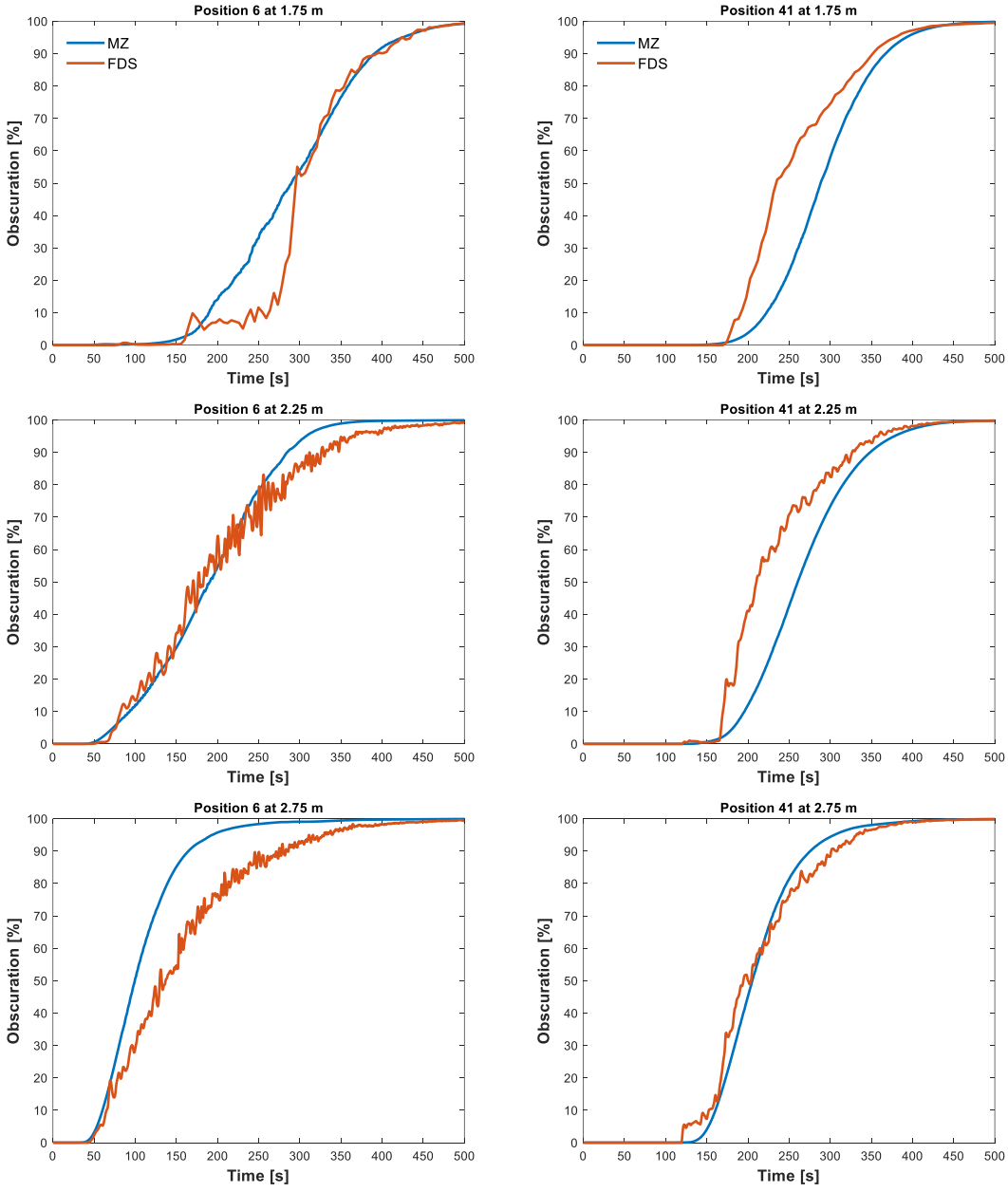

Figure 21 Obscuration changes with time compared between MZ fire model and FDS for the office scenario in positions 6 and 41 at the heights of 1.75, 2.25 and 2.75 m.

4.2 Supermarket scenario

Figure 22 shows the supermarket scenario temperature profiles at 300 s, 600 s, 1200 s, 1800 s, 2400 s and 3045 s at y = 9 meters for MZ fire model simulation. This figure provides temperature information at discrete data points with a uniform temperature in each 6 x 6 x 0.5 m^3 cell.

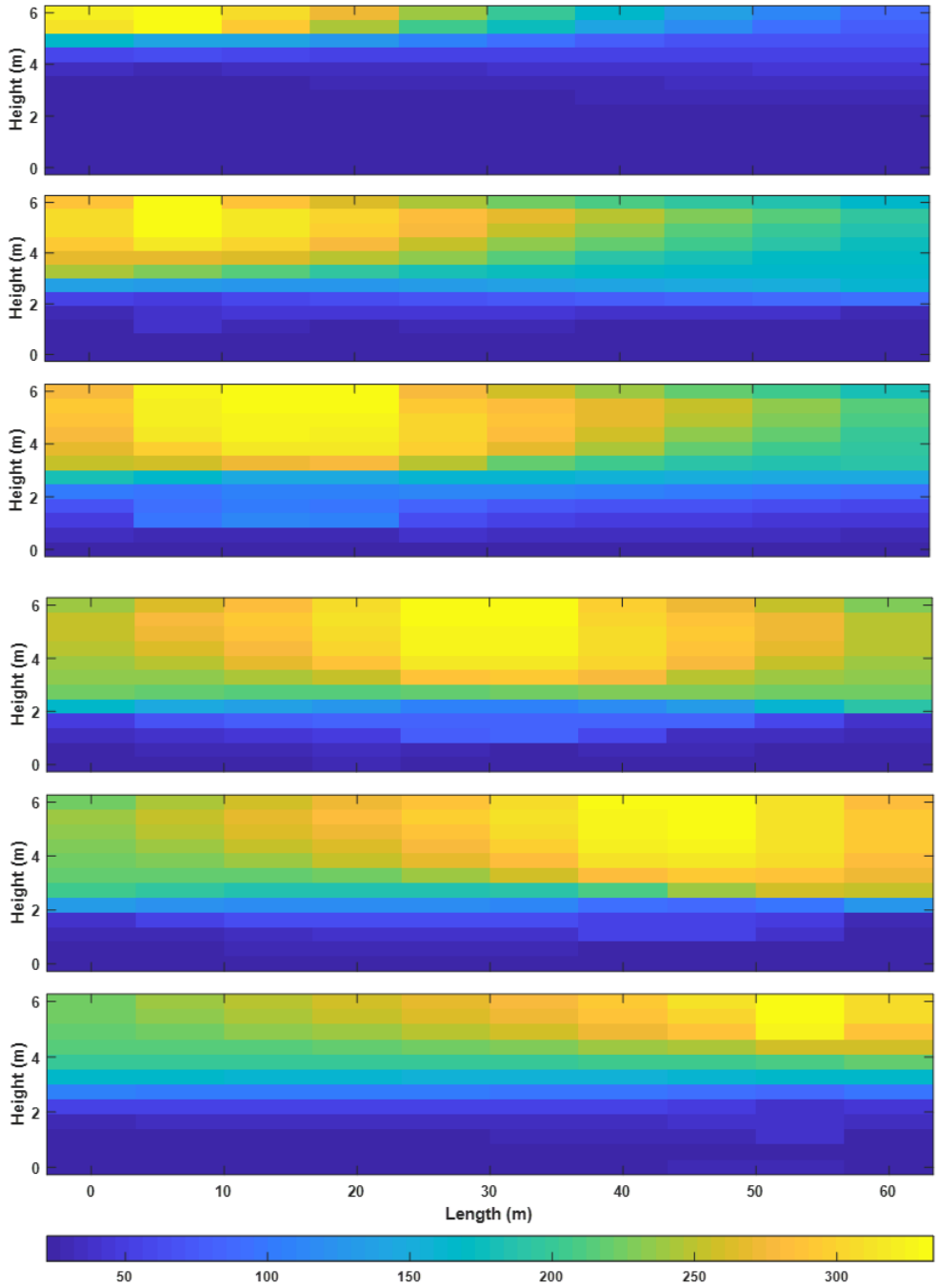

Figure 22 Temperature profiles generated in MATLAB® from MZ fire model outputs for the supermarket scenario at different times (from top down) 300 s, 600 s, 1200 s, 1800 s, 2400 s and 3045 s at y = 9 m (SLCF 9) as shown in Figure 8.

Temperature averaging is done over a 20 s period in MZ fire model, whereas in FDS this period is kept as similar to MZ fire model as possible. The differences in time steps does not allow

selection of identical averaging periods. The averaging periods (Table 8) are chosen having in mind that MZ fire model is tested for prediction of far field temperatures.

Table 8 Averaging periods [s] for positions 3, 5, 10 in the supermarket scenario.

	Averaging periods [s]		
Position	**1**	**2**	**3**
3	1500-1520	2500-2520	2800-2820
5	200-220	500-520	700-720
10	500-520	700-720	1000-1020

Position 3 is located close to the ignition package, position 5 is located in the middle of the enclosure at about 24 meters away from the ignition point, and position 10 is located 43 meters away from the ignition point (see Figure 23). During the first averaging period (1500-1520 s), thirteen packages are involved in the fire. During the second averaging period (2500-2520 s), eleven packages are involved in the fire. And, during the third averaging period (2800-2820 s), only four fuel packages are burning.

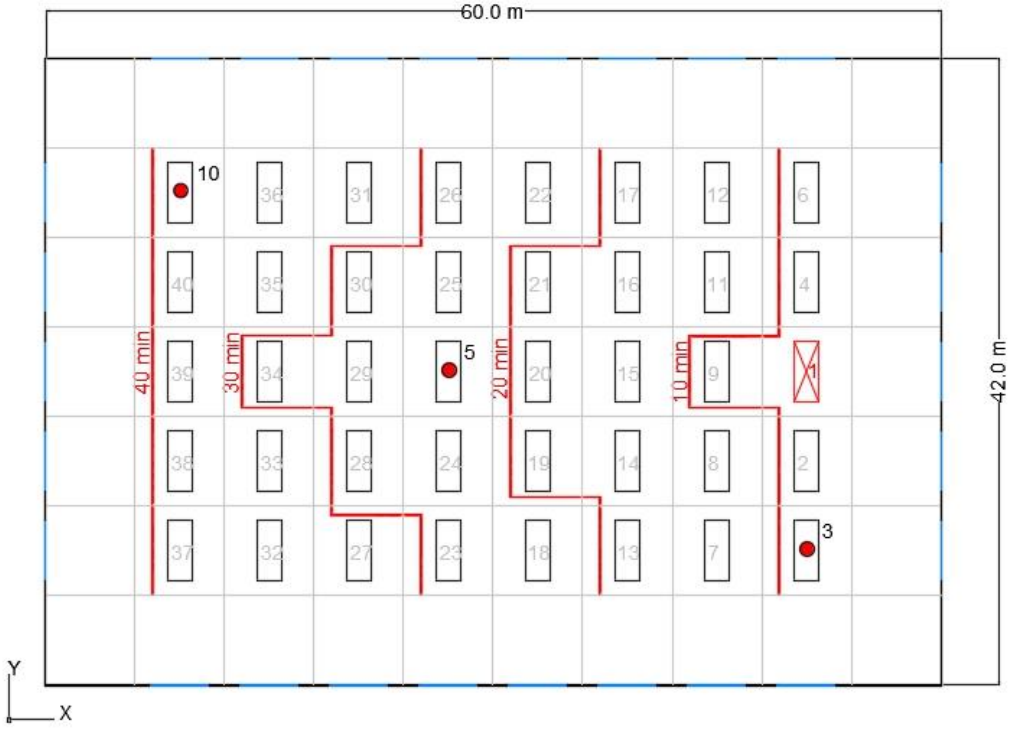

Figure 23 The supermarket layout, showing the fire spread with times red lines and the measurement positions for temperature and obscuration (3, 5 and 10).

Figure 24 shows the results of temperature measurements at positions 3, 5 and 10. The values are averaged as described in Table 9. This table shows percentage difference in average temperatures between MZ fire model and FDS taken at a height of 3 m for different time periods.

Table 9 Percentage difference in average temperatures between MZ fire model and FDS from the height of 3 m up to the ceiling taken at different times (periods) for each measurement position.

	Difference MZ - FDS [%]		
Position	**Period 1**	**Period 2**	**Period 3**
3	26.9	19.2	20.8
5	-7.3	23	33.3
10	9.4	19.5	24.1

Figure 24 shows temperature results for the supermarket scenario. MZ fire model shows higher temperatures compared to FDS at most locations. In position 3, temperatures are on average 19-27 % (Table 9) higher in MZ fire model than in FDS. In position 5, predictions made by MZ fire model are similar to the predictions made by FDS in averaging period 1, with only on average 7.3 % differences. After 500 s, when four packages are involved in fire, MZ fire model shows 23% higher temperatures and after 700 s the differences are on average about 33%. Position 10 is located furthest away from the ignition point. The best agreement in this position is achieved during the first averaging period (500 - 520 s), with MZ fire model showing on average 9.4 % higher temperatures. For the second and the third averaging periods, MZ fire model shows on average 20-24% higher predictions.

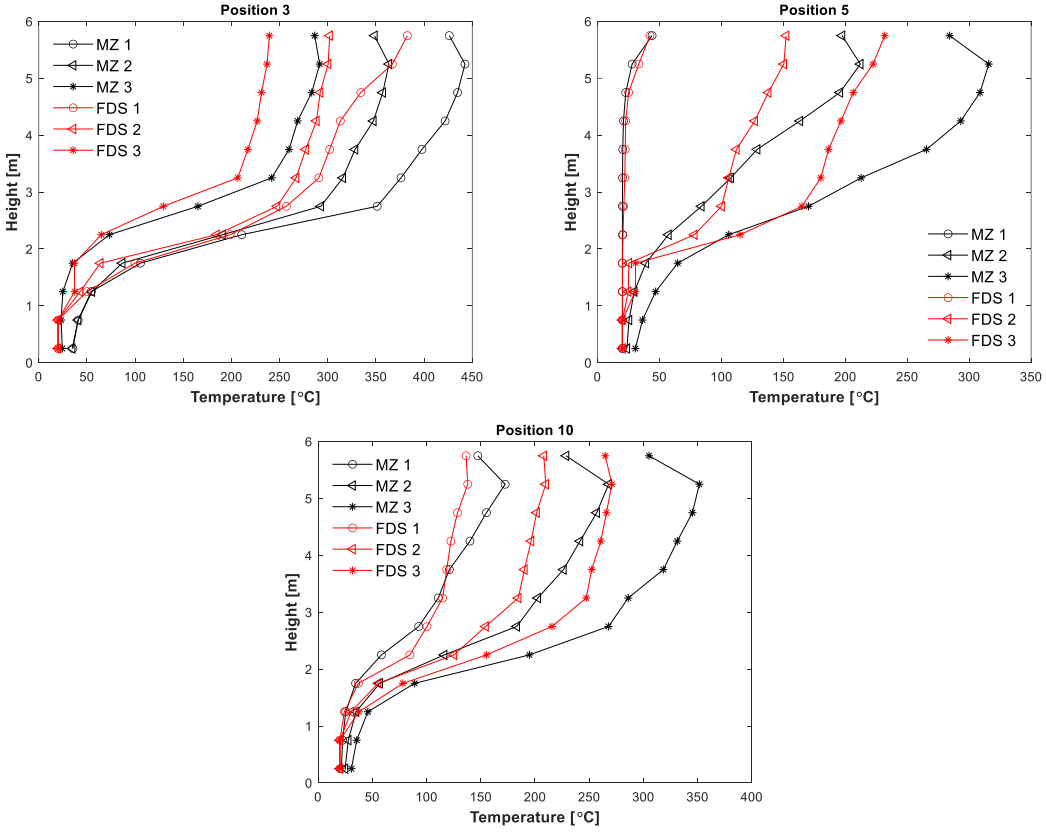

Figure 24 Average temperatures over the height for MZ fire model and FDS for the supermarket case.

Figure 25 shows obscuration [%] for the supermarket scenario in position 5 at six different heights (for position locations see Figure 17). Only position 5 is presented because it shows

similar results to other positions (3 and 10). The results for the other positions are contained in Appendix D. The measurements start from 2.75 m above the floor based on the bottom height of the openings. Figure 25 shows that measurements are better at the upper heights. The best agreement between the models is found directly under the ceiling, at the height of 5.75 m. At the lower heights (2.75–4.25 m), MZ fire model reaches 100% obscuration later compared to FDS. The obscuration in FDS has a fluctuating profile, whereas MZ fire model profile is smooth, which can be explained by resolution and model differences.

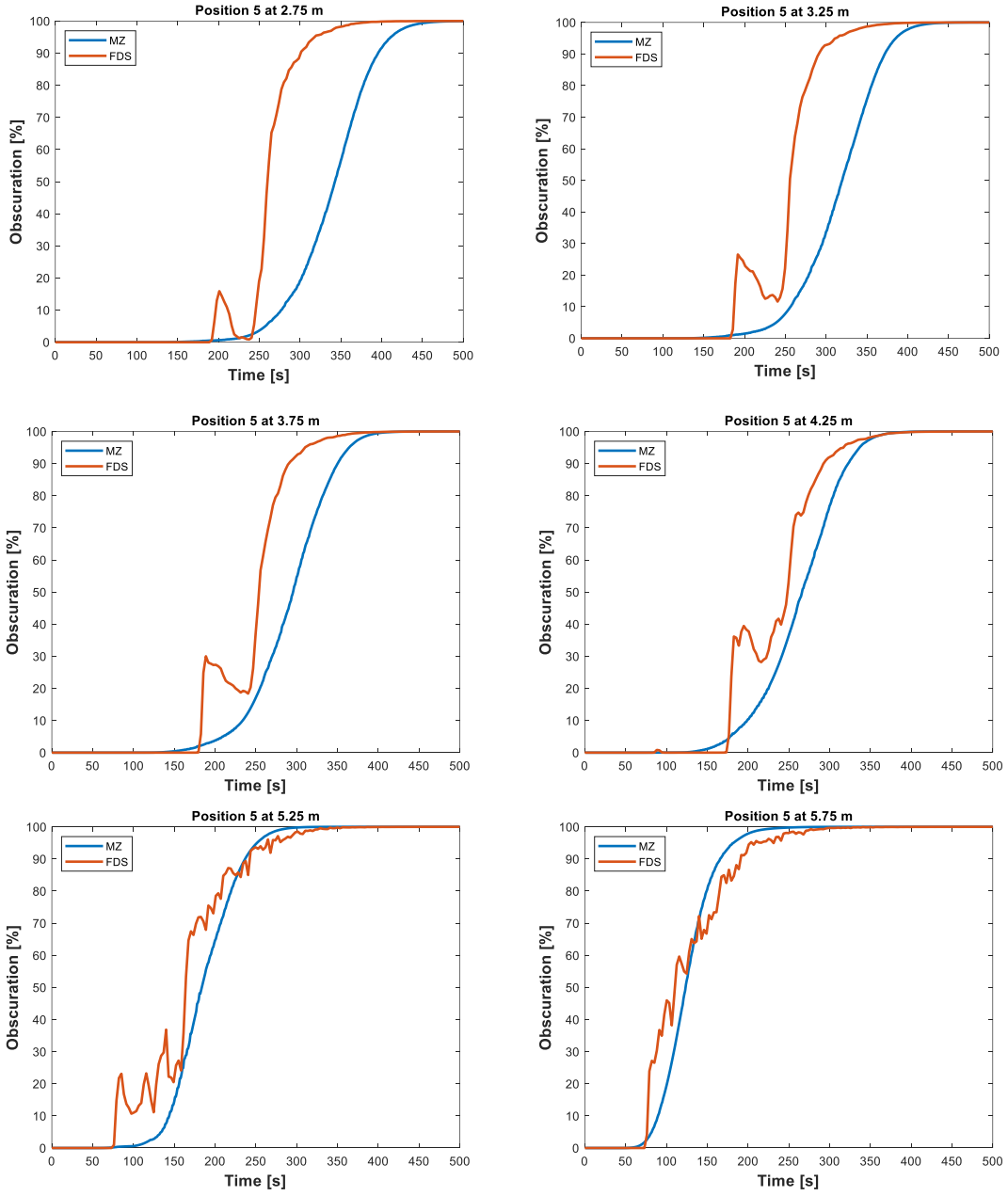

Figure 25 Obscuration comparison for MZ fire model and FDS in position 5 at different heights (for the position see Figure 23). Obscuration results for positions 3 and 10 can be found in Appendix D.

Figure 26 shows a comparison of average temperature for MZ fire model and FDS. The figure covers a time range of 490 – 510 s in positions 3 (located at 0 m from fire), position 5 (located at 17.2 m from fire) and position 10 (located at 37.2 m from fire). The values are provided for heights of 1.75 m and 3.25 m. This figure shows that the difference in temperatures at the height of 1.75 m is large near the fire and becomes increasingly smaller with distance from the fire. At a height of 3.25 m the differences become smaller at all positions.

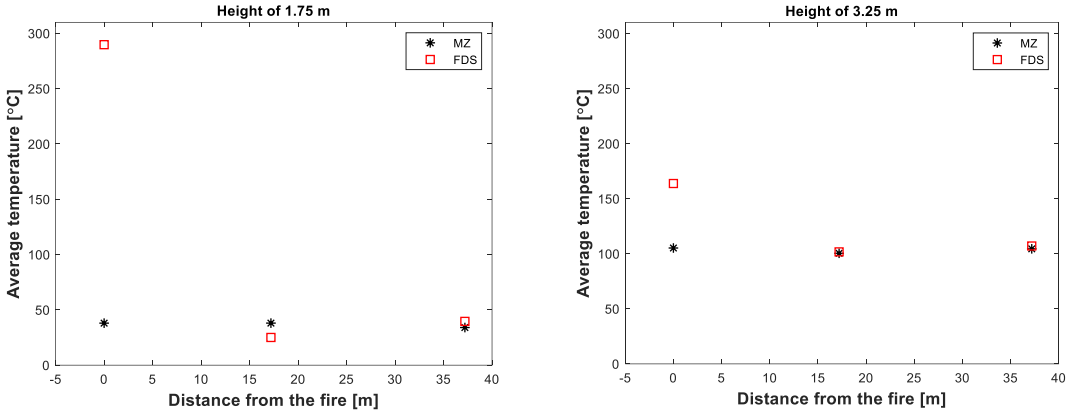

Figure 26 Comparison of temperatures over the distance for the supermarket case at the heights of 1.75 m and 3.25 m. Temperatures are averaged over the period of 490 – 510 s, when the fire is located at 0 m from fire (position 3), 17.2 m from fire (position 5) and 37.2 m from fire (position 10).

4.3 Tisova fire test

Figure 27 shows a horizontal temperature map for the Tisova fire test at 6000 s for z = 3.75 m. This temperature map is generated using MATLAB® based on MZ fire model simulation output. The figure provides temperature information as discrete data points, with a uniform temperature in each 3 x 3 x 0.5 m^3 cell.

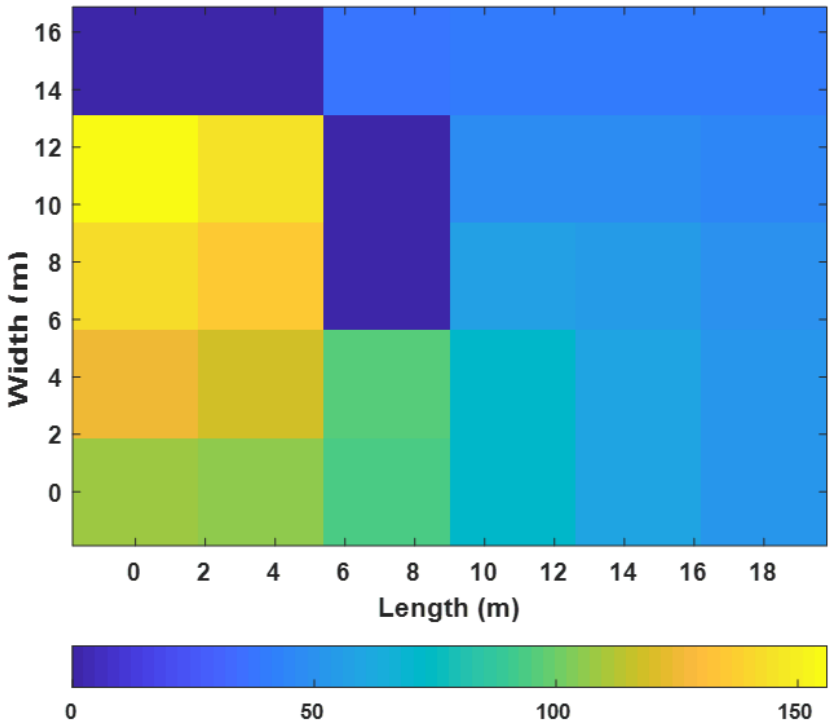

Figure 27 Horizontal temperature map generated in MATLAB® from MZ fire model output at 6000 s at the height z= 3.75 m.

Several positions for temperature devices are considered to compare the results from MZ fire model with the data from the experiment: positions 1, 8, 46, 63, 68 and 76 (as named in the experimental results), see Figure 28. These positions are located at different distances from the fire. The corresponding thermocouple data are taken from the experimental results, published in (Rush, et al., 2020) and compared to MZ fire model and FDS. Results presented below only show data from positions 1, 8, 68 and 76. Results from the positions 46 and 63 can be found in the Appendix E.

Figure 28 shows FDS temperature slices at z = 3.75 m height, taken within the averaging time periods at (a) 1020 s, (b) 3040 s and (c) 5050 s. This figure helps to visualize temperature changes in the Tisova fire experiment for the time periods used in the analysis. The location of devices 1, 8, 68 and 76 on Figure 28 is denoted with numbers. The choice is made to limit the temperature to 80 °C because the maximum temperature rises to approximately 130 °C in FDS was noted only in position 1 during the last averaging period. The rest of the data shows temperatures below 80 °C. During the first averaging period (Figure 28 (a) 1020 s), only one package is burning, and the temperatures stay around 30 °C at the measurement points. Burning is very slow (0.5 mm/s fire spread rate) for the entire simulation. After one hour, the burning front advances for an approximate distance of 1.8 m (Rush, et al., 2021).

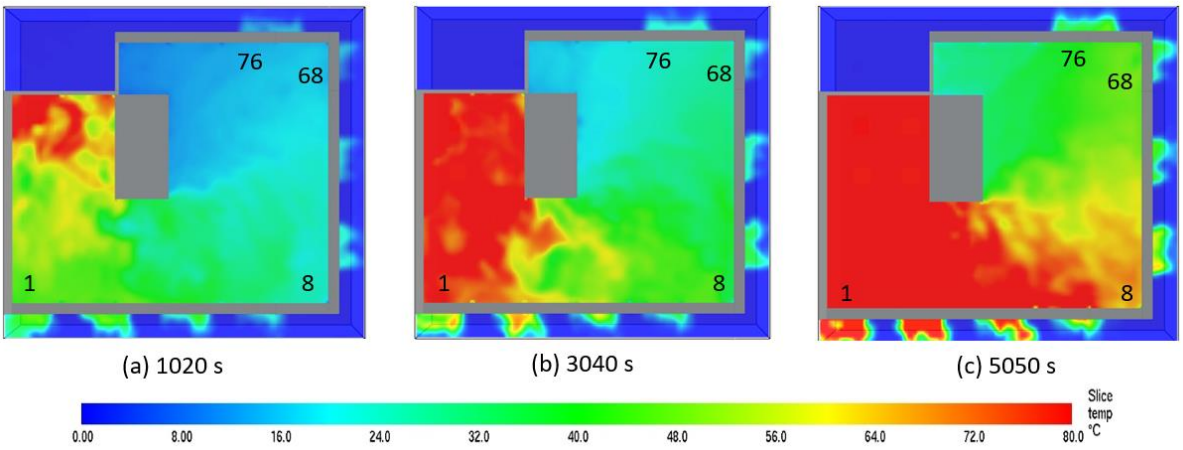

Figure 28 Temperature slices in FDS at z = 3.75 m height, taken within the averaging time periods at (a) 1020 s, (b) 3040 s and (c) 5050 s. Numbers denote the locations of the measurement positions.

Table 10 shows temperature difference in percentage between MZ fire model, FDS and experiment. The results for position 1 and 8 averaged over time intervals of 1020-1080 s, 3000-3060 s and 5040-5100 s are shown in Figure 29. In general, FDS had better agreement with experimental results than MZ fire model. This is true for both locations and at all time intervals. Comparison between MZ fire model and experimental results show higher values (23-63 %) for MZ fire model. Position 1 showed good results for periods 1 and 2, with FDS temperatures being on average 3.5-5.4 % higher. In period 3, FDS predicted on average 22.5 % higher temperatures. Position 8 showed on average 70-80 % higher temperatures in FDS. Even higher differences exist between MZ fire model and experimental results.

Table 10 Percentage difference in average temperatures between FDS and MZ fire model/ Experiment and MZ fire model above the height of 2.5 m, taken at different times (periods) for each measurement position.

	Difference FDS - MZ [%]			Difference Experiment - MZ [%]		
Position	**Period 1**	**Period 2**	**Period 3**	**Period 1**	**Period 2**	**Period 3**
1	3.5	5.4	22.5	62.7	34.4	-23.5
8	78.6	80.3	69.4	96.8	147.5	64.3
68	46.1	43.9	36.5	0	66.6	47.3
76	26.8	30.7	18.1	-67	0.5	18.4

Figure 30 shows experimental results from MZ fire model and FDS. The results are for positions 68 and 76 and are averaged over the same time intervals. The initial ambient temperature in the compartment prior the test was estimated to be 1.6 °C. Figure 30 shows that experimental temperatures in these positions did not raise over 50 °C. In general, predictions from MZ fire model and FDS at position 68 were poor compared to experimental values and also were not consistent with each other. Position 76 shows slightly better results with FDS model, being 18–31 % higher on average.

Figure 31 compares obscuration at heights of 1.3, 3.3 and 3.9 m for positions 68 and 8. The measurements from MZ fire model were done in the 3 x 3 x 0.5 m cells. In FDS the obscuration path devices were placed in the same positions, spanning the width of the cell to measure the

obscuration in %. The obscuration predictions vary depending on the heights. At the lower heights, the differences are large, and the fluctuations of obscuration measurements are high, see Figure 31 at 1.3 m. At a height of 3.3 m, FDS reaches the same obscuration faster than MZ fire model. At a height of 3.9 m, MZ fire model reaches the same obscuration earlier than FDS.

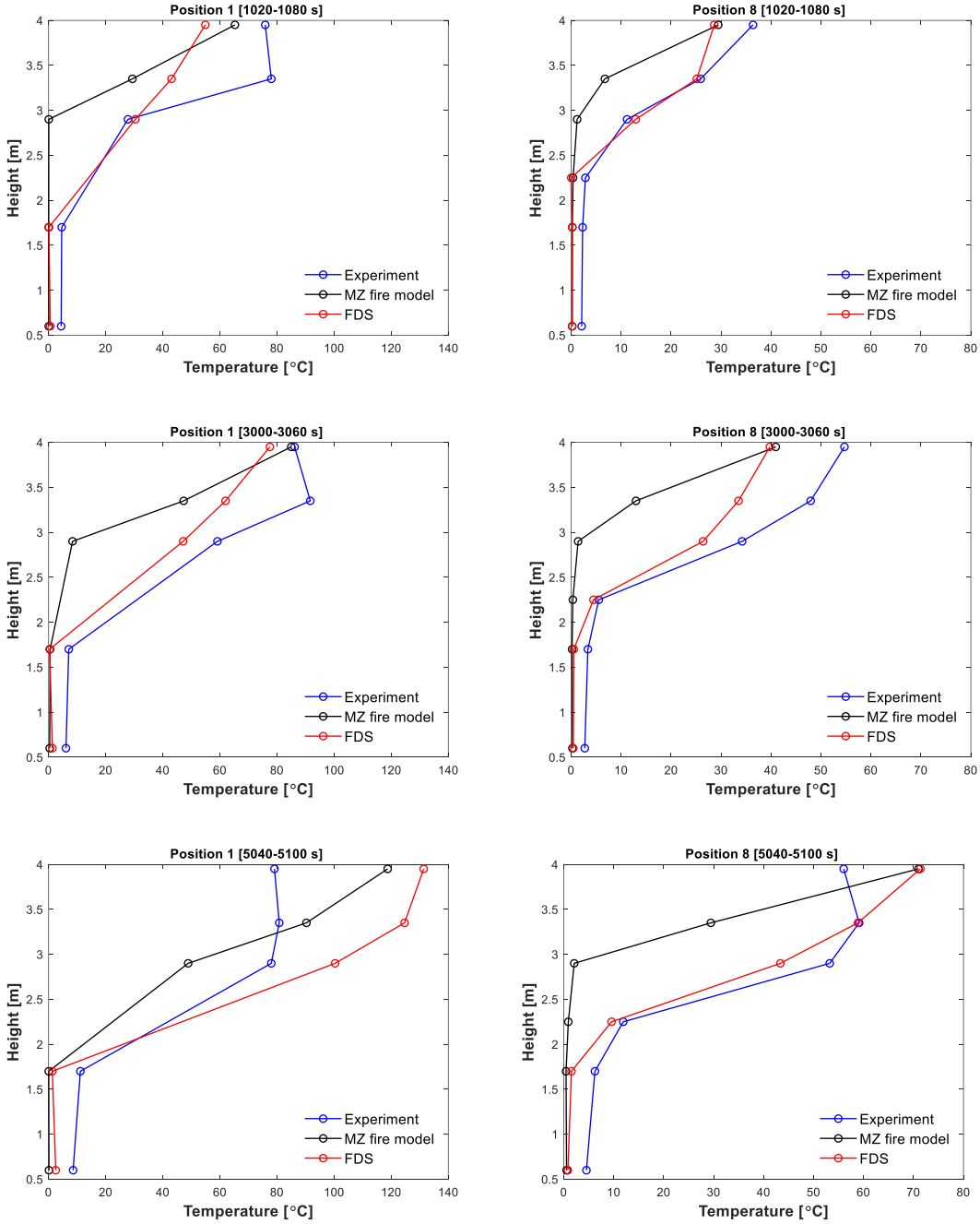

Figure 29 The Tisova fire test temperature results comparison to MZ fire model and FDS for positions 1 and 8 averaged over time intervals of 1000-1020 s, 3000-3060 s and 5040-5100 s.

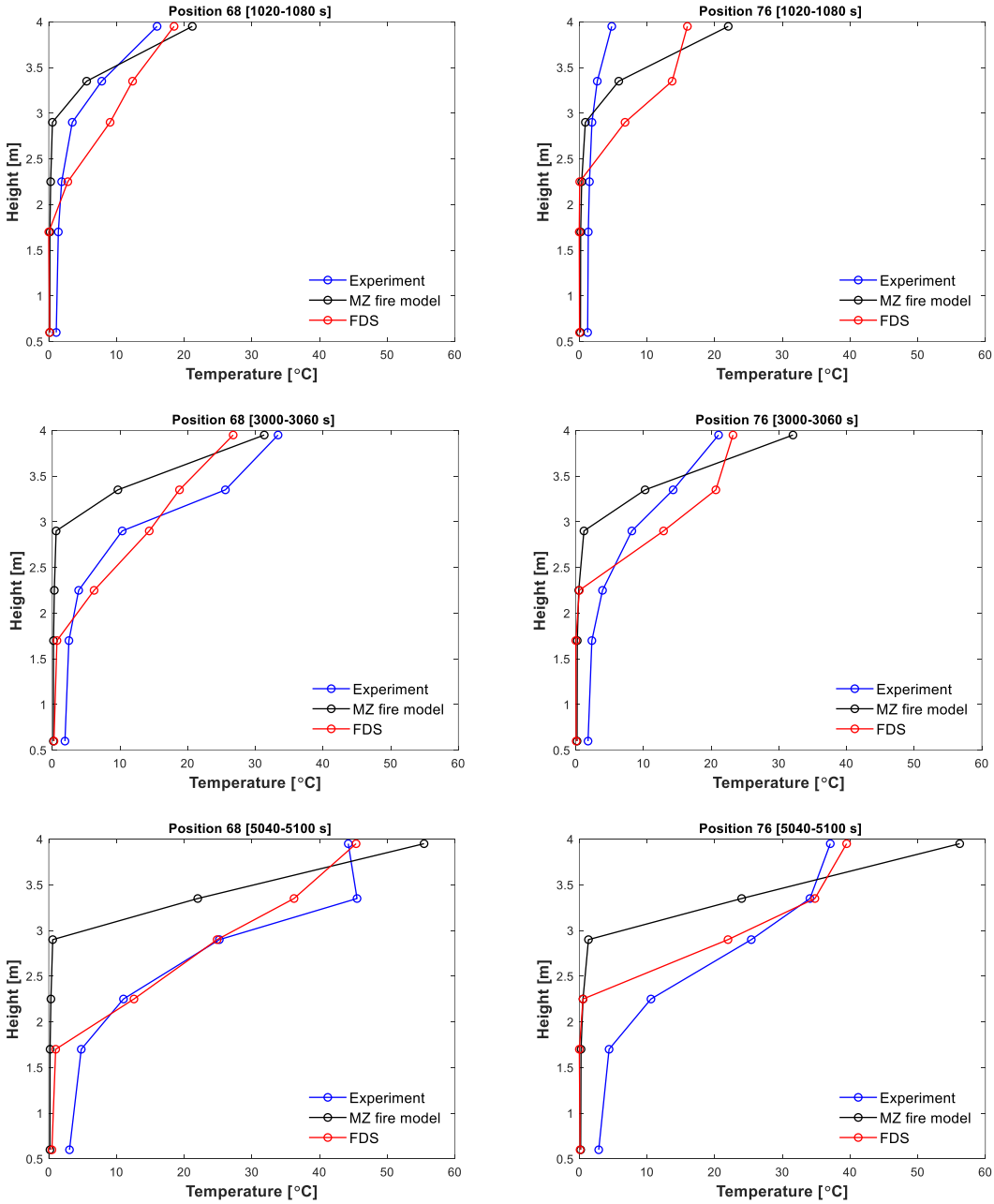

Figure 30 The Tisova fire test temperature results comparison to MZ fire model and FDS for positions 68 and 76 averaged over time intervals of 1000-1020 s, 3000-3060 s and 5040-5100 s.

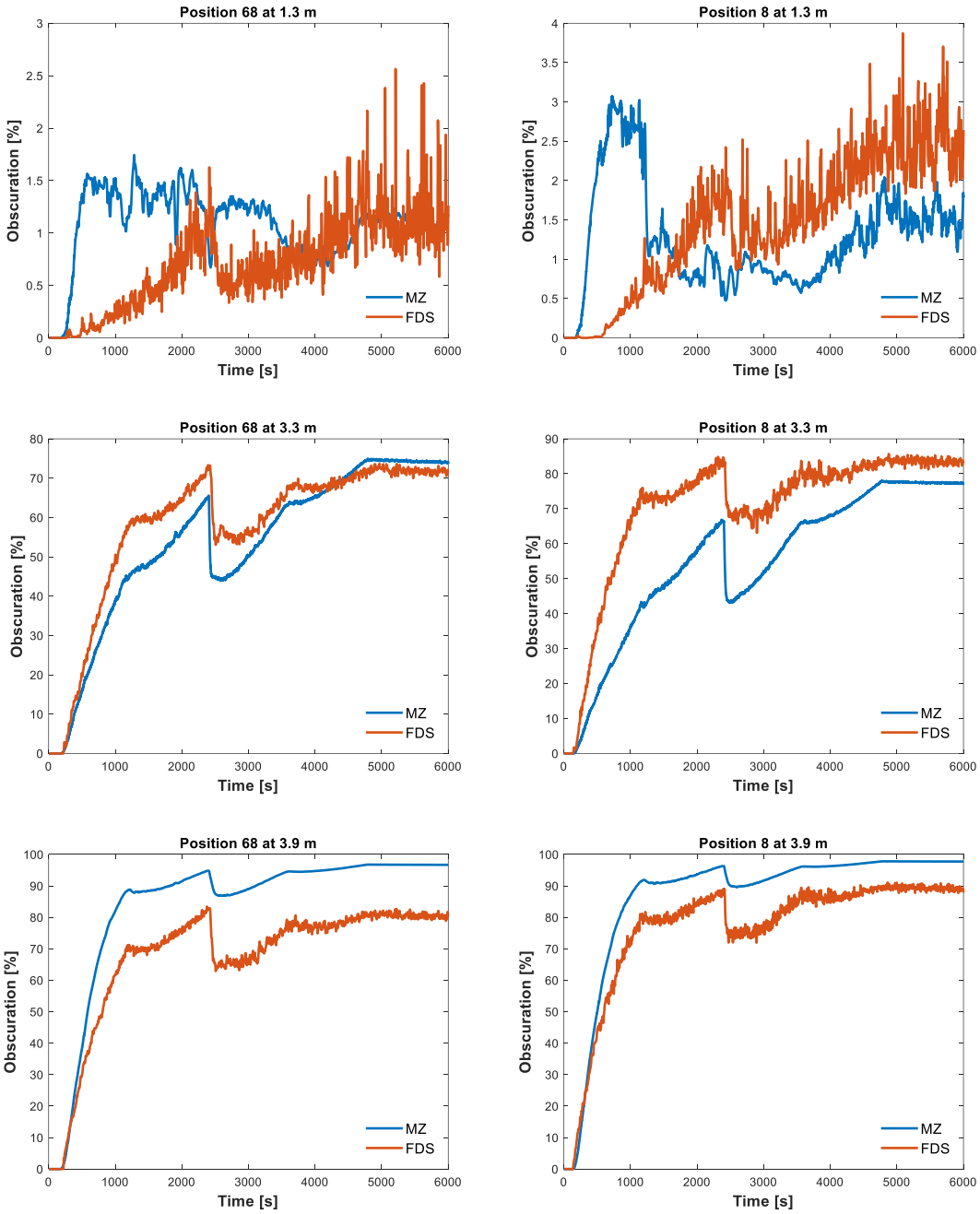

Figure 31 Obscuration for the Tisova fire test modelled with MZ fire model and FDS at heights of 1.3, 3.3 and 3.9 m.

Figure 32 presents comparison of predicted temperatures (MZ fire model and FDS) to temperatures estimated using Alpert's ceiling jet correlation (Karlsson & Quintiere, 2000, p. 156). The Alpert correlation has been used in previous studies (Johansson, et al., 2013) (Rackauskaite, et al., 2015) (Dai, et al., 2018) to estimate far field temperatures, and it is therefore interesting to compare it to the current results. The distance *r* in Alpert correlation is a constantly changing distance from the centre of the travelling fire to position 1. Temperatures between MZ fire model and FDS vary on average 11% for the whole duration of the measurement, while Alpert correlation's temperatures are on average 40-70% lower than FDS temperatures. It shows that Alpert correlation does not work well for confined enclosures, such as the Tisova test enclosure.

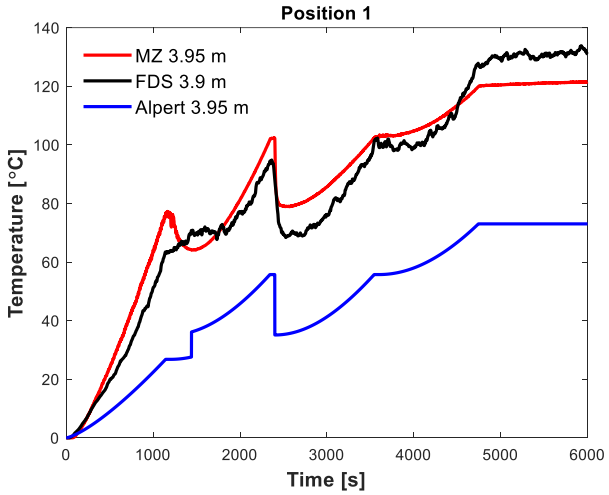

Figure 32 Temperature in position 1 at the approximate height of 3.95 m with MZ fire model, FDS and Alpert's correlation.

It is not known how an adjacent zone being in direct contact with a vent influences the temperatures. Therefore, an additional MZ fire model simulation was performed in a similar way as in FDS, i.e., with an extended domain outside of the building. Extension of the domain outside the building showed no significant differences, see Appendix J for additional information.

Additional work was done in attempt to improve the fitting of geometry (height) into MZ fire model. For this, both MZ fire model and FDS had to be rerun with the new settings. In MZ fire model, the 4.2 meters height of the compartment was divided by 0.42 m heigh cells. The results of temperature comparison are reported in Appendix K. The resulting temperatures are similar in the near field. In the far field, MZ fire model showed higher temperatures near the ceiling.

4.4 Edinburgh Tall Building Fire Test (ETFT)

Figure 33 shows for the ETFT fire scenario a top view of the temperature distribution at the time of ignition for each couple of burners (i.e., 154 s, 302 s, 454 s, 602 s and 752 s.). This figure provides a temperature map with discrete data points.

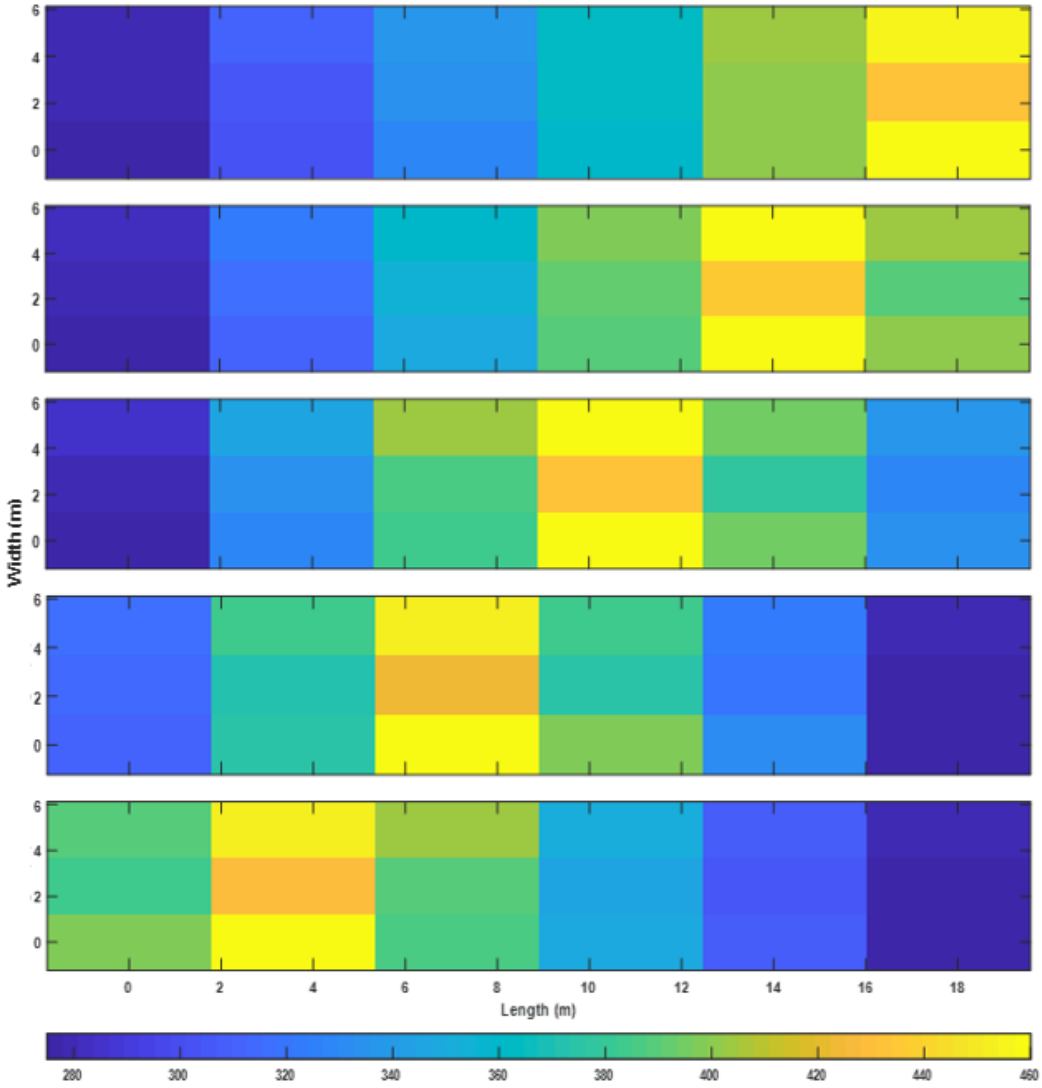

Figure 33 Top view on the temperature distribution, generated in MATLAB® from MZ fire model output at different ignition times (from top down): 154 s, 302 s, 454 s, 602 s and 752 s.

Figure 34 shows positions of temperature (D21_1, B01_1 and G01_1) and obscuration devices (D21_1 and D2_2). In this figure, positions of the burners activated during the averaging periods are marked with red lines. The three averaging periods are the same for all measurement positions.

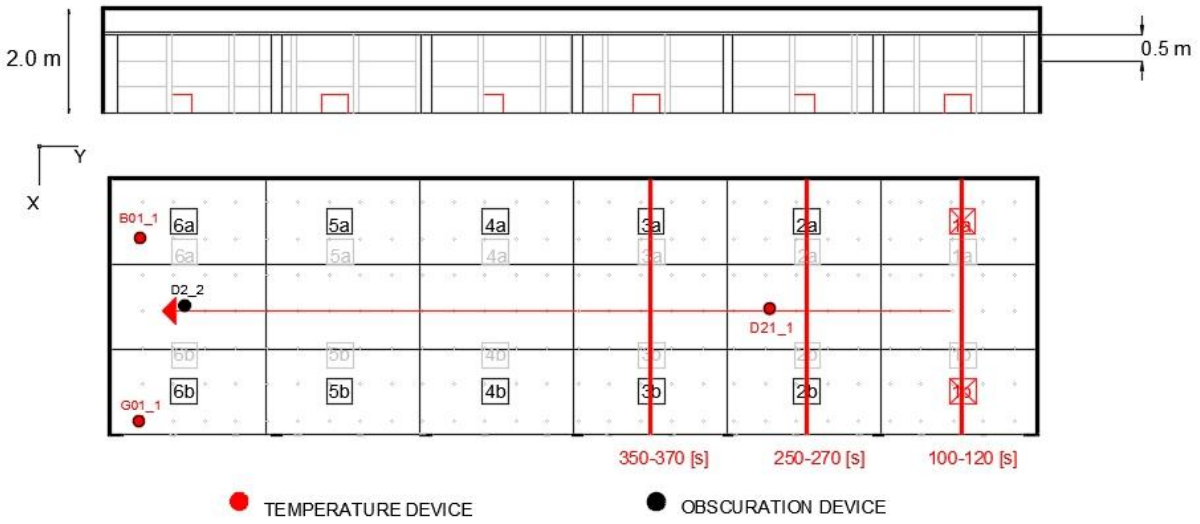

Figure 34 Layout of the ETFT fire test, showing measurement device's locations. The positions of the burners, that are burning during the averaging period 1 (100-120 s), period 2 (250-270 s) and period 3 (350-370 s), are marked with red lines.

Table 11 shows the percentage difference in average temperatures between MZ fire model, FDS and experimental results for a height of 1.6 m up to the ceiling. The table covers three different periods for each measurement position.

Table 11 Percentage difference in average temperatures between MZ fire model, FDS and experiment over the height of 1.6 m at different times (periods) for each measurement position.

	Difference MZ-FDS [%]			Difference MZ-Experiment [%]		
Position	**Period 1**	**Period 2**	**Period 3**	**Period 1**	**Period 2**	**Period 3**
D21_1	3.4	-6.2	-13.7	130	97	82
G01_1	11.1	19.8	27.8	86	91	90
B01_1	9.7	3.0	10.2	111	118	112

Figure 35 compares temperatures from the experiment to the simulation results from MZ fire model and FDS. Only the results from averaging periods 1 and 3 are shown in the Figure 35. The graphs for averaging period 2 are presented in Appendix F. Position D21_1 is located 4 m from the first couple of burners (1a – 1b), whereas positions B01_1 and G01_1 are located 15.5 m from the ignition source. In position D21_1, MZ fire model shows approximately 3 – 14 % temperature differences compared to FDS. Higher percentage differences (14%) for the third period can be explained by proximity to the combustion. In position B01_1, located in the corner, temperatures predicted by MZ fire model are 3 – 10 % higher than those predicted by FDS. Higher differences (11-28 %) are observed at position G01_1 (located close to the openings). Both models significantly overpredict experimental results and temperature measurements are on average 82-130 % higher with MZ fire model compared to the experiments. It is reasonable to expect a better agreement between FDS and experimental results. MZ fire model simulation was run with an extended domain. An attempt was made to model the same scenario without an extended domain. For the results of this simulation compared to a simulation without domain extension see Appendix J.

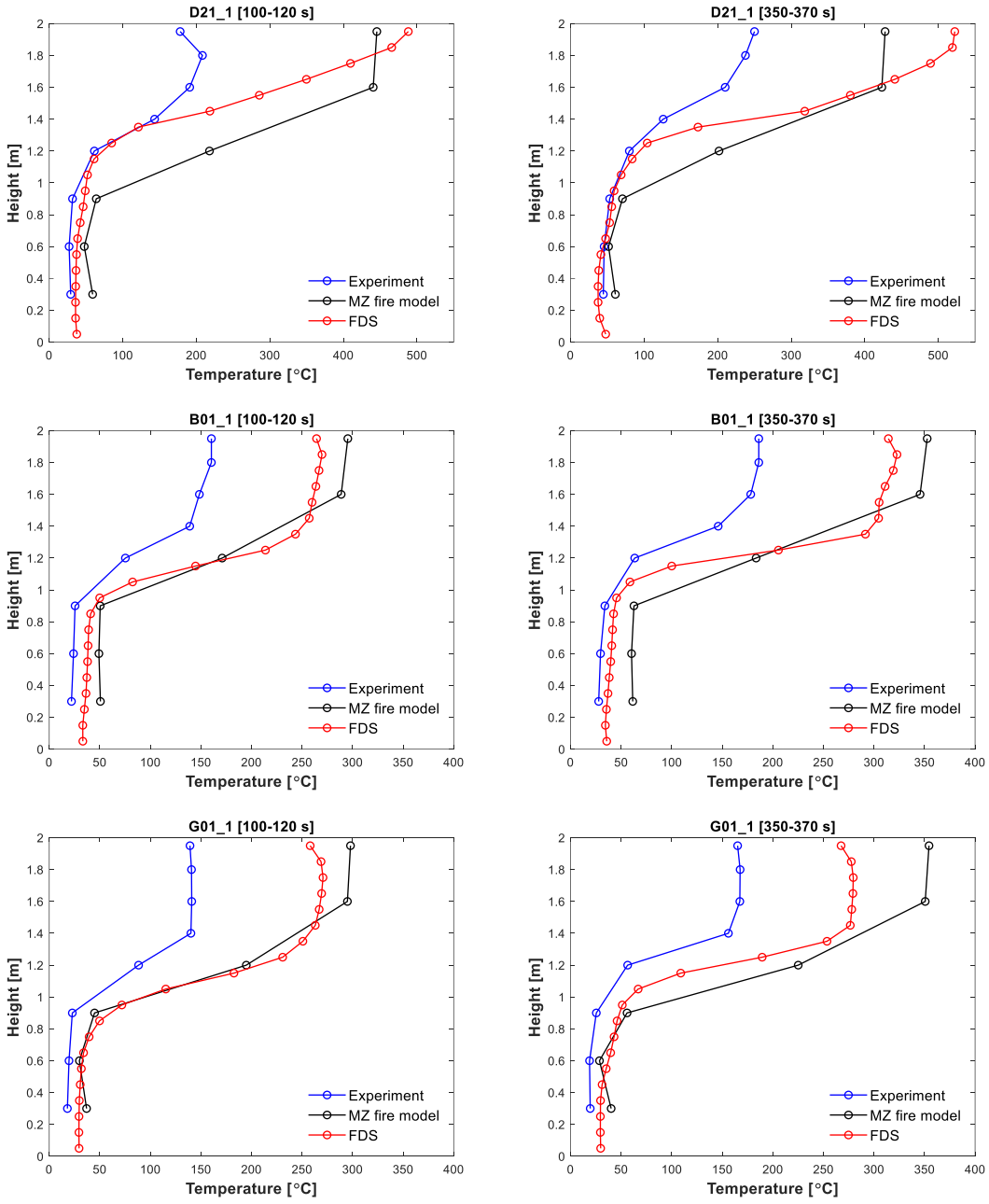

Figure 35 Average temperature profiles over the height of the ETFT fire test compartment for MZ fire model, FDS and the experiment.

The obscuration was predicted using FDS and MZ fire models at different heights in positions D21_1 and D2_2 (see Figure 34). No experimental data on obscuration is available. Figure 36 shows that obscuration results predicted by MZ fire model are similar in position D21_1 to result from FDS at the height of 1.75 m. However, the difference is larger at the lower height (1.25 meters). In position D21_1 at 1.75 m (close to the ignition point) the obscuration peak is reached simultaneously in MZ fire model and FDS. At the height of 1.75 m, overall obscuration results are similar, but FDS shows more fluctuations. Note also that MZ fire model's profile is smoother. The obscuration goes down every 150 s due to the burners being switched off and on. In position D2_2, which is located further away from the burning packages, the results are closer at the 1.25 m height. FDS reaches peak % obscuration faster. Obscuration % was also

plotted for the heights from 0.25 m to 1.75 m (not shown here) indicating large deviations between the two models at the lower heights.

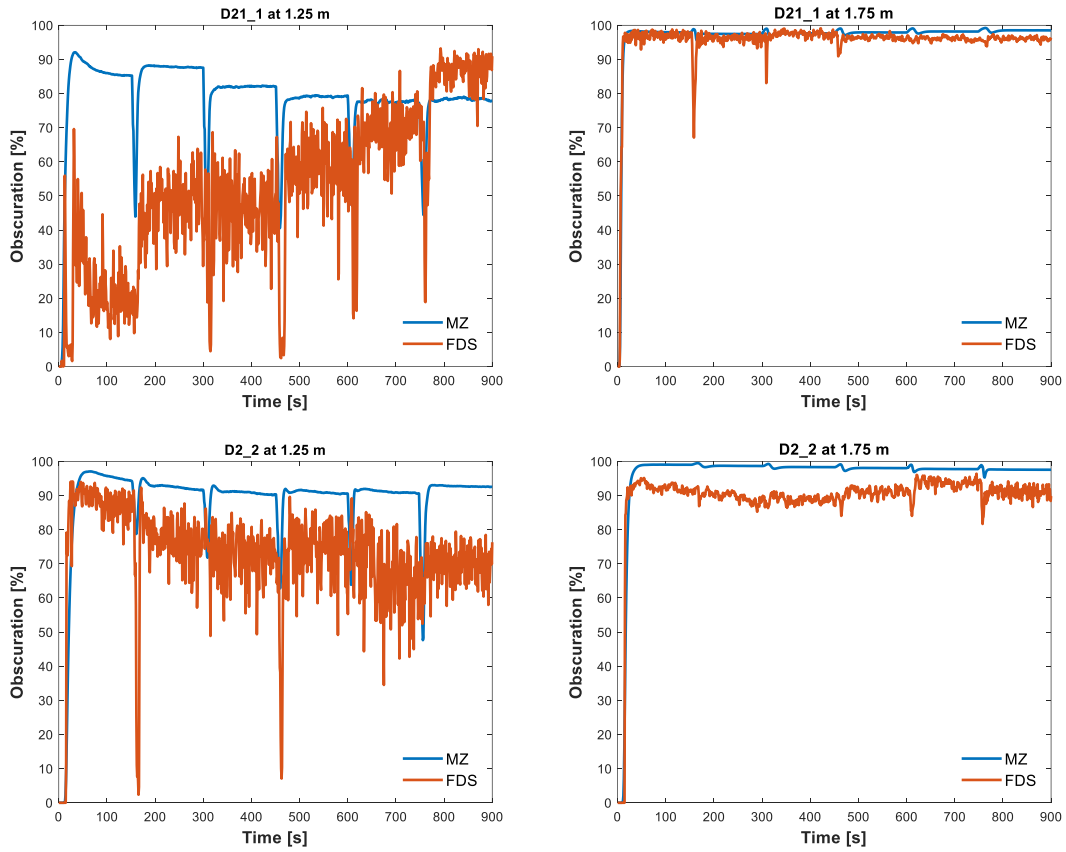

Figure 36 Obscuration comparison for MZ fire model and FDS for positions D21_1 and D2_2, at 1.25 m and 1.75 m heights.

Figure 37 presents comparison of predicted temperatures (MZ fire model and FDS) to temperatures estimated using Alpert's ceiling jet correlation (Karlsson & Quintiere, 2000, p. 156) The distance *r* in Alpert correlation is a constantly changing distance from position B01_1 to the centre of travelling fire. Temperatures between MZ fire model and FDS vary on average 10% until the fire reaches the measurement point, where differences become very large. Alpert correlation temperatures are on average 60-70% lower than FDS temperatures, before the combustion takes place. The Alpert correlation does not lead to accurate results due to the fact that flames may reach the ceiling, which was not the case in Alpert's experiments. Also, the ceiling in ETFT fire test is confined by the walls of the enclosure.

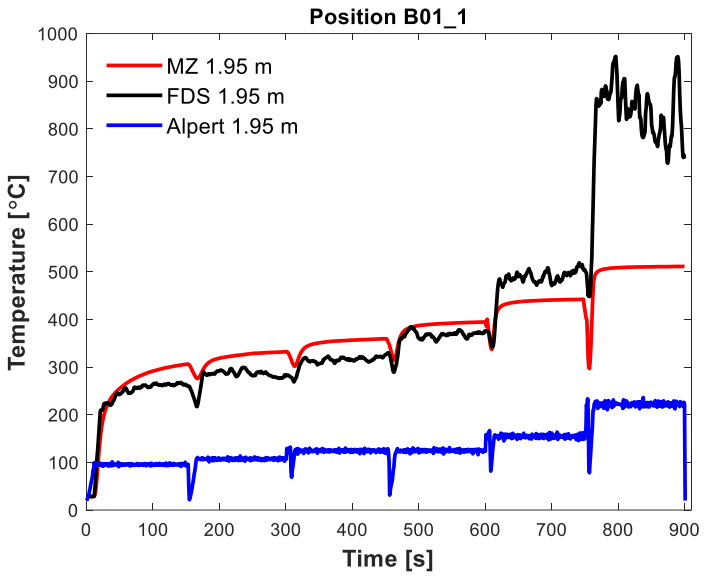

Figure 37 Temperature in position B01_1 at the height of 1.95 m with MZ fire model, FDS and Alpert's correlation.

4.5 Computational time

MZ fire model has a distinct advantage of low computational time in comparison to the FDS simulations. This advantage makes it possible to run the simulations on a personal computer. Previous models used for MZ fire model validations (Johansson, 2021) were run in minutes, but in this study, it took hours to run a simulation (Table 12). It took longer to run the simulations because the computational time depends on dimensions of the enclosure, the fire's characteristics, and boundary conditions. The current simulations used more obstructions and a more fires. For example, extending the domain outside the openings in MZ fire model for the ETFT fire test scenario doubled the computational time from 0.46 to 0.86 hours.

Wall clock time for MZ fire model and FDS is compared in Table 12. The table shows that depending on the scenario, the computational time can be reduced from 10 (the Tisova fire test) to 40 (Supermarket case) times when using MZ fire model. This demonstrates the significant advantage of using MZ fire model for parametric studies. All FDS cases were run on a computer cluster, where each mesh was assigned to an MPI process. MZ fire model simulations were performed on a laptop, powered by an Intel® Core I7 CPU@2.3 GHz. The computational time comparison is not strictly possible because the models were run in a different way, but it is anyway interesting to show the resulting wall clock times for both models.

Table 12 Wall clock time for simulations performed for MZ fire model and FDS.

Simulation	Duration [s]	MZ number of cells	FDS number of cells	MZ fire model Wall Clock Time [h]	FDS Wall Clock Time [h]	Mesh size FDS [cm]	Time [h] FDS/MZ
Office	4712	360	527340	1.4	26.7	20	19
Supermarket	3045	840	2390528	2.6	104.8	20	40
Tisova fire test	6000	240	211090	1.6	15	20	9
ETFT fire test (extended)	900	144	334800	0.86	11.6	10	13.5

5 Discussion

This chapter discusses uncertainties in experiments and models. A discussion on a comparison of temperature and obscuration results between the models and the corresponding experiments is included. Additionally, information is given on the problems that were experienced when working on this thesis. Finally, MZ fire model limitations and recommended further work are discussed.

5.1 Uncertainties in the models and experiments

In this thesis, MZ fire model was tested for fire scenarios in large, well-ventilated spaces. All scenarios included travelling fires, i.e., a fire that spreads throughout a compartment. Four scenarios were evaluated. Two scenarios were prescribed by the user and two were based on previously conducted experiments. All four scenarios were run using both MZ fire model and FDS. Temperature and obscuration measurement devices used in the scenario were placed in the same positions for both models to facilitate comparison of results.

There are different kinds of uncertainties that must be considered. There are user influence uncertainties that can arise from assumptions, errors, and insufficient knowledge (Johansson & Ekholm, 2018). In the experiments, thermal material properties are not always tested or tested in time. One such example is wood moisture content tested after the experiment in the Tisova fire test model. Testing after the experiment showed 16-18% moisture content (MC) instead of the ordered 11%. Measuring procedures of the MC in itself include uncertainties and storage conditions will affect the outcome. Uncertainties can arise from errors in measurements (experimental uncertainty) or from calculated flow properties (model uncertainties). Model uncertainties can be a consequence of boundary conditions or choice of model equations. For example, MZ fire model uses an empirical correlation to model the plume. It also does not model turbulence and the flows are driven by temperature differences. The total uncertainty is a combination of all the above-mentioned factors (user's effect, experimental uncertainties, and model uncertainties).

In many cases, differences between a model and its corresponding experiment are due to uncertainties in the input variables, simplifications in the models and/or lack of information about the experiment. When there is a lack of information for the experiment, it can help to compare MZ fire model to FDS model results. Observed differences are attributable to the inherent difference in the computation method of the model. It is emphasized that MZ fire model is a much simpler model compared to FDS. The more extensive simplifications of the MZ model limit its capability and therefore it is not expected to generate simulations as accurately as an FDS model.

5.2 Experienced problems

Setting up the models (MZ fire model and FDS) based on the experimental data (Tisova and ETFT fire tests) was challenging due to the lack of information about the experiment. It was an additional challenge to adapt the available experimental information to MZ fire model. But an erroneous assumption in a model of an experiment would increase the differences in the results. The descriptions of experiments did not facilitate accurate modelling. It was challenging to represent a continuous bed of wood cribs with discretely located burners, along with fitting the geometry of the building into MZ fire model. Another challenge was to evaluate the design fire

curve, including decisions on how the fire was travelling in the compartment. Without a priori HRR information, there is a room for uncertainty in the output due to user decisions. Information about the travelling fire was particularly challenging to extract from the Tisova fire test papers. As discussed earlier, substantially different information on the flame spread rates, timing of windows closing and usage of accelerators was published in two related papers (Rush, et al., 2021) (Lange, et al., 2018).

To model the ETFT fire test in MZ fire model, several simplifications for the material thermal properties and thicknesses were necessary. These simplifications were needed because MZ fire model crashed when the material properties were assigned as reported in the experiment. The original compartment was made of different sandwich materials that had high insulating properties. When tested using reported conductivity values, the model crashed with negative or very high temperatures in the output. In total, 11 different material settings were tested before the final choice of materials was made. Another challenge was to fit the ETFT test geometry and at the same time keep the burners at the original position. Several attempts were made to divide the domain in the x-direction into 5, 4 and 3 cells while keeping the burners as the location used in the experiment; the attempts were not successful. After multiple attempts to maintain the burners' position, it was decided to move the burners into the centre of the cells. This change likely had some impact the temperature results; however, the magnitude of this difference is not known.

5.3 MZ fire model in large spaces

The first attempt to use MZ fire model for large spaces is reported in (Johansson, 2018), where two fictive cases were modelled using a travelling fire concept. The enclosure for the two fire scenarios was 20 x 32 x 4 m^3 with a single opening (12 x 3 m^2). The fire travelled through four and nine fuel packages. Comparison of MZ fire model simulation with FDS results showed a good agreement for vertical temperatures (20% difference) for the scenario with higher HRR (nine fuel packages burning). MZ fire model was also tested by Waldeck B. (Waldeck, 2020) for a large enclosure fire scenario (60 x 40 x 10 m^3) with one fuel package. Waldeck reported that there was good agreement in general between the models.

Similar to (Johansson, 2018), an attempt was made to compare MZ fire model with FDS using scenarios for large spaces, including an office (40 x 24 x 3 m^3) and a supermarket (60 x 42 x 6 m^3) scenario. This research used a larger number of fuel packages located throughout the space (48 and 40 respectively). In these scenarios the travelling fire was set up based on the predefined ignition time, which was estimated using Modak's equation. Tests were also made to set up the same scenarios based on the ignition temperature. This approach was deemed not possible for MZ fire model due to the very low surface temperatures, compared to FDS.

For the office scenario, some positions and averaging period as predicted by MZ fire model were similar to those predicted by FDS. In other cases, FDS predictions yielded on average 10% higher temperatures. This said, there were higher differences for positions close to the burning packages. This is attributed to the inability to model flame and turbulence in MZ fire model. Whereas FDS can model these parameters in the near field region. It was also clear from the results that temperature measured in the corners of the building were not well represented in MZ fire model. This maybe a result of the openings influence for openings located next to the zone of the measurement. The corner temperatures up to about one meter are rather low.

MZ fire model for the supermarket showed higher temperatures compared to FDS. Differences ranged between 7.3–33 % on average. Despite the greater differences in comparison to the office scenario, the data showed that when looking at heights over 1.75 m and distances over 15 m from the fire, the differences between average temperatures become relatively small.

5.4 MZ fire model comparison to experiments

There is a lack of experimental data on large-scale fires, suitable for MZ fire model validation. In the previous work (Johansson, 2021), several comparisons with well-known validation cases were performed. These cases included the International Fire Model Benchmarking and Validation Exercise #3 (21.7 x 7 x 3.8 m^3), Murcia Fire Test (19.5 x 19.5 x 20 m^3), PolyU/USTC Atrium (22.4 x 11.9 x 27 m^3) (McGrattan, 2007). As a result of this study, a good correspondence between FDS and MZ fire model was observed (5% difference), with larger deviations compared to the experiments (10% difference).

For this thesis, two cases on experiments with travelling fires were found: the Tisova fire test (18 x 15 x 4 m^3) and the ETFT fire test (17.8 x 4.9 x 2 m^3). The former fire test used wood cribs, and the latter had a series of tests with propane burners. There were several challenges in setting up simulations for these experiments, described in the Section 6.2. These tests are more challenging to model, compared to the cases tested previously in (Johansson, 2021). Namely, it is more difficult to get the temperatures right when the fire is moving, and also when the ceiling heights are as low as in the ETFT test (2 m). Temperature results for both Tisova and ETFT models with MZ fire model had large differences compared to the experimental results.

The Tisova fire test results were on average 4-80 % higher in FDS than in MZ fire model. The differences between experimental results and MZ fire model were very large (0-148%). Only position 1 have shown comparable results between FDS and MZ fire model, which can be due to very low temperatures measured in the far field positions, because the settings in both programs were identical. In general, Tisova model had a large number of uncertainties, but also, it had to be limited in simulation duration, due to the change in ventilation conditions. The fire growth during this time was very slow, and there were a lot of uncertainties in how such slow travelling fire could be modelled. In hindsight, an alternative design fire could be tested in MZ fire model. Instead of discrete fuel packages, a burner covering the same area as the cribs can be tested. The peak HRR and the HRR curve, will therefore have to be updated. As for the current attempt, it is questionable on whether a pallet stack of such a low height, is a good estimate of HRR. More information on HRR would be of a large help for modelling purposes. An extension of domain outside the openings was tested for the current Tisova model, which showed insignificant temperature differences in a few positions, but doubled the computational time.

In the ETFT fire test, both FDS and MZ fire model over-predicted temperatures reported in experiment significantly (MZ fire model showed 82-130 % higher temperatures), whereas differences between MZ fire model and FDS results on average varied between 3–28 %. FDS predictions were closer to the experiment. The reason behind such a large discrepancy between the models and the experiment is not known. Some of the causes can be in the difference of material properties or in the change of the burners location. MZ fire model did not allow for modelling of obstructions with thermal properties, as reported in the experiment. This can also be the reason why FDS predictions are not as close to experiment as expected, the choice of

material properties was set in FDS, as in MZ fire model. The HRR was compared after running both programs, with the rest of the setting being identical (see Appendix I).

As for Tisova fire model, no similar problems were encountered with materials properties where concrete core was tested in the laboratory prior to experiment. Some uncertainty is still possible with masonry properties that were taken from (Degler & Eliasson, 2015) because data from reports were not available. A minor change was made to an opening (made 12 cm smaller) in order to fit the geometry into MZ fire model. This change should not have a large impact on temperatures, because the window is located far from the fire source. Not modelling the continuous fuel bed, used in the experiment can be argued to cause large differences between the models and the experiment.

5.5 Obscuration

The obscuration prediction can be used for comparison to a predefined performance criterion in Performance-Based Design. MZ fire model has the capability of measuring the obscuration based on the species concentration. No visibility or obscuration data was available from the experiments (Tisova and ETFT); therefore, a comparison was made only between MZ fire model and FDS. For this purpose, a "path obscuration" device was used in FDS to measure obscuration along the length of a corresponding MZ fire model cell.

By default, FDS generates the smoke in proportion to the HRR (McGrattan, et al., 2019). In this way, soot yield defines the density of soot being transported to the cells. FDS obscuration calculation has been verified (McGrattan & et.al., 2019) and validated (McGrattan, et al., 2020). Obscuration predictions by FDS for wood has been reported to overpredict the experimental results (Rinne, et al., 2007).

Waldeck B. (Waldeck, 2020) made the first comparison of obscuration between MZ fire model and FDS. It was done by converting the obscuration into a visibility value, and then comparing to the visibility output from the FDS simulation. The results reported in (Waldeck, 2020) show a visibility difference of a few meters for some tests and greater differences for a wide enclosure (38 x 38 m^2). This comparison is problematic because conversion of obscuration to a visibility value is not assured of being conducted in exactly the same manner.

In this thesis, the results of obscuration showed a decreasing difference with increasing measurement height (i.e., closer to the ceiling). Also, smaller differences were noted further away from the combustion zone. However, in such positions the results were quite similar. As for the experimental cases, where the differences between FDS and MZ fire model were larger (i.e., Tisova fire), the obscuration differences were also larger, even at heights close to the ceiling. In the models that were well defined, such as the office and supermarket cases, the smoke layer descending time differed. Sometimes the smoke layer descended faster in FDS and other times faster in MZ fire model. The reasons for this result can be traced back to the model differences, specifically zone sizes. It is, therefore, possible that the differences might be smaller if the zone size in the z-direction is decreased.

Overall, the average obscuration value (taken in the zone at a height of 0.5 m and width of 6 x 6 m) will not be the same as an average value taken along a path of 20 cm in FDS cells. There will be differences even if the path obscuration (in FDS) is measured in the same position and is the same length as the size of one cell in MZ fire model. The differences are especially

apparent when the smoke is descending past the measurement position in both models. It can also be argued that, when using hydrostatic pressure difference and no turbulence modelling, the plume spread in the horizontal direction can give additional clues to the difference in results.

5.6 MZ fire model limitations and further work

This research included comparisons between MZ fire model and FDS. Clearly, MZ fire model has certain inherent limitations compared to a CFD model developed in FDS. Some of the limitations are obvious, such as the larger cell size in MZ fire model. This limitation can make the geometry fitting quite challenging. This constraint repeatedly caused difficulties when trying to closely simulate the geometry reported in experiments. For example, it was not feasible to accurately model numerous fine obstructions, such as the many different dimensions of the down-stands in the Tisova fire. These inaccuracies potentially have an impact on smoke dynamics. Another limitation is that MZ fire model cannot be used to model under-ventilated fires. For this reason, the Tisova fire model had to be limited in time due to changes in ventilation conditions. These limitations were apparent from beginning of this project. There are also several other limitations, that have been encountered during the course of this work.

It was challenging to fit a simple rectangular compartment geometry from the ETFT experiment into MZ fire model. The cells were chosen in order to keep the burners' position in the middle of the cells as much as possible, even though this is not a limitation in the program. To make this possible, a larger number of smaller cells is needed; however, there is a maximum limit to the number of cells possible. This maximum limit was reached by a division of the height in 6 cells and the length in 6 cells. These limits may be dependent on the openings height. In this case, it is concluded that the maximum number of cells in the z-direction for an opening is 5. The flow in a zone can only have one direction when positioned flush with an opening. This said, having lower number of cells at the opening can make it difficult to capture the flow.

Other limitations of MZ model worth mentioning for future research are the use of ramp functions and the definition of openings. An attempt was made to represent the decay phase using multiple ramps in MZ fire model, but it is not possible to assign individual ramps for each fuel package in the current program version. When defining an opening in MZ fire model, the rule is to avoid multiple openings in a single cell. This proved especially important because the cells in MZ fire model can be quite large (e.g., 6 x 6 m^2) and can contain two closely positioned windows.

Another challenge was to represent a well-insulated boundary condition in the ETFT experiment. Using the actual experimental thermal material properties resulted in a program crash. This can be explained by the number of nodes in the boundaries being very high for an insulator with a low conductivity, and by the thickness of an obstruction. The more nodes there are, the more calculations that are needed in each time step. This was discovered to cause a problem with an insulated floor and ceiling in the simulations of the ETFT test. The heat transfer has to be regulated and the number of nodes in the boundaries limited. Users are cautioned to carefully consider trade-offs by making obstructions thinner and adjusting insulation properties.

There is no straight forward way to determine the size of MZ fire model cells. It is suggested in (Johansson, 2020) to use a cell size that is large enough to cover the plume. An attempt was made in this thesis research to follow this advice. A well-designed sensitivity study for MZ fire

model cell size would provide helpful guidance to future users. Additionally, a parameter study could be performed to see how the changes in HRR magnitude, thickness of the boundaries, and thermal properties influence the computational time. During the work on this thesis, some tests were done with a total HRR of 80 MW, which was accomplished by included more fires. Predictably, this resulted in a very slow calculation that ran for several hours. The slower computation can be explained by the time-consuming heat transfer calculations. Performing sensitivity and parameter studies would be valuable for future users.

Within this research effort, an attempt was made to find a suitable large-scale experiment with a travelling fire. Experiments often use wood cribs to model a fire, but an accurate representation of such an experiment is challenging because of difficulties in accounting for the fire spread. For future work, it would be advantageous to perform large-scale experiments in conjunction with development of MZ fire models, thereby affording opportunities to minimize difference between the experimental setup and MZ fire model.

Based on the current work, further development of MZ fire model may include adjustments in node resolution for conduction modelling. This will expand the capabilities for modelling insulating material types and sizes. Another possible improvement could be implementation of interpolation of cell values for the output of devices, similar to FDS. Moreover, MZ model can potentially be used in the inversed recovery methodology (Overholt & Ezekoye, 2012) to search for HRR satisfying the temperature data available. A G.U.I (graphical user interphase) would help users with the simulation setup. This could potentially be implemented in SmokeView. Additionally, development of a ramp function would help to better represent experimental HRRs. Ultimately, MZ fire model can be developed to predict near field temperatures with a suitable sub-model.

6 Conclusion

This thesis compared the predictive capabilities of MZ fire model to that of a comparable FDS model. The comparisons were done using two fictive fire scenarios that were designed to represent fires in large space, i.e., office and supermarket. Additionally, MZ fire model was compared to test results from two live-fire experiments (the Tisova and ETFT fire tests). Due to the high number of experimental uncertainties, MZ fire model was also compared to FDS models for the experiments. The study focused on large space compartments, where the fire results is a fuel-limited travelling fire (i.e., a fire that does not flash over) The temperature and obscuration results from MZ fire model were compared for the four different scenarios.

The temperature results with the design fire scenarios (office and supermarket) show good agreement between MZ fire model and FDS (on average 10% differences in the office scenario and 7.3–33 % differences in the supermarket scenario). The differences are higher than in the previously reported cases, which is attributed to several factors, including the numerous uncertainties and higher HRR in combination with accuracy limitations for modeling a travelling fire. Comparison to the ETFT experiment resulted in similar temperature differences between the models (3–28 %), but larger differences between MZ fire model and the experimental results (82–130 %). The Tisova fire test results had larger temperature differences in general, which indicates that experimental conditions were not successfully represented. Alpert's correlations showed on average 40-70 % lower temperatures than MZ fire model and FDS, mainly due to the unconfined enclosure assumption. A way to improve the results accuracy in MZ fire model is to divide the domain in z-direction in a larger number of cells. Larger number of cells at the openings can potentially improve the temperature predictions.

The obscuration results showed larger differences on the lower heights and better agreement at heights near the ceiling. The reasons for these differences are in the size of the cells, where the obscuration is measured and averaged. Some other reasons may include the differences in modelling, i.e., the use of static pressure lines for the horizontal smoke movement and no turbulence modelling. For these reasons, using obscuration results from MZ fire model for tenability purposes is not advisable. Further refinements to MZ model and modelling process are necessary before this tool is viable for actual production work.

This thesis has shown that despite conceptually significant differences on how FDS and MZ fire models calculate temperatures, MZ fire model gives reasonably good predictions of far-field temperatures, provided that scenarios are similarly well-defined.

Multiple tests of MZ fire model have revealed areas for future development and testing, as well as exposing problems with lack of reliable and clear information for modelling of experiments on travelling fires. This study has also shown that there are great advantages of MZ fire model, most notably the substantially shorter computational time and the simplicity of use.

Fire safety engineers already familiar with FDS can use the MZ fire model with little additional training; the modelling concepts are similar, as is the general process. There are several important aspects regarding the setting up the zones that needs to be considered for the current version of the MZ fire model:

- number of cells spanning the height of an opening has to be as large as possible;
- the maximum number of openings placed in a cluster of cells in z-direction is one;

- the measurement devices and a fire vent should not be placed on the cell boundaries;
- the maximum number of fire vents in a zone is one;
- the minimum number of cells in each domain's direction is 3;
- materials with low conductivity (< 0.02 kW/mK) can cause problems, and therefore needs to be tested;
- thermal thickness of material, high HRR may influence the computational time.

Notwithstanding the problems in validation, the comparison with FDS offers valuable insights into the capabilities of the MZ fire model. It has the potential to be an effective engineering tool for parametric studies and a priori testing for large scale experiments with travelling fires.

7 References

Anderson, J. et al., 2020. *FDS simulations and modelling efforts of travelling fires in a large elongated compartment.* s.l., s.n.

Arvidson, M., 2005. *Potato Crisps and Cheese Nibbles Burn Fiercely,* s.l.: Brandposten .

Babrauskas, V., 1986. Free Burning Fires. *Fire Safety Journal,* 11(1-2), pp. 35-51.

Babrauskas, V., 2014. *Ignition Handbook.* London: Fire Science Publishers.

Bong, W. J., 2011. *Limitations of zone models and CFD models for natural smoke filling in large spaces,* Christchurch: University of Canterbury.

BSI, P. 7.-1., 2003. *Application of fire safety engineering principles to the design of buildings. Part 1,* s.l.: s.n.

CEN, 2004. *Eurocode 1: Actions on structures Part 1-2: General actions - Actions on structures exposed to fire,* s.l.: CEN.

Chaipanich, A. & Chindaprasirt, P., 2015. *The properties and durability of autoclaved aerated concrete masonry blocks,* s.l.: Elsevier.

Chow, W., 1996. Multi-Cell concept for simulating fires in big enclosures using a Zone Model. *Journal of fire sciences,* Volume 14.

Clifton, G. C., 1996. *Fire Models for Large Firecells.* HERA Report R4-83 c a cura di s.l.:HERA.

Czajkowski, L., Olek, W., Weres, J. & Guzenda, R., 2015. Thermal properties of wood-based panels: specific heat determination. *Wood Sci Technol,* Volume 50, p. 537–545.

Daia, X., W. S. & Usmani, A., 2017. A critical review of “travelling fire” scenarios for performance-based structural engineering. *Fire safety journal,* Volume 91, pp. 568-578.

Dai, X., Weich, S. & Usmani, A., 2018. *Structural implications due to an extended travelling fire methodology (ETFM) framework using SIFBuilder.* s.l., s.n.

Dai, X., Welch, S. & Usmani, A., 2017. A critical review of “travelling fire” scenarios for performance-based structural engineering. *Fire Safety Journal,* Volume 91, pp. 568-578.

de Korte, A. & Brouwers, H., 2009. *Thermal Conductivity of Gypsum Plasterboard, At ambient temperature and exposed to fire,* s.l.: Czech Technical University of Prague.

Degler, J. & Eliasson, A., 2015. *A Priori Modeling of the Tisova Fire Test in FDS,* s.l.: s.n.

Degler, J. & Eliasson, A., 2015. *ltu.diva-portal.org.* [Online]
Available at: http://ltu.diva-portal.org/smash/get/diva2:1025534/FULLTEXT02.pdf
[Consultato il giorno 01 March 2021].

DiNenno, P. J., 2002. *Handbook of Fire Protection Engineering.* Third Edition a cura di s.l.:SFPE.

Drysdale, D. D., 2010. *An introduction to fire dynamics.* Third Edition a cura di s.l.:Wiley.

E1355-12, A., 2018. *Standard Guide for Evaluating the Predictive Capability of Deterministic Fire Models,* s.l.: ASTM.

Engineering ToolBox, 2003. *Specific Heat of Food and Foodstuff.* [Online]
[Consultato il giorno 25 February 2021].

EU, 2010. *Directive 2010/31/EU of the European Parliament and the Council of 19 May 2010 on the energy performance of buildings.* Bruxelles: Off. J. Eur. Union 13.

Gottfried, J. S. & Rein, G., 2012. Travelling fires for structural design - Part I: Literature review. *Fire Safety Journal,* Volume 54, pp. 74-85.

Hamins, A. et al., 2005. *Experiments and Modeling of Multiple Workstations Burning in a Compartment,* s.l.: NIST.

Hidalgo, J. P. et al., 2017. An experimental study of full-scale openfloor plan enclosure fires. *Fire safety journal,* Volume 89, pp. 22-40.

Hidalgo, J. P. et al., 2018. *Edinburgh Tall Building Fire Tests [dataset],* Edinburgh: University of Edinburgh.

Hidalgo, J. P. et al., 2019. The Malveira fire test: Full-scale demonstration of fire modes in open-plan compartments. *Fire Safety Journal,* Volume 108.

Hietaniemi, J. & Mikkola, E., 2010. *Design Fires for Fire Safety Engineering,* s.l.: JULKAISIJA - UTGIVARE.

Hua, J., Wang, J. & Kumar, K., 2005. Development of a hybrid field and zone model for fire smoke propagation simulation in buildings. *Fire Safety Journal,* Volume 40, pp. 99-119.

Hurley, M. J., 2016. *SFPE handbook of fire protection enginering.* 5 a cura di s.l.:Springler.

Iqbal, N. & Salley, M., 2004. *Quantitative Fire Hazard Analysis Methods for the U.S.Nuclear Regulatory Commission Fire Protection Inspection Program,* Washington, DC: NUREG.

Johansson, N., 2017. *Estimating gas temperatures in large enclosures.* Lund, Lund University.

Johansson, N., 2018. *A case study of Far-Field Temperatures in Progressing Fires.* s.l., s.n.

Johansson, N., 2020. *Multi Zone Fire Model.* [Online]
Available at: https://mzfiremodel.com/
[Consultato il giorno 2021].

Johansson, N., 2020. *Multi-Zone Fire Model – General Documentation and Users Guide.* Lund: s.n.

Johansson, N., 2021. Evaluation of a zone model for fire safety engineering in large spaces [in press]. *Fire Safety Journal*.

Johansson, N. & Ekholm, M., 2018. Variation in Results due to User Effects in a Simulation with FDS. *Fire Technology,* Volume 54, pp. 97-116.

Johansson, N., Wahlqvist, J. & Van Hees, P., 2013. *Simple Ceiling Jet Correlation Derived from Numerical Experiments.* Lund, Lund University.

Karlsson, B. & Quintiere, J., 2000. *Enclosure fire Dynamics.* Boca Raton: CRC Press.

Kirby, B. R. et al., 1999. Natural fires in large scale compartments. *International Journal on Engineering Performance-Based Fire Codes,* 1(2), pp. 43-58.

Lange, D., Rush, D., Dai, X. & Boström, L., 2018. *The Tisova fire test part 1: test report,* s.l.: RISE.

Lonnermark, A. & Bjorklund, A., 2008. *Smoke Spread and Gas Temperatures during Fires in Retails Premises - Experiments and CFD Simulations,* s.l.: SP Technical Research Institute of Sweden.

Madrzykowsky, D., 2012. *Unpublished test results,* s.l.: s.n.

McGrattan, K., 2007. *Verification and Validation of Selected Fire Models for Nuclear Power Plant Applications Volume 7: Fire Dynamics Simulator (FDS),* Rockville: NUREG.

McGrattan, K., Baum, H. & Rehm, R., 1998. Large Eddy Simulations of Smoke Movement. *Fire Safety Journal,* Volume 30, pp. 161-178.

McGrattan, K. B., Bouldin, C. & Forney, G. P., 2005. *Computer Simulation of The Fires in the World Trade Center Towers,* s.l.: NIST.

McGrattan, K. & et.al., 2019. *Fire Dynamics Simulator Technical Reference Guide Volume 2: Verification, NIST Special Publication 1018-2,* Gaithersburg, Maryland, USA: National Institute of Standards and Technology.

McGrattan, K. et al., 2019. *Fire dynamics simulator user's guide.* s.l.:NIST.

McGrattan, K. et al., 2020. *Fire Dynamics Simulator Technical Reference Guide Volume 3: Validation.* 6 a cura di s.l.:NIST Special Publication 1018-3.

Nishino, T. & Kagiya, K., 2019. A multi-layer zone model including flame spread over linings for simulation of room-corner fire behavior in timber-lined rooms. *Fire Safety Journal,* Volume 110.

NRC, 2007. *Verification and Validation of Selected Fire Models for Nuclear Power Plant Applications ,* Washington D.C.: NUREG-U.S. Nuclear Regulatory Commission.

NUREG, 2012. *Nuclear Power Plant Fire Modeling Analysis Guidelines,* Washington D.C.: U.S.NRC.

Ohllemiller, T. et al., 2005. *Fire tests of single office workstations,* s.l.: NIST NCSTAR 1-5C.

Overholt, K. J. & Ezekoye, O. A., 2012. Characterizing heat release rates using an inverse fire modeling technique. *Fire Technology,* Volume 48, pp. 893-909.

Peacock, R. D., Forney, G. P. & A, R. P., 2021. *CFAST - Consolidated Fire and Smoke Transport (Version 7) Volume 3: Verification and Validation Guide,* s.l.: NIST.

Pope, S. B., 2000. *Turbulent Flows.* s.l.:Cambridge University Press.

Rackauskaite, E., Hamel, C., Law, A. & Rein, G., 2015. Improved Formulation of Travelling Fires and Application to Concrete and Steel Structures. *Structures,* Volume 3, pp. 250-260.

Rein, G. et al., 2007. Multi-storey fire analysis for high-rise buildings. *11th Interflam,* pp. 605-616.

Rinne, T., Hietaniemi, J. & Hostikka, S., 2007. *Experimental Validation of the FDS Simulations of Smoke and Toxic Gas Concentrations,* s.l.: VTT Technical Research Centre of Finland.

ROCKWOOL, 2021. *Beamclad thermal property.* [Online]
Available at: https://www.rockwool.com/uk/products-and-applications/product-overview/fire-protection-solutions/beamclad-en-gb/?selectedCat=downloads
[Consultato il giorno 20 march 2021].

ROCKWOOL, s.d. *Rockroof flexi plus.* [Online]
Available at: https://www.rockwool.be/producten/hellend-dak/rockroof-flexi-plus/
[Consultato il giorno March 2021].

Rush, D., Dai, X. & Lange, D., 2020. *Tisova Fire Test Data, [dataset],* Edimburgh: University of Edinburgh. School of Engineering.

Rush, D., Dai, X. & Lange, D., 2021. Tisova Fire Test - Fire behaviours and lessons learnt. *Fire Safety Journal,* 121(103261), pp. 0379-7112.

Stern-Gottfried, J. et al., 2016. A Performance Based Methodology Using Travelling Fires for Structural Analysis. *SFPE.*

Stern-Gottfried, J. & Rein, G., 2012. Travelling fires for structural design–Part I: Literature review. *Fire Safety Journal,* Volume 54, pp. 74-85.

Stern-Gottfried, J., Rein, G., Bisby, L. A. & L, T. J., 2010. Experimental review of the

homogeneous temperature assumption in post-flashover compartment fires. *Fire safety journal,* Volume 45, p. 249–261.

Sun-Yeo, M., Cheol-Hong, H. & Sung-Chan, K., 2019. CO and Soot Yields of Wood Combustibles for a Fire Simulation. *Fire Science Engineering,* 33(1), pp. 76-84.

Suzuki, K., Tanaka, T., Harada, K. & Yoshida, H., 2004. *An application of Multi-Layer Zone Model to a tunnel fire..* Daegu, Korea, 6th Asia-Oceania Symposium on Fire Science and Technology.

Suzuki, K., Tanaka, T., Harada, K. & Yoshida, H., 2004. Prediction model for vertical gas temperature distribution in spaces involved in fire. Development of multi-layer zone smoke movement model Part 1. *J. Environ. Eng.,* Volume 590, pp. 1-7.

Suzuki, K., Tanaka, T., Harada, K. & Yoshida, H., 2005. Improvement and verification of prediction model for vertical distribution of gas temperature and concentrations in fire compartment, and calculation of ceiling jet temperature considered entrainment of gas to fire plume. Part 2. *J. Environ.E.,* pp. 1-7.

SYKTYVKAR, s.d. *Handbook SyPly.* [Online]
Available at: https://www.syply.com/syply/birch/

Tewardson, A., 1995. *SFPE Handbook of Fire Protection Engineering.* 2nd a cura di s.l.:Springer.

Torero, J., Majdalani, A., Abecassis-Empis, C. & Cowlard, A., 2014. Revisiting the Compartment Fire. *Fire Safety Science,* Volume 11, pp. 28-45.

Tuomo, R., Hietaniemi, J. & Hostikka, S., 2007. *Experimental Validation of the FDS Simulations of Smoke and Toxic Gas Concentrations,* Espoo: VTT.

Waldeck, B., 2020. *A Comparison Between FDS and the Multi-Zone Fire Model Regarding Gas Temperature and Visibility in Enclosure Fires,* s.l.: s.n.

Xiaojun, C., Lizhong, Y., Zhihua, D. & Weicheng, F., 2005. A multi-layer zone model for predicting fire behaviour in a fire room. *Fire Safety Journal,* Volume 40, pp. 267-281.

Yudong, L. & Drysdale, D., s.d. Measurement of the Ignition Temperature of Wood. *IAFSS,* pp. 380-385.

8 Appendices

Appendix A: Sensitivity analysis

FDS uses large eddy simulation (LES), and it is therefore important to perform a cell sensitivity analysis. As a first rough estimate, cell size should fall into an inertial subrange of the energy spectrum. The following expression can be used (Pope, 2000, p. 184):

$$l_{EI} = \frac{l_0}{6} \qquad \text{Equation 3}$$

where l_{ei} is the inertial subrange length scale, and l_0 is the characteristic length scale of the largest eddies. Using the equation above, taking l_0 as the burner dimension (2.4 m – office and 1.6 m – supermarket), resulting in l_{ei} for the office - 0.4 m and for the supermarket – 0.26 m. Another rough measure for the cell size can be made using a ratio between characteristic fire diameter and nominal cell size D^*/δ_x, with D^* is defined as (McGrattan, et al., 2019):

$$D^* = \left(\frac{\dot{Q}}{\rho_\infty \cdot T_\infty \cdot c_p \cdot \sqrt{g}}\right)^{\frac{2}{5}} \qquad \text{Equation 4}$$

where $\dot{Q}$ is the heat release rate [kW], ρ_∞ is the ambient air density [1.204 kg/m^3], T_∞ is the ambient temperature [293 K], c_p is the heat capacity [1.005 kJ/kgK] and g is the gravity [9.81 m/s^2].

The D^*/δ_x can be calculated as a function of time for three different cell sizes (0.2, 0.1 and 0.05 m) that have been chosen based on the preliminary analysis made above. This points at the fact that the first choice of cell size should not exceed 0.24 m. Figure 38 shows the results, which imply that the initial choice of mesh size for the burning process may be considered too large. After 1500 s, the ratio D^*/δ_x fluctuates on a fixed level, following the HRR. The values for the ratio D^*/δ_x at that time are 15.9, 31.8 and 63.7 for mesh sizes of 0.2, 0.1 and 0.05 m respectively.

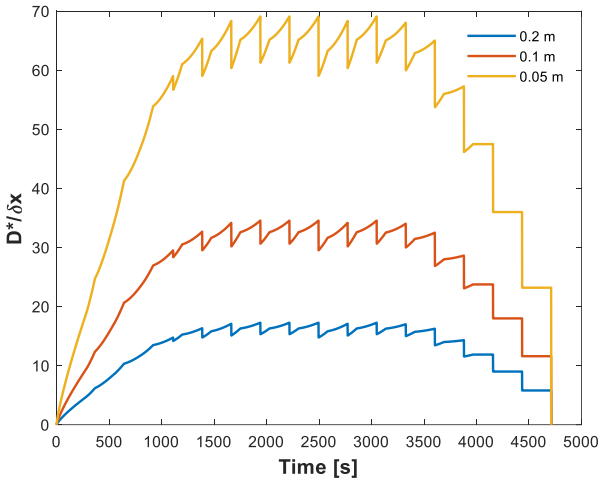

Figure 38 Non-dimensional ratio changes with the time for three mesh sizes: 0.2, 0.1 and 0.05 m.

Table 13 below provides an overview of mesh sizes used in the sensitivity study for the office scenario and the non-dimensional ratio D^*/δ_x at 300 s.

Table 13 Mesh sizes used in the cell sensitivity study for the office scenario.

Case	D^*	Name	Mesh size [m]	D^*/δ_x at 300 s	Total number of cells (whole domain)	Total number of cells (half domain)	Wall clock time (whole domain) [days]	Wall clock time (half domain) [h]
Office	2.4	Coarse	0.2	5	493 680	250 920	3	30
		Moderate	0.1	10	3 949 440	1 974 720	16	195
		Fine	0.05	20	31 595 520	15 797 760	151	1814

The size of the compartment is a challenge for the sensitivity study because of the high computational cost. The total number of cells for the office compartment with different mesh sizes is shown in the Table 13 above. To simplify this, the domain is divided into two parts on the y-axis symmetry. Thus, only the left part is modelled for the sensitivity study (Figure 39). This facilitates a substantial computational saving, as seen in Table 13. The clock time for the 5 cm simulation is estimated using linear interpolation because it was only modelled up to 1102 s, which took 7 weeks on 6 MPI processes. The total number of cells is slightly higher than half of the total number due to the extension of the domain outside the centre of the building to facilitate free smoke flow. The devices that are used for the sensitivity study are marked on Figure 39 below. The ignition position is marked with a red cross and the fire front times are marked with a red line.

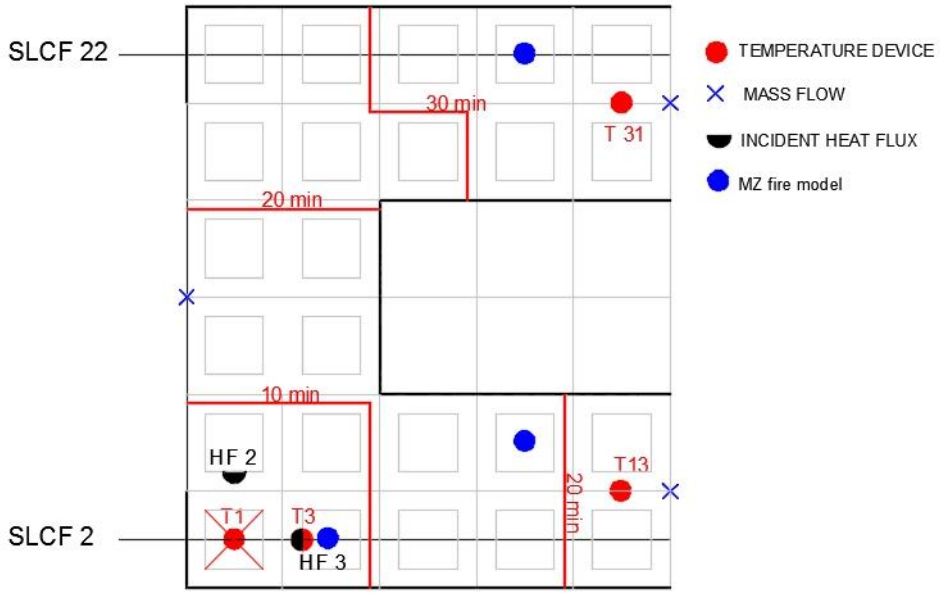

Figure 39 Device positions and the domain simplification used in sensitivity study. It shows temperature (red), mass flow and heat flux measurement positions. SLCF denotes positions of slices, made for both temperature and velocity.

Figure 40 shows the temperature profiles, averaged between 1440 to 1460 s of simulations for two meshes: 20 and 10 cm. The averaging differs slightly between the two meshes due to the differences in time steps. Temperatures in all four locations (T1, T3, T13 and T31, see Figure 39) show good agreement above a height of 1.5 m. The best agreement is achieved for position T31, which is located 32 m away from the initial ignition source, (Figure 39). The highest differences are at position T1, where ignition takes place. This shows that the prediction for far

field regions have reasonable agreement for both, 20 and 10 cm mesh.

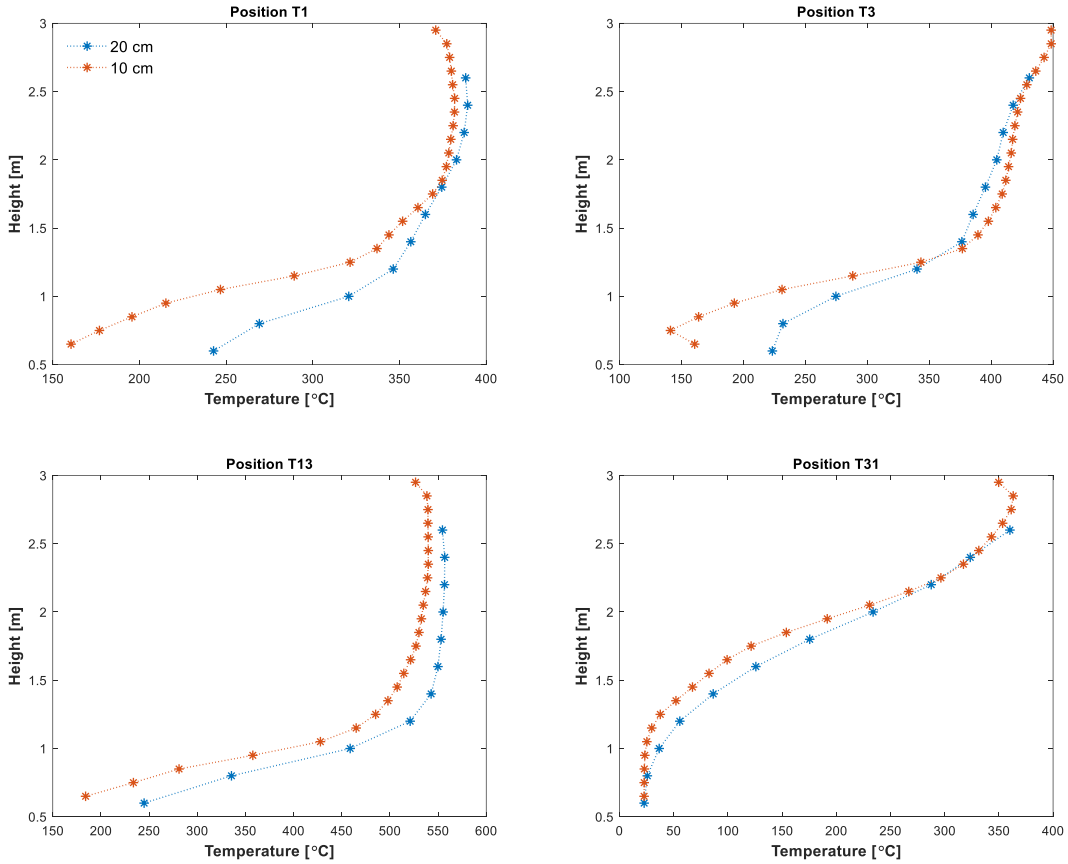

Figure 40 Comparison of average temperatures in FDS for mesh sizes of 20 and 10 cm for positions shown in Figure 39.

Figure 41 shows instantaneous temperature slices for 20 cm (a), 10 cm (b) and 5 cm (c) in the position marked as SLCF 2 in Figure 39 at the time of 1102 s. This slice shows that the 20 cm (a) mesh fails to capture the detailed fire dynamics, but nonetheless shows reasonable predictions.

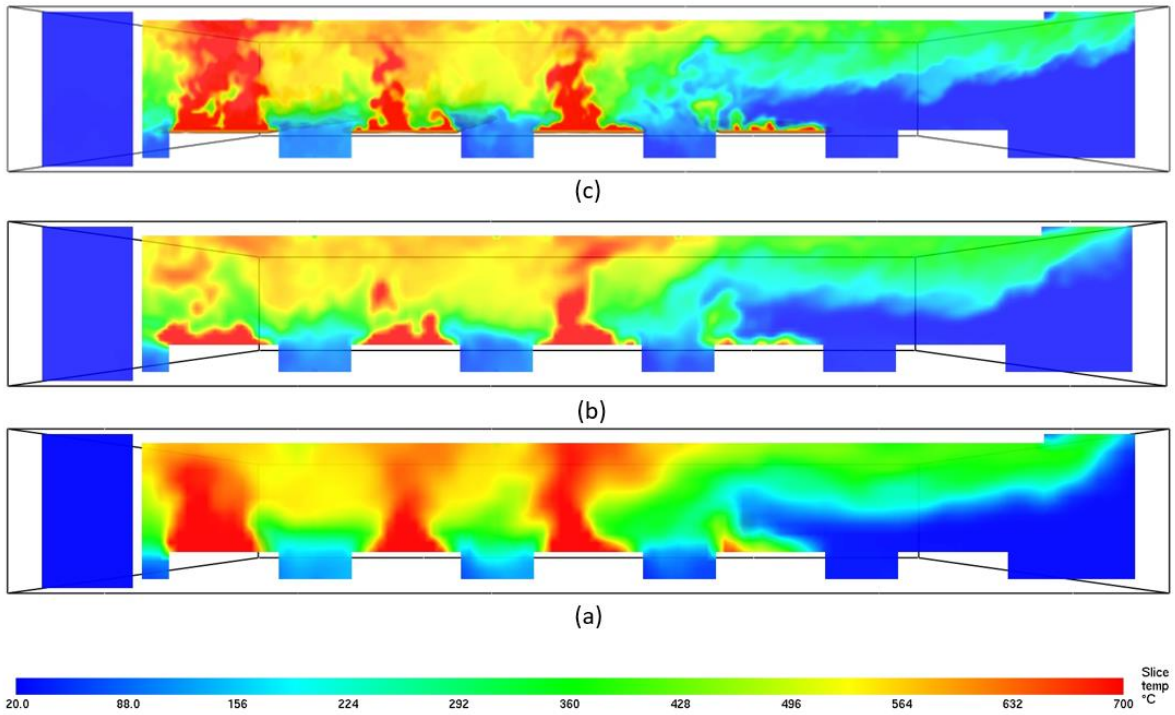

Figure 41 Temperature slices (SLCF 2, in Figure 39) at Y= 2.0 m taken at 1102 s. Comparison between 20 cm (a), 10 cm (b) and 5 cm (c) meshes.

Vector velocity slices are shown in Figure 42 for mesh sizes of 20 cm (a), 10 cm (b) and 5 cm (c). The slices on 10 and 5 cm meshes had to be changed slightly to increment the number of vectors skipped. Consequently, some of the visual differences may be explained by this slight alteration. Overall, the velocity flow in the far field is very similar in the three meshes, which is also confirmed by the temperature results in Figure 42.

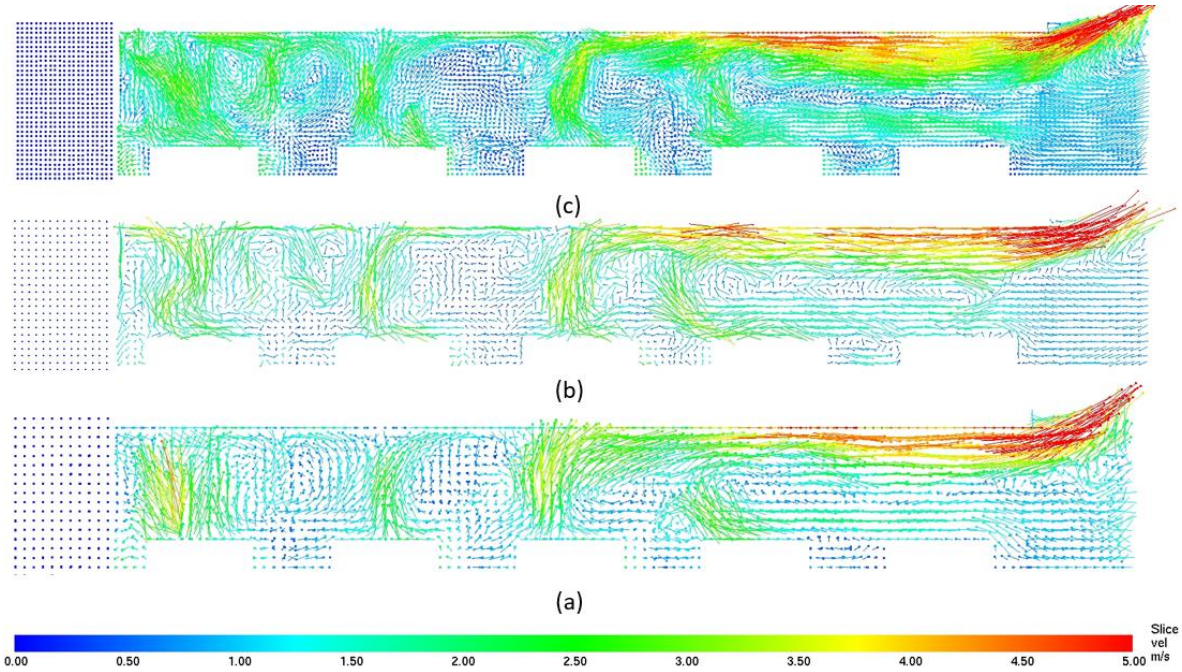

Figure 42 Vector velocity slices for 20 cm (a), 10 cm (b) and 5 cm (c) meshes taken at 1102 s in position Y=22 m (SLCF 22).

Figure 43 shows changes in heat flux at positions 2 and 3 for 20, 10 and 5cm mesh sizes. There is a spike of heat flux at around 604 s for position 2 and around 627 s for position 3. These spikes correspond to the ignition of a near-by fuel package. The heat flux for position 2 measured on the 5 cm mesh is 14% higher at the peak and significantly higher at position 3 during ignition of a near-by fuel package.

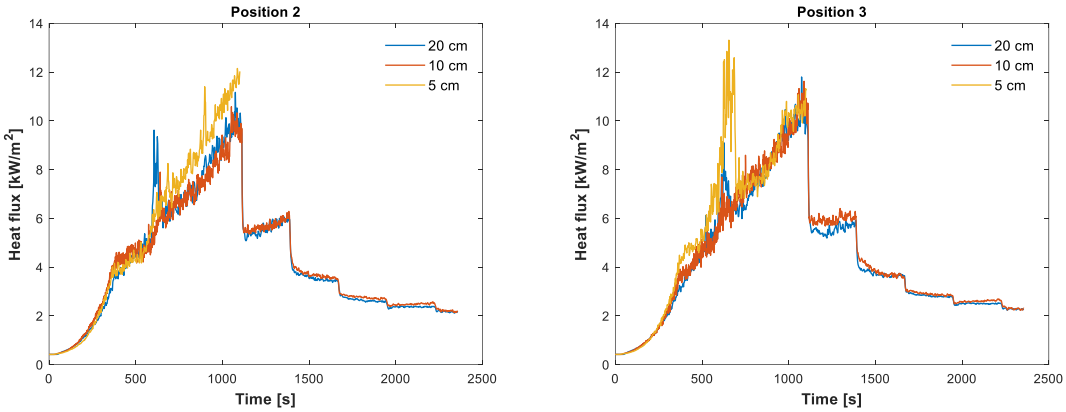

Figure 43 Heat flux changes with time in positions 2 and 3.

Temperature measurement at the ignition position (position 1) is shown in Figure 44, where an instantaneous temperature signal is averaged using 20 s window. The figure shows that for near-field temperature (i.e., temperature in the combustion location), the sensitivity study has to be continued because temperature results have not converged.

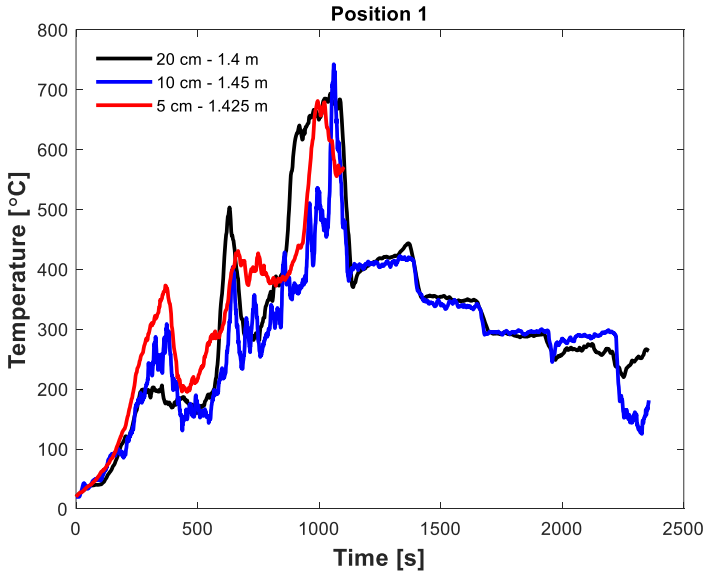

Figure 44 Temperature measurement comparison in position 1 for 20, 10 and 5 cm meshes. Temperatures at 800 - 1000 s are higher with coarser mesh. The signal is averaged using moving average with a window of 20 s.

Simplification of the domain was accomplished y considering only half the full domain. This resulted in a substantial CPU cost savings for the sensitivity study simulations. Nevertheless, simulations for the study itself have to be made using the full geometry, which implies that the CPU time to run it will be even higher – see the estimates in the Table 13. The half domain case was run on 6 processors in parallel, assigning one processor to each mesh. The full domain can

be split into more meshes, nevertheless the time to run all the simulations for this thesis on 10 cm or 5 cm meshes is beyond the time constraints for the project scope.

With regard to the 5 cm mesh simulation, it had a high computational cost and, therefore, it was not possible to include it into the comparison of averaged temperatures (Figure 40). Up to the time of 1102 s, no clear hot layer was fully formed, thus no attempt of averaging/comparing temperatures was performed. Instead, the comparison of temperature versus time is shown in Figure 45, where the temperature is compared in the far-field at a height of approximately 2.6 m in positions 13 and 31. This data indicates that the 10 and 5 cm results converge up to the 1102 s time. The results for 20 cm mesh are consistently higher (roughly 20% at most) than with the 10 and 5 cm meshes. This shows that for further work within this area it is preferrable that FDS simulations be performed on the finer mesh.

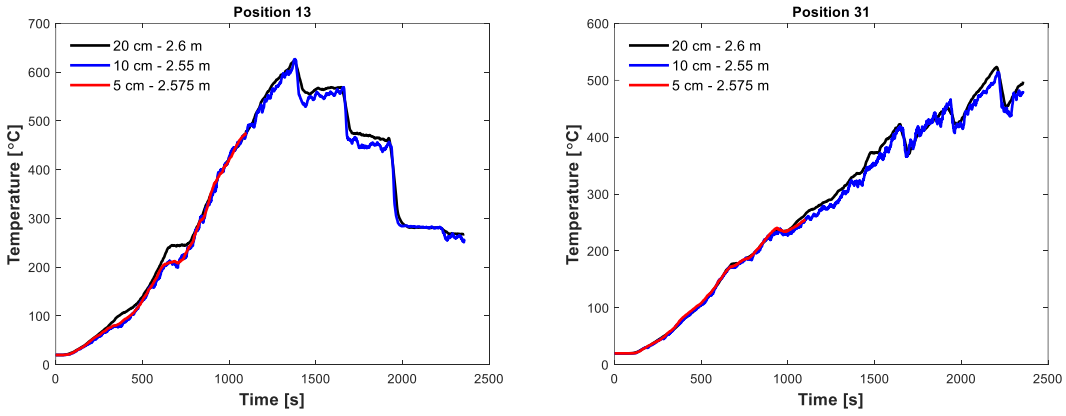

Figure 45 Temperature measured in positions 13 and 31 (far field) with three different meshes: 20, 10 and 5 cm. 10 cm mesh shows similar results to 5 cm, up until the 1102 s.

Simplification of the domain by considering only a half provided a CPU cost savings for the sensitivity study simulations. Nevertheless, simulations for the study itself have to be made using the full geometry, which implies that the CPU time will be even higher, see the estimates in Table 13. The half of the domain was run on 6 processors in parallel, assigning one processor to each mesh. The full domain can be split into more meshes, nevertheless the time to run all the simulations for this thesis on 10 cm mesh has a too high of a CPU cost for the scope of this project. Figure 43 and Figure 44 show that the convergence has not been reached in the near-field region, and that the sensitivity study shall be continued. Nevertheless, the choice is made to use 20 cm mesh in the office, supermarket and the Tisova fire scenarios, and 10 cm in ETFT because of the smaller size of the compartment.

Appendix B-1: Calculation of ignition time for the different scenarios

The full calculation was performed in Excel and is not showed here. Instead, only one step is included to show how the ignition time was calculated using Modak's equation. In Modak's equation, X_r is the radiation fraction [-], R_o is the distance of the target from the flame [m] and $\dot{Q}$ is the HRR [kW].

Office case:

At 277 s the HRR reached 920.748 kW (Figure 5). Therefore, the heat flux of 10 kW/m^2 is reached:

$$\dot{q''} = \frac{X_r \dot{Q}}{4\pi R_0^2} = \frac{0.35 * 920.748}{4\pi * 1.6^2} \approx 10 \quad [\frac{kW}{m^2}]$$

Supermarket case:

At 166 s the HRR reached 1295.13 kW (Figure 10), therefore:

$$\dot{q''} = \frac{X_r \dot{Q}}{4\pi R_0^2} = \frac{0.35 * 1295.13}{4\pi * 2.0^2} \approx 9 \quad [\frac{kW}{m^2}]$$

At 258 s the HRR reached 4692.76 kW (Figure 16), therefore:

$$\dot{q''} = \frac{X_r \dot{Q}}{4\pi R_0^2} = \frac{0.35 * 4692.76}{4\pi * 4.4^2} \approx 7 \quad [\frac{kW}{m^2}]$$

Appendix B-2: Calculation of the opening areas and global equivalence ratio

To estimate the minimum openings area for a fire in a scenario to be fuel-controlled, the formula for maximum heat release rate can be used (Karlsson & Quintiere, 2000, p. 130):

Office case:

$$A_0 = \frac{Q_{max}}{1.518 * \sqrt{H_0}} = \frac{25}{1.518 * \sqrt{1.0}} \approx 16.5\ m^2$$

Supermarket case:

$$A_0 = \frac{Q_{max}}{1.518 * \sqrt{H_0}} = \frac{80}{1.518 * \sqrt{3}} \approx 30\ m^2$$

The global equivalence ratio (Φ), the ratio of the mass flux of a fuel to the mass flux of oxygen in a compartment, divided by the stoichiometric ratio. Φ indicates if the fire is fuel or ventilation controlled (Peacock, et al., 2021). Results for each case are reported in Table 14. In the equations below, $\dot{Q}$ is the HRR [kW], $\dot{m}_{O_2}$ is the mass flux of oxygen into the compartment, A_0 is the area [m^2] and H_0 [m] is the height of the openings in the enclosure.

$$\Phi = \frac{\dot{m}_f}{r \cdot \dot{m}_{O_2}} \equiv \frac{\dot{Q}}{13100\ \dot{m}_{O_2}} \qquad \text{Equation 5}$$

$$\dot{m}_{0_2} = \frac{1}{2} \cdot 0.23 \cdot A_0 \cdot \sqrt{H_0} \qquad \text{Equation 6}$$

Table 14 Global Equivalent Ratio (G.E.R) for all the cases in the thesis.

CASE	m02	HRR [MW]	Φ	
Office	11.04	70	0.48	fuel controlled
Supermarket	65.33	80	0.09	fuel controlled
TISOVA fire test	8.72	2.32	0.02	fuel controlled
ETFT fire test	7.17	2.47	0.11	fuel controlled

Appendix B-3: Calculation of the diameter of the fire plume

It is not obligatory but recommended to fit the plume into a single cell at the ceiling. A rough estimate of fire plume diameter is computed assuming a 15-degree angle for vertical inclination of the plume and the ideal plume theory (Karlsson & Quintiere, 2000, p. 60). The radius of the plume can be calculated as:

$b = \frac{6}{5} \cdot \alpha \cdot z$ where α is a constant equal to 0.15, and z is the height of the enclosure in metres.

For the **office case**, considering the fuel package height, a value of b = 0.54 m was found. Considering the diagonal of the fuel package as $2.4 \cdot \sqrt{2} = 3.39$ m, which is then added twice to the plume radius and gives the final dimension of **4.47** m. This is slightly larger, than the cell used in this case (4.0 x 4.0 m).

For the **supermarket case**, b = 1.08 m, and the final plume's diameter estimate is **6.16** m, which is close to the cell size (6.0 x 6.0 m).

For the **Tisova fire test**, b = 0.72 m, and the final plume's diameter estimate is **2.85** m, which is within the cell size (3.0 x 3.0 m).

For the **ETFT fire test**, b = 0.36 m, and the final plume's diameter estimate is **1.42 m**, which is within the cell size (2.96 x 1.63 m).

Appendix B-4: Calculation of conductivity values

Determination of conductivity values for the walls was estimated based on the layers of concrete aerated block, FLEXI® insulation, and plasterboard. Conductivity was estimated using thermal transmittance of the sandwich wall as follows:

$$k = U \cdot thickness \ = 0.18 \cdot 0.115 = 0.0207 \approx 0.021 \ \frac{W}{mK}$$

Appendix C: Comparison of MZ fire model with sensitivity study results

Figure 46 presents a comparison of the office scenario MZ fire model result with the sensitivity study results. Near field temperatures for MZ fire model are about 20% greater (T1, T3) compared to the results with 20 and 10 cm meshes. For the measurements at T13 (2 m) the MZ fire model shows 43% lower temperatures than predicted by FDS compared to the 10 cm mesh. The prediction for the position T31 is 36% greater, which is below FDS predictions for the height of 2.5 m.

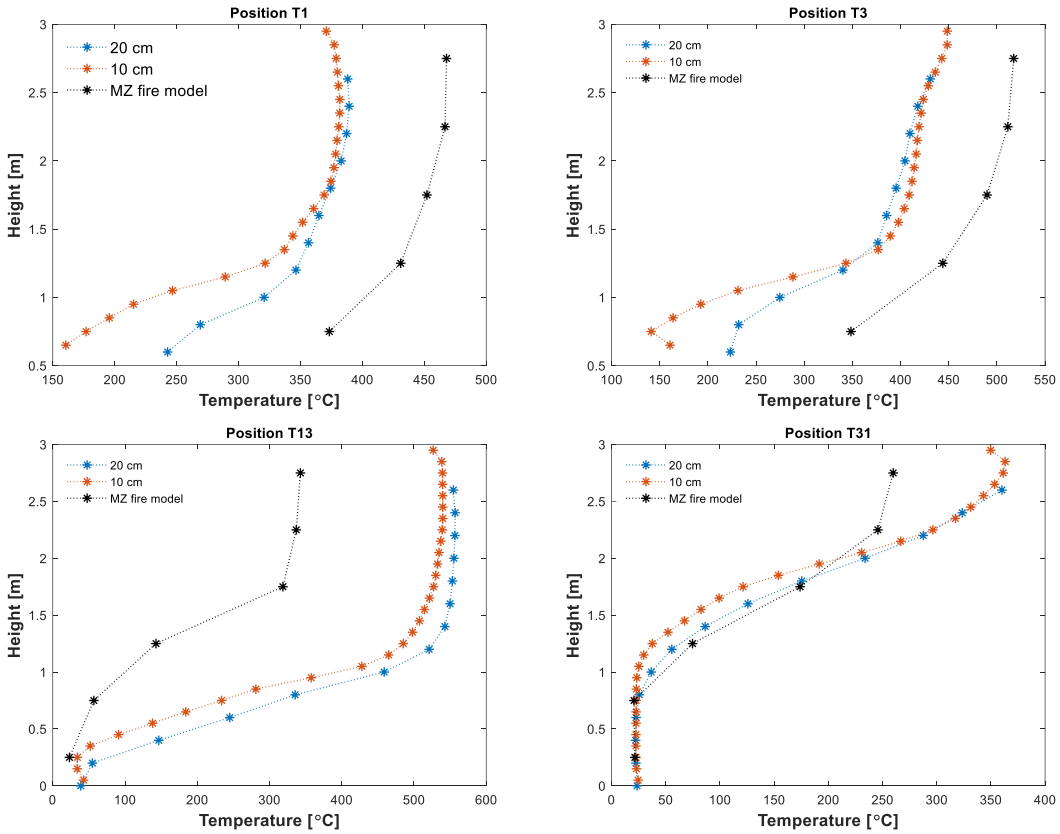

Figure 46 Comparison of MZ fire model temperature results to sensitivity study results, averaged over the period of 1440-1460 s for positions 1, 3, 13 and 31.

Appendix D: Obscuration results (supermarket scenario)

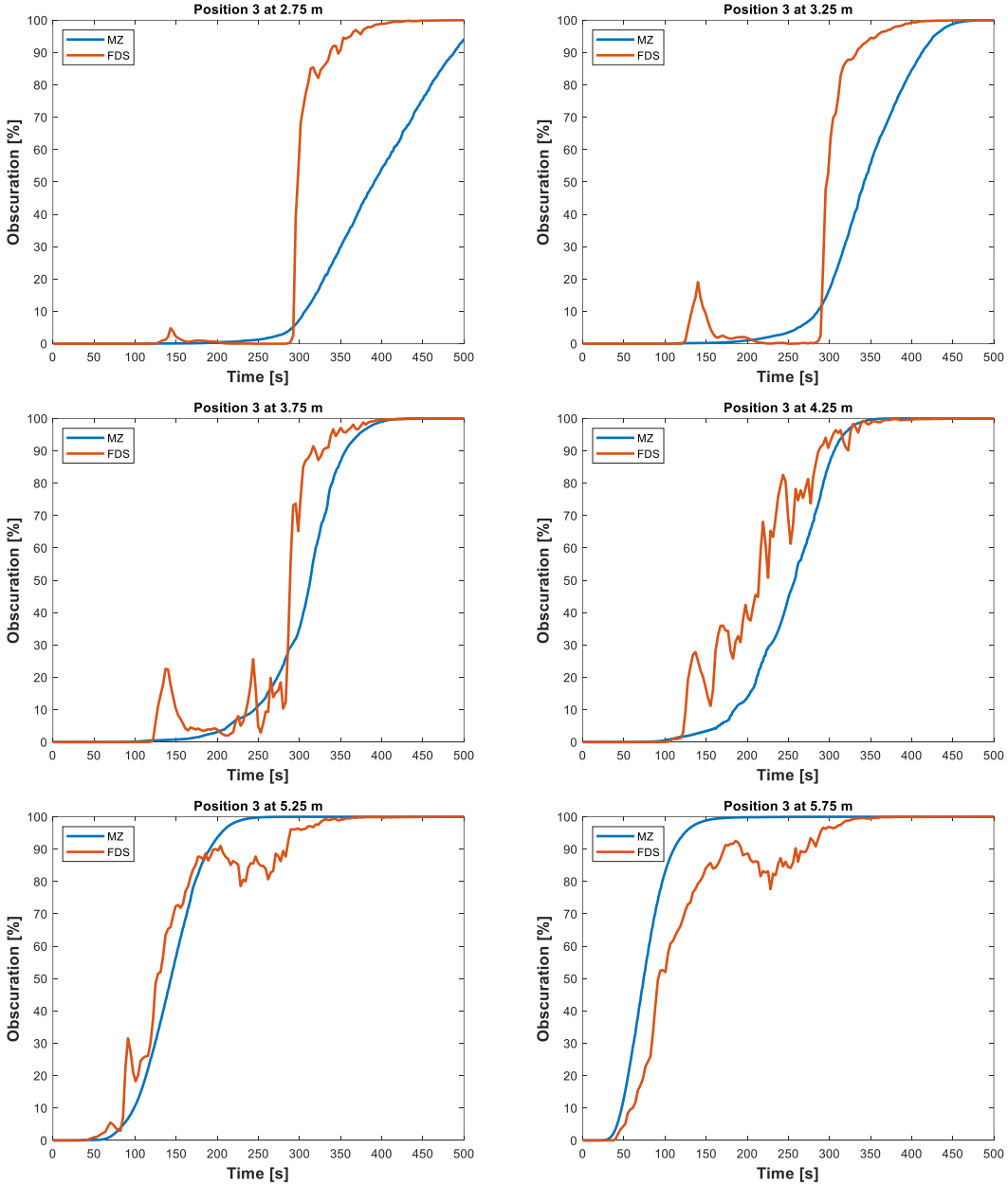

Figure 47 Obscuration comparison for supermarket scenario in position 3, at 6 different heights.

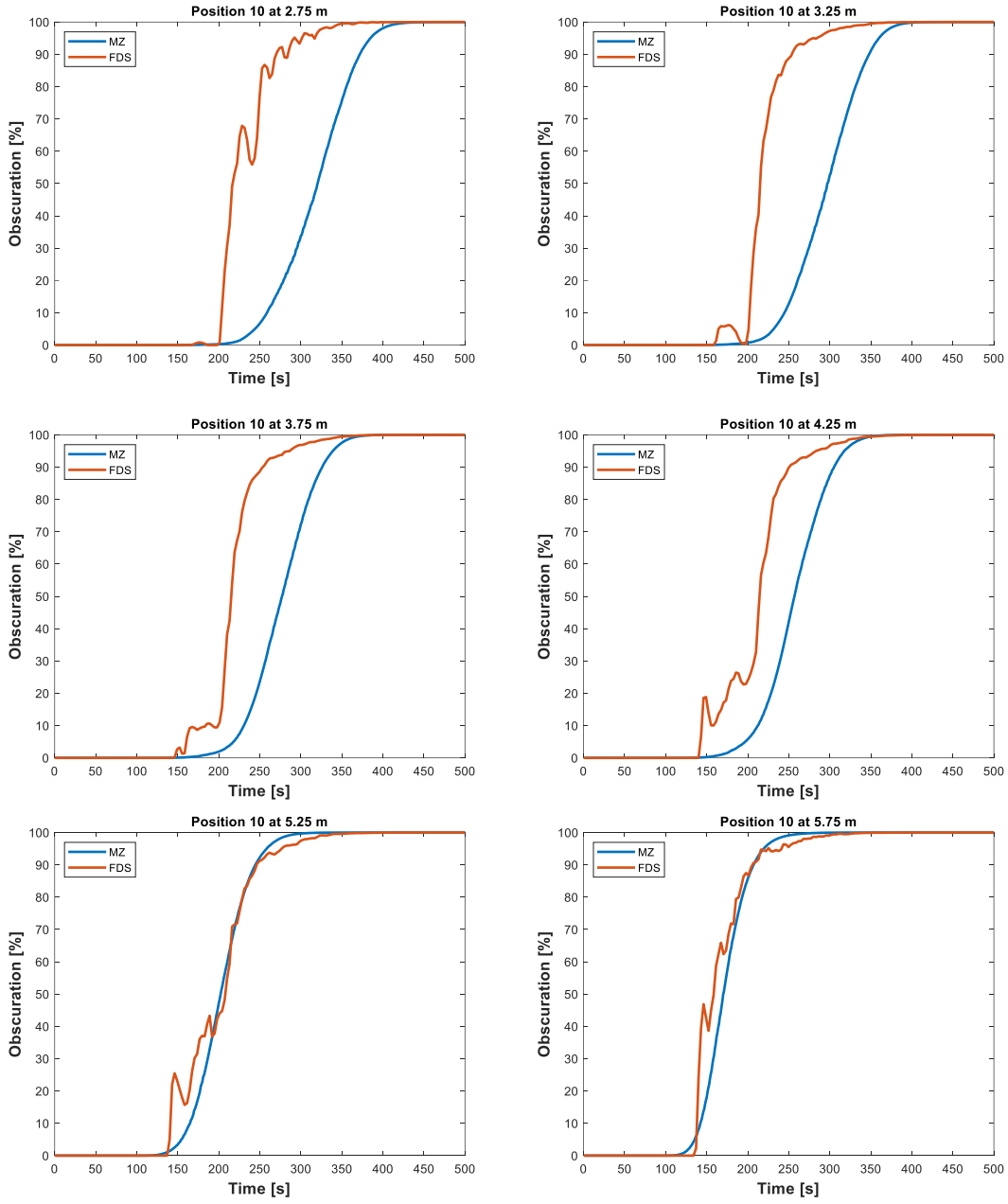

Figure 48 Obscuration comparison for supermarket scenario in position 10, at 6 different heights.

Appendix E: Temperature comparison – Tisova fire test

Figure 49 shows temperature profiles for MZ fire model and FDS compared to the experimental results. Significant differences are seen between the average temperatures in positions 63 and 46. In position 46, experimental results show higher temperatures lower in the domain (i.e., under 2.5 m), which can be explained by the impact of air from the openings. Temperature differences become greater at higher temperatures.

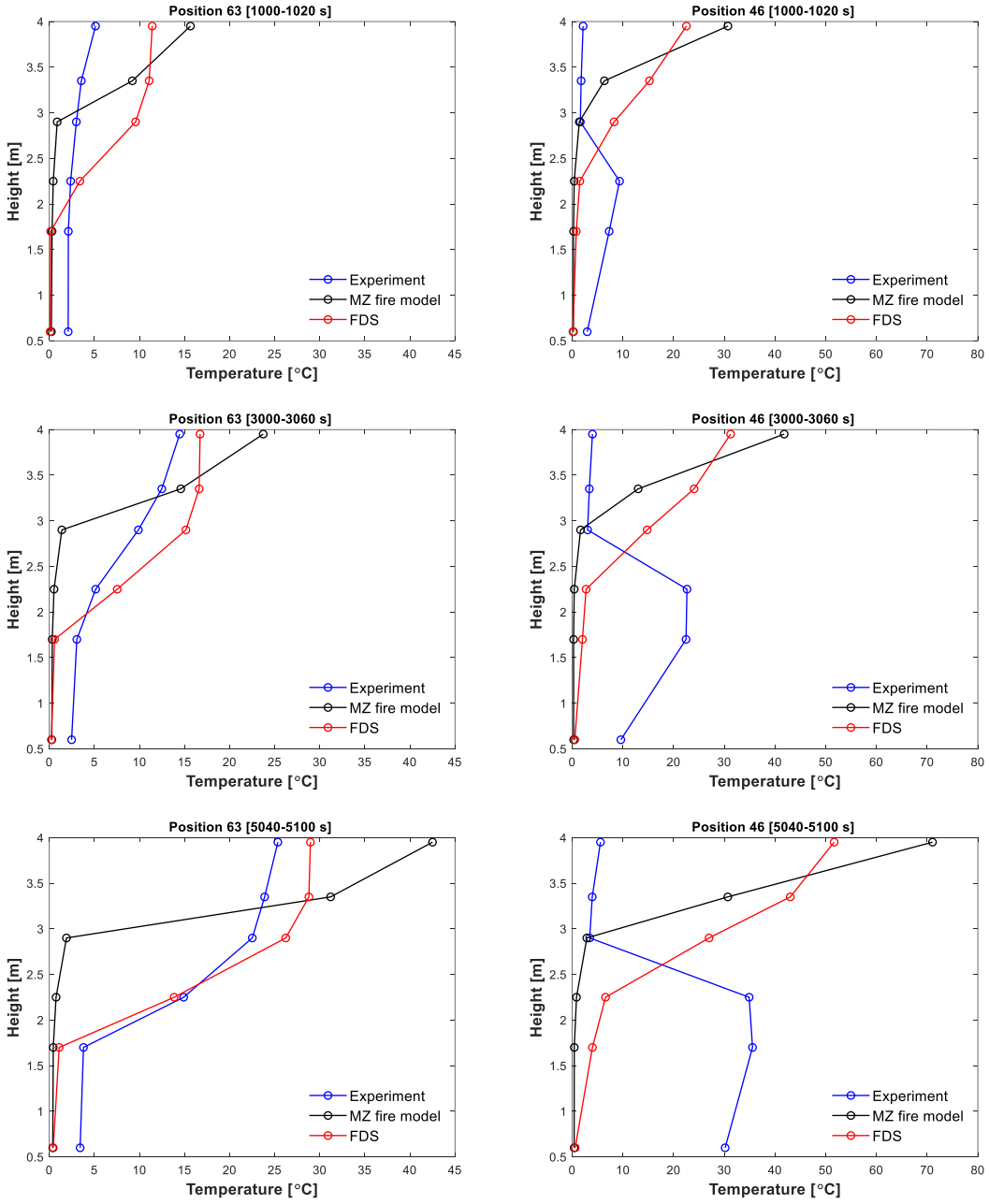

Figure 49 The Tisova fire test temperature profiles comparison of experimental data to MZ fire model and FDS in positions 63 and 46.

Appendix F: Temperature comparison – ETFT fire test

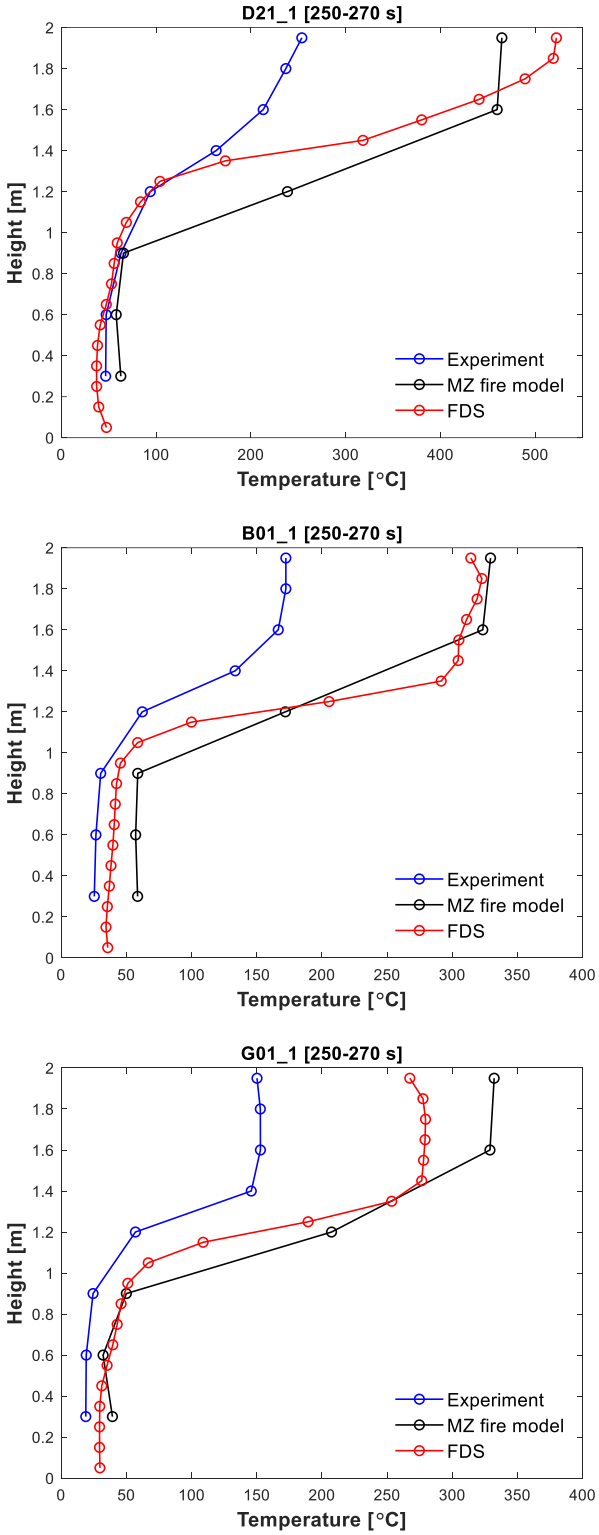

Figure 50 ETFT fire test temperature comparison (averaging period 2, 250-270 s) to FDS and MZ fire model results for three measurement positions D21_1, B01_1 and G01_1.

Appendix G: Office scenario code: FDS

```
&HEAD CHID='office_20'/

&TIME T_END=4712.0/

&MISC TMPA=20.0/

############## MESHES 20 cm ##############

#####&MESH ID='MESH', IJK=220,141,17, XB=-2.0,42.0,-2.0,26.2,-0.2,3.2/  527340

&MESH ID='MESH1', IJK=30,141,17, XB=-2.0,4.0,-2.0,26.2,-0.2,3.2/  71910 cells
&MESH ID='MESH2', IJK=20,141,17, XB=4.0,8.0,-2.0,26.2,-0.2,3.2/   47940 cells
&MESH ID='MESH3', IJK=20,141,17, XB=8.0,12.0,-2.0,26.2,-0.2,3.2/
&MESH ID='MESH4', IJK=20,141,17, XB=12.0,16.0,-2.0,26.2,-0.2,3.2/
&MESH ID='MESH5', IJK=20,141,17, XB=16.0,20.0,-2.0,26.2,-0.2,3.2/
&MESH ID='MESH6', IJK=20,141,17, XB=20.0,24.0,-2.0,26.2,-0.2,3.2/
&MESH ID='MESH7', IJK=20,141,17, XB=24.0,28.0,-2.0,26.2,-0.2,3.2/
&MESH ID='MESH8', IJK=20,141,17, XB=28.0,32.0,-2.0,26.2,-0.2,3.2/
&MESH ID='MESH9', IJK=20,141,17, XB=32.0,36.0,-2.0,26.2,-0.2,3.2/
&MESH ID='MESH10', IJK=30,141,17, XB=36.0,42.0,-2.0,26.2,-0.2,3.2/

############## MATERIAL SPECS ##############

&MATL ID='CONCRETE',
   CONDUCTIVITY=1.1,
   SPECIFIC_HEAT=0.88,
   DENSITY=2100/   from Karlsson & Quintiere book

&MATL ID='PARTICLEBOARD',
   DENSITY=637,
   CONDUCTIVITY=0.1081,
   SPECIFIC_HEAT=1.424,
   EMISSIVITY=0.9/ from Czajkowski paper

############## FUEL CHARACTERISTICS ##############

&REAC FUEL='PARTICLEBOARD',
   C=3.4
   H=5.78
   O=2.448
   N=0.0034
   SOOT_YIELD=0.015,
   HEAT_OF_COMBUSTION=1.8E4,
   RADIATIVE_FRACTION=0.35/ soot yield PB=0.008 here changed

############## SURFACES ##############
```

```
&SURF ID='FLOOR',
   MATL_ID='CONCRETE',
   THICKNESS=0.2,
   RGB=192,192,192/

&SURF ID='DESK',
   MATL_ID='PARTICLEBOARD',
   COLOR='TAN',
   THICKNESS=0.6/

&SURF ID='BURN',
   MATL_ID='PARTICLEBOARD',
   COLOR='RED',
   HRRPUA=279.0,
   THICKNESS=0.6,
   RAMP_Q='deskramp'/

############## OUTER BOUNDARY WALLS ##############

&OBST XB=-0.2,40.2,-0.2,24.2,-0.2,0.0, SURF_ID='FLOOR', RGB=192,192,192/
&OBST XB=-0.2,40.2,-0.2,24.2,3.0,3.2, SURF_ID='FLOOR', RGB=192,192,192/
&OBST XB=-0.2,40.2,24.0,24.2,0.0,3.2, SURF_ID='FLOOR', RGB=192,192,192/ north wall
&OBST XB=-0.2,40.2,-0.2,0.0,0.0,3.2, SURF_ID='FLOOR', RGB=192,192,192/ south wall
&OBST XB=-0.2,0.0,-0.2,24.2,0.0,3.2, SURF_ID='FLOOR', RGB=192,192,192/ left wall
&OBST XB=40.0,40.2,-0.2,24.2,0.0,3.2, SURF_ID='FLOOR', RGB=192,192,192/ right wall
&OBST XB=8.0,32.0,8.0,16.0,-0.2,3.2, SURF_ID='FLOOR', RGB=0,0,0/ Concrete core

############## OPENINGS ##############

&HOLE XB=-0.3,0.3,4.0,20.0,0.0,1.0/ left
&HOLE XB=39.9,40.3,4.0,20.0,0.0,1.0/ right
&HOLE XB=4.0,36.0,23.9,24.3,0.0,1.0/ north
&HOLE XB=4.0,36.0,-0.2,0.3,0.0,1.0/ south

############## FUEL PACKAGE RAMP ##############

&RAMP ID='deskramp',T=0,F=0/
&RAMP ID='deskramp',T=10,F=0.000747/
&RAMP ID='deskramp',T=20,F=0.002986/
&RAMP ID='deskramp',T=30,F=0.006719/
&RAMP ID='deskramp',T=40,F=0.011944/
&RAMP ID='deskramp',T=50,F=0.018663/
&RAMP ID='deskramp',T=60,F=0.026874/
&RAMP ID='deskramp',T=70,F=0.036579/
&RAMP ID='deskramp',T=80,F=0.047777/
```

```
&RAMP ID='deskramp',T=90,F=0.060468/
&RAMP ID='deskramp',T=100,F=0.074651/
&RAMP ID='deskramp',T=110,F=0.090328/
&RAMP ID='deskramp',T=120,F=0.107498/
&RAMP ID='deskramp',T=130,F=0.126161/
&RAMP ID='deskramp',T=140,F=0.146317/
&RAMP ID='deskramp',T=150,F=0.167966/
&RAMP ID='deskramp',T=160,F=0.191108/
&RAMP ID='deskramp',T=170,F=0.215742/
&RAMP ID='deskramp',T=180,F=0.24187/
&RAMP ID='deskramp',T=190,F=0.269491/
&RAMP ID='deskramp',T=200,F=0.298606/
&RAMP ID='deskramp',T=210,F=0.329213/
&RAMP ID='deskramp',T=220,F=0.361313/
&RAMP ID='deskramp',T=230,F=0.394906/
&RAMP ID='deskramp',T=240,F=0.429992/
&RAMP ID='deskramp',T=250,F=0.466571/
&RAMP ID='deskramp',T=260,F=0.504643/
&RAMP ID='deskramp',T=270,F=0.544209/
&RAMP ID='deskramp',T=280,F=0.585267/
&RAMP ID='deskramp',T=290,F=0.627818/
&RAMP ID='deskramp',T=300,F=0.671862/
&RAMP ID='deskramp',T=310,F=0.7174/
&RAMP ID='deskramp',T=320,F=0.76443/
&RAMP ID='deskramp',T=330,F=0.812954/
&RAMP ID='deskramp',T=340,F=0.86297/
&RAMP ID='deskramp',T=350,F=0.914479/
&RAMP ID='deskramp',T=360,F=0.967482/
&RAMP ID='deskramp',T=366,F=1.0/
&RAMP ID='deskramp',T=1110,F=1.0/
&RAMP ID='deskramp',T=1111,F=0.0/

############## MESH VENTS ##############

&VENT MB='XMIN', SURF_ID='OPEN'/ left big side
&VENT MB='XMAX', SURF_ID='OPEN'/ right big side
&VENT MB='YMIN', SURF_ID='OPEN'/ left big side
&VENT MB='YMAX', SURF_ID='OPEN'/ right big side
&VENT MB='ZMIN', SURF_ID='OPEN'/ left big side
&VENT MB='ZMAX', SURF_ID='OPEN'/ right big side

############## OFFICE STATIONS ##############
##### DESK 1 ignited at time 0 seconds

&OBST ID='DESK1', XB=0.8,3.2,0.8,3.2,0.0,0.6, SURF_ID='DESK', RGB=240,230,140/
```

```
&DEVC ID='TIMER', XYZ=0.8,0.8,1.6, QUANTITY='TIME', SETPOINT=1.0 / top
&VENT XB=0.8,3.2,0.8,3.2,0.6,0.6,  SURF_ID='BURN', DEVC_ID='TIMER', RGB=255,0,0 /

##### DESK 2 ignited at time 277 seconds

&OBST ID='DESK2', XB=0.8,3.2,4.8,7.2,0.0,0.6, SURF_ID='DESK', RGB=240,230,140/

&DEVC ID='TIMER2', XYZ=0.8,4.8,1.6, QUANTITY='TIME', SETPOINT=277 / top
&VENT XB=0.8,3.2,4.8,7.2,0.6,0.6,  SURF_ID='BURN', DEVC_ID='TIMER2', RGB=240,230,140 /

##### DESK 3 ignited at time 277 seconds

&OBST ID='DESK3', XB=4.8,7.2,0.8,3.2,0.0,0.6, SURF_ID='DESK', RGB=240,230,140/

&DEVC ID='TIMER3', XYZ=4.8,0.8,1.6, QUANTITY='TIME', SETPOINT=277 / top
&VENT XB=4.8,7.2,0.8,3.2,0.6,0.6,  SURF_ID='BURN', DEVC_ID='TIMER3', RGB=240,230,140  /

##### DESK 4 ignited at time 277 seconds

&OBST ID='DESK4', XB=4.8,7.2,4.8,7.2,0.0,0.6, SURF_ID='DESK', RGB=240,230,140/

&DEVC ID='TIMER4', XYZ=4.8,4.8,1.6, QUANTITY='TIME', SETPOINT=277 / top
&VENT XB=4.8,7.2,4.8,7.2,0.6,0.6,  SURF_ID='BURN', DEVC_ID='TIMER4', RGB=240,230,140 /

##### DESK 5 ignited at time 554 seconds

&OBST ID='DESK5', XB=0.8,3.2,8.8,11.2,0.0,0.6, SURF_ID='DESK', RGB=240,230,140/

&DEVC ID='TIMER5', XYZ=0.8,8.8,1.6, QUANTITY='TIME', SETPOINT=554 / top
&VENT XB=0.8,3.2,8.8,11.2,0.6,0.6,  SURF_ID='BURN', DEVC_ID='TIMER5', RGB=240,230,140 /

##### DESK 6 ignited at time 554 seconds

&OBST ID='DESK6', XB=4.8,7.2,8.8,11.2,0.0,0.6, SURF_ID='DESK', RGB=240,230,140/

&DEVC ID='TIMER6', XYZ=4.8,8.8,1.6, QUANTITY='TIME', SETPOINT=554 / top
&VENT XB=4.8,7.2,8.8,11.2,0.6,0.6,  SURF_ID='BURN', DEVC_ID='TIMER6', RGB=240,230,140 /

##### DESK 7 ignited at time 554 seconds

&OBST ID='DESK7', XB=8.8,11.2,0.8,3.2,0.0,0.6, SURF_ID='DESK', RGB=240,230,140/

&DEVC ID='TIMER7', XYZ=8.8,0.8,1.6, QUANTITY='TIME', SETPOINT=554 / top
&VENT XB=8.8,11.2,0.8,3.2,0.6,0.6,  SURF_ID='BURN', DEVC_ID='TIMER7', RGB=240,230,140 /

##### DESK 8 ignited at time 554 seconds
```

```
&OBST ID='DESK8', XB=8.8,11.2,4.8,7.2,0.0,0.6, SURF_ID='DESK', RGB=240,230,140/

&DEVC ID='TIMER8', XYZ=8.8,4.8,1.6, QUANTITY='TIME', SETPOINT=554 / top
&VENT XB=8.8,11.2,4.8,7.2,0.6,0.6,  SURF_ID='BURN', DEVC_ID='TIMER8', RGB=240,230,140 /

##### DESK 9 ignited at time 831 seconds

&OBST ID='DESK9', XB=12.8,15.2,4.8,7.2,0.0,0.6, SURF_ID='DESK', RGB=240,230,140/

&DEVC ID='TIMER9', XYZ=12.8,4.8,1.6, QUANTITY='TIME', SETPOINT=831 / top
&VENT XB=12.8,15.2,4.8,7.2,0.6,0.6,  SURF_ID='BURN', DEVC_ID='TIMER9', RGB=240,230,140 /

##### DESK 10 ignited at time 831 seconds

&OBST ID='DESK10', XB=12.8,15.2,0.8,3.2,0.0,0.6, SURF_ID='DESK', RGB=240,230,140/

&DEVC ID='TIMER10', XYZ=12.8,0.8,1.6, QUANTITY='TIME', SETPOINT=831 / top
&VENT XB=12.8,15.2,0.8,3.2,0.6,0.6,  SURF_ID='BURN', DEVC_ID='TIMER10', RGB=240,230,140 /

##### DESK 11 ignited at time 831 seconds

&OBST ID='DESK11', XB=0.8,3.2,12.8,15.2,0.0,0.6, SURF_ID='DESK', RGB=240,230,140/

&DEVC ID='TIMER11', XYZ=0.8,12.8,1.6, QUANTITY='TIME', SETPOINT=831 / top
&VENT XB=0.8,3.2,12.8,15.2,0.6,0.6,  SURF_ID='BURN', DEVC_ID='TIMER11', RGB=240,230,140 /

##### DESK 12 ignited at time 831 seconds

&OBST ID='DESK12', XB=4.8,7.2,12.8,15.2,0.0,0.6, SURF_ID='DESK', RGB=240,230,140/

&DEVC ID='TIMER12', XYZ=4.8,12.8,1.6, QUANTITY='TIME', SETPOINT=831 / top
&VENT XB=4.8,7.2,12.8,15.2,0.6,0.6,  SURF_ID='BURN', DEVC_ID='TIMER12',  RGB=240,230,140/

##### DESK 13 ignited at time 1108 seconds

&OBST ID='DESK13', XB=16.8,19.2,0.8,3.2,0.0,0.6, SURF_ID='DESK', RGB=240,230,140/

&DEVC ID='TIMER13', XYZ=16.8,0.8,1.6, QUANTITY='TIME', SETPOINT=1108 / top
&VENT XB=16.8,19.2,0.8,3.2,0.6,0.6,  SURF_ID='BURN', DEVC_ID='TIMER13', RGB=240,230,140 /

##### DESK 14 ignited at time 1108 seconds

&OBST ID='DESK14', XB=16.8,19.2,4.8,7.2,0.0,0.6, SURF_ID='DESK', RGB=240,230,140/

&DEVC ID='TIMER14', XYZ=16.8,4.8,1.6, QUANTITY='TIME', SETPOINT=1108 / top
```

```
&VENT XB=16.8,19.2,4.8,7.2,0.6,0.6,  SURF_ID='BURN', DEVC_ID='TIMER14', RGB=240,230,140 /

##### DESK 15 ignited at time 1108 seconds

&OBST ID='DESK15', XB=0.8,3.2,16.8,19.2,0.0,0.6, SURF_ID='DESK', RGB=240,230,140/

&DEVC ID='TIMER15', XYZ=0.8,16.8,1.6, QUANTITY='TIME', SETPOINT=1108 / top
&VENT XB=0.8,3.2,16.8,19.2,0.6,0.6,  SURF_ID='BURN', DEVC_ID='TIMER15', RGB=240,230,140 /

##### DESK 16 ignited at time 1108 seconds

&OBST ID='DESK16', XB=4.8,7.2,16.8,19.2,0.0,0.6, SURF_ID='DESK', RGB=240,230,140/

&DEVC ID='TIMER16', XYZ=4.8,16.8,1.6, QUANTITY='TIME', SETPOINT=1108 / top
&VENT XB=4.8,7.2,16.8,19.2,0.6,0.6,  SURF_ID='BURN', DEVC_ID='TIMER16', RGB=240,230,140 /

##### DESK 17 ignited at time 1385 seconds

&OBST ID='DESK17', XB=0.8,3.2,20.8,23.2,0.0,0.6, SURF_ID='DESK', RGB=240,230,140/

&DEVC ID='TIMER17', XYZ=0.8,20.8,1.6, QUANTITY='TIME', SETPOINT=1385 / top
&VENT XB=0.8,3.2,20.8,23.2,0.6,0.6,  SURF_ID='BURN', DEVC_ID='TIMER17', RGB=240,230,140 /

##### DESK 18 ignited at time 1385 seconds

&OBST ID='DESK18', XB=4.8,7.2,20.8,23.2,0.0,0.6, SURF_ID='DESK', RGB=240,230,140/

&DEVC ID='TIMER18', XYZ=4.8,20.8,1.6, QUANTITY='TIME', SETPOINT=1385 / top
&VENT XB=4.8,7.2,20.8,23.2,0.6,0.6,  SURF_ID='BURN', DEVC_ID='TIMER18', RGB=240,230,140 /

##### DESK 19 ignited at time 1385 seconds

&OBST ID='DESK19', XB=20.8,23.2,0.8,3.2,0.0,0.6, SURF_ID='DESK', RGB=240,230,140/

&DEVC ID='TIMER19', XYZ=20.8,0.8,1.6, QUANTITY='TIME', SETPOINT=1385 / top
&VENT XB=20.8,23.2,0.8,3.2,0.6,0.6,  SURF_ID='BURN', DEVC_ID='TIMER19', RGB=240,230,140 /

##### DESK 20 ignited at time 1385 seconds

&OBST ID='DESK20', XB=20.8,23.2,4.8,7.2,0.0,0.6, SURF_ID='DESK', RGB=240,230,140/

&DEVC ID='TIMER20', XYZ=20.8,4.8,1.6, QUANTITY='TIME', SETPOINT=1385 / top
&VENT XB=20.8,23.2,4.8,7.2,0.6,0.6,  SURF_ID='BURN', DEVC_ID='TIMER20', RGB=240,230,140 /

##### DESK 21 ignited at time 1662 seconds
```

```
&OBST ID='DESK21', XB=24.8,27.2,4.8,7.2,0.0,0.6, SURF_ID='DESK', RGB=240,230,140/

&DEVC ID='TIMER21', XYZ=24.8,4.8,1.6, QUANTITY='TIME', SETPOINT=1662 / top
&VENT XB=24.8,27.2,4.8,7.2,0.6,0.6,  SURF_ID='BURN', DEVC_ID='TIMER21', RGB=240,230,140 /

##### DESK 22 ignited at time 1662 seconds

&OBST ID='DESK22', XB=24.8,27.2,0.8,3.2,0.0,0.6, SURF_ID='DESK', RGB=240,230,140/

&DEVC ID='TIMER22', XYZ=24.8,0.8,1.6, QUANTITY='TIME', SETPOINT=1662 / top
&VENT XB=24.8,27.2,0.8,3.2,0.6,0.6,  SURF_ID='BURN', DEVC_ID='TIMER22', RGB=240,230,140  /

##### DESK 23 ignited at time 1662 seconds

&OBST ID='DESK23', XB=8.8,11.2,20.8,23.2,0.0,0.6, SURF_ID='DESK', RGB=240,230,140/

&DEVC ID='TIMER23', XYZ=8.8,20.8,1.6, QUANTITY='TIME', SETPOINT=1662 / top
&VENT XB=8.8,11.2,20.8,23.2,0.6,0.6,  SURF_ID='BURN', DEVC_ID='TIMER23', RGB=240,230,140 /

##### DESK 24 ignited at time 1385 seconds

&OBST ID='DESK24', XB=8.8,11.2,16.8,19.2,0.0,0.6, SURF_ID='DESK', RGB=240,230,140/

&DEVC ID='TIMER24', XYZ=8.8,16.8,1.6, QUANTITY='TIME', SETPOINT=1385 / top
&VENT XB=8.8,11.2,16.8,19.2,0.6,0.6,  SURF_ID='BURN', DEVC_ID='TIMER24', RGB=240,230,140 /

##### DESK 25 ignited at time 1662 seconds

&OBST ID='DESK25', XB=12.8,15.2,16.8,19.2,0.0,0.6, SURF_ID='DESK', RGB=240,230,140/

&DEVC ID='TIMER25', XYZ=12.8,16.8,1.6, QUANTITY='TIME', SETPOINT=1662 / top
&VENT XB=12.8,15.2,16.8,19.2,0.6,0.6,  SURF_ID='BURN', DEVC_ID='TIMER25', RGB=240,230,140 /

##### DESK 26 ignited at time 1939 seconds

&OBST ID='DESK26', XB=12.8,15.2,20.8,23.2,0.0,0.6, SURF_ID='DESK', RGB=240,230,140/

&DEVC ID='TIMER26', XYZ=12.8,20.8,1.6, QUANTITY='TIME', SETPOINT=1939 / top
&VENT XB=12.8,15.2,20.8,23.2,0.6,0.6,  SURF_ID='BURN', DEVC_ID='TIMER26', RGB=240,230,140  ,

##### DESK 27 ignited at time 1939 seconds

&OBST ID='DESK27', XB=28.8,31.2,4.8,7.2,0.0,0.6, SURF_ID='DESK', RGB=240,230,140/

&DEVC ID='TIMER27', XYZ=28.8,4.8,1.6, QUANTITY='TIME', SETPOINT=1939 / top
&VENT XB=28.8,31.2,4.8,7.2,0.6,0.6,  SURF_ID='BURN', DEVC_ID='TIMER27', RGB=240,230,140  /
```

```
##### DESK 28 ignited at time 1939 seconds

&OBST ID='DESK28', XB=28.8,31.2,0.8,3.2,0.0,0.6, SURF_ID='DESK', RGB=240,230,140/

&DEVC ID='TIMER28', XYZ=28.8,0.8,1.6, QUANTITY='TIME', SETPOINT=1939 / top
&VENT XB=28.8,31.2,0.8,3.2,0.6,0.6,  SURF_ID='BURN', DEVC_ID='TIMER28', RGB=240,230,140 /

##### DESK 29 ignited at time 2216 seconds

&OBST ID='DESK29', XB=32.8,35.2,4.8,7.2,0.0,0.6, SURF_ID='DESK', RGB=240,230,140/

&DEVC ID='TIMER29', XYZ=32.8,4.8,1.6, QUANTITY='TIME', SETPOINT=2216 / top
&VENT XB=32.8,35.2,4.8,7.2,0.6,0.6,  SURF_ID='BURN', DEVC_ID='TIMER29', RGB=240,230,140 /

##### DESK 30 ignited at time 2216 seconds

&OBST ID='DESK30', XB=32.8,35.2,0.8,3.2,0.0,0.6, SURF_ID='DESK', RGB=240,230,140/

&DEVC ID='TIMER30', XYZ=32.8,0.8,1.6, QUANTITY='TIME', SETPOINT=2216 / top
&VENT XB=32.8,35.2,0.8,3.2,0.6,0.6,  SURF_ID='BURN', DEVC_ID='TIMER30', RGB=240,230,140 /

##### DESK 31 ignited at time 2216 seconds

&OBST ID='DESK31', XB=16.8,19.2,20.8,23.2,0.0,0.6, SURF_ID='DESK', RGB=240,230,140/

&DEVC ID='TIMER31', XYZ=16.8,20.8,1.6, QUANTITY='TIME', SETPOINT=2216 / top
&VENT XB=16.8,19.2,20.8,23.2,0.6,0.6,  SURF_ID='BURN', DEVC_ID='TIMER31', RGB=240,230,140 /

##### DESK 32 ignited at time 1939 seconds

&OBST ID='DESK32', XB=16.8,19.2,16.8,19.2,0.0,0.6, SURF_ID='DESK', RGB=240,230,140/

&DEVC ID='TIMER32', XYZ=16.8,16.8,1.6, QUANTITY='TIME', SETPOINT=1939 / top
&VENT XB=16.8,19.2,16.8,19.2,0.6,0.6,  SURF_ID='BURN', DEVC_ID='TIMER32', RGB=240,230,140 /

##### DESK 33 ignited at time 2493 seconds

&OBST ID='DESK33', XB=20.8,23.2,20.8,23.2,0.0,0.6, SURF_ID='DESK', RGB=240,230,140/

&DEVC ID='TIMER33', XYZ=20.8,20.8,1.6, QUANTITY='TIME', SETPOINT=2493 / top
&VENT XB=20.8,23.2,20.8,23.2,0.6,0.6,  SURF_ID='BURN', DEVC_ID='TIMER33', RGB=240,230,140 /

##### DESK 34 ignited at time 2216 seconds

&OBST ID='DESK34', XB=20.8,23.2,16.8,19.2,0.0,0.6, SURF_ID='DESK', RGB=240,230,140/
```

```
&DEVC ID='TIMER34', XYZ=20.8,16.8,1.6, QUANTITY='TIME', SETPOINT=2216 / top
&VENT XB=20.8,23.2,16.8,19.2,0.6,0.6,  SURF_ID='BURN', DEVC_ID='TIMER34', RGB=240,230,140 /

##### DESK 35 ignited at time 2493 seconds

&OBST ID='DESK35', XB=36.8,39.2,4.8,7.2,0.0,0.6, SURF_ID='DESK', RGB=240,230,140/

&DEVC ID='TIMER35', XYZ=36.8,4.8,1.6, QUANTITY='TIME', SETPOINT=2493 / top
&VENT XB=36.8,39.2,4.8,7.2,0.6,0.6,  SURF_ID='BURN', DEVC_ID='TIMER35', RGB=240,230,140 /

##### DESK 36 ignited at time 2493 seconds

&OBST ID='DESK36', XB=36.8,39.2,0.8,3.2,0.0,0.6, SURF_ID='DESK', RGB=240,230,140/

&DEVC ID='TIMER36', XYZ=36.8,0.8,1.6, QUANTITY='TIME', SETPOINT=2493 / top
&VENT XB=36.8,39.2,0.8,3.2,0.6,0.6,  SURF_ID='BURN', DEVC_ID='TIMER36', RGB=240,230,140 /

##### DESK 37 ignited at time 2770 seconds

&OBST ID='DESK37', XB=24.8,27.2,20.8,23.2,0.0,0.6, SURF_ID='DESK', RGB=240,230,140/

&DEVC ID='TIMER37', XYZ=24.8,20.8,1.6, QUANTITY='TIME', SETPOINT=2770 / top
&VENT XB=24.8,27.2,20.8,23.2,0.6,0.6,  SURF_ID='BURN', DEVC_ID='TIMER37', RGB=240,230,140 /

##### DESK 38 ignited at time 2493 seconds

&OBST ID='DESK38', XB=24.8,27.2,16.8,19.2,0.0,0.6, SURF_ID='DESK', RGB=240,230,140/

&DEVC ID='TIMER38', XYZ=24.8,16.8,1.6, QUANTITY='TIME', SETPOINT=2493 / top
&VENT XB=24.8,27.2,16.8,19.2,0.6,0.6,  SURF_ID='BURN', DEVC_ID='TIMER38', RGB=240,230,140 /

##### DESK 39 ignited at time 3047 seconds

&OBST ID='DESK39', XB=28.8,31.2,20.8,23.2,0.0,0.6, SURF_ID='DESK', RGB=240,230,140/

&DEVC ID='TIMER39', XYZ=28.8,20.8,1.6, QUANTITY='TIME', SETPOINT=3047 / top
&VENT XB=28.8,31.2,20.8,23.2,0.6,0.6,  SURF_ID='BURN', DEVC_ID='TIMER39', RGB=240,230,140 /

##### DESK 40 ignited at time 2770 seconds

&OBST ID='DESK40', XB=28.8,31.2,16.8,19.2,0.0,0.6, SURF_ID='DESK', RGB=240,230,140/

&DEVC ID='TIMER40', XYZ=28.8,16.8,1.6, QUANTITY='TIME', SETPOINT=2770 / top
&VENT XB=28.8,31.2,16.8,19.2,0.6,0.6,  SURF_ID='BURN', DEVC_ID='TIMER40', RGB=240,230,140 /
```

```
##### DESK 41 ignited at time 2493 seconds

&OBST ID='DESK41', XB=32.8,35.2,8.8,11.2,0.0,0.6, SURF_ID='DESK', RGB=240,230,140/

&DEVC ID='TIMER41', XYZ=32.8,8.8,1.6, QUANTITY='TIME', SETPOINT=2493 / top
&VENT XB=32.8,35.2,8.8,11.2,0.6,0.6,  SURF_ID='BURN', DEVC_ID='TIMER41', RGB=240,230,140 /

##### DESK 42 ignited at time 2770 seconds

&OBST ID='DESK42', XB=36.8,39.2,8.8,11.2,0.0,0.6, SURF_ID='DESK', RGB=240,230,140/

&DEVC ID='TIMER42', XYZ=36.8,8.8,1.6, QUANTITY='TIME', SETPOINT=2770 / top
&VENT XB=36.8,39.2,8.8,11.2,0.6,0.6,  SURF_ID='BURN', DEVC_ID='TIMER42', RGB=240,230,140 /

##### DESK 43 ignited at time 2770 seconds

&OBST ID='DESK43', XB=32.8,35.2,12.8,15.2,0.0,0.6, SURF_ID='DESK', RGB=240,230,140/

&DEVC ID='TIMER43', XYZ=32.8,12.8,1.6, QUANTITY='TIME', SETPOINT=2770 / top
&VENT XB=32.8,35.2,12.8,15.2,0.6,0.6,  SURF_ID='BURN', DEVC_ID='TIMER43', RGB=240,230,140 /

##### DESK 44 ignited at time 3047 seconds

&OBST ID='DESK44', XB=36.8,39.2,12.8,15.2,0.0,0.6, SURF_ID='DESK', RGB=240,230,140/

&DEVC ID='TIMER44', XYZ=36.8,12.8,1.6, QUANTITY='TIME', SETPOINT=3047 / top
&VENT XB=36.8,39.2,12.8,15.2,0.6,0.6,  SURF_ID='BURN', DEVC_ID='TIMER44',RGB=240,230,140  /

##### DESK 45 ignited at time 3047 seconds

&OBST ID='DESK45', XB=32.8,35.2,16.8,19.2,0.0,0.6, SURF_ID='DESK', RGB=240,230,140/

&DEVC ID='TIMER45', XYZ=32.8,16.8,1.6, QUANTITY='TIME', SETPOINT=3047 / top
&VENT XB=32.8,35.2,16.8,19.2,0.6,0.6,  SURF_ID='BURN', DEVC_ID='TIMER45', RGB=240,230,140 /

##### DESK 46 ignited at time 3324 seconds

&OBST ID='DESK46', XB=36.8,39.2,16.8,19.2,0.0,0.6, SURF_ID='DESK', RGB=240,230,140/

&DEVC ID='TIMER46', XYZ=32.8,16.8,1.6, QUANTITY='TIME', SETPOINT=3324 / top
&VENT XB=36.8,39.2,16.8,19.2,0.6,0.6,  SURF_ID='BURN', DEVC_ID='TIMER46', RGB=240,230,140 /

##### DESK 47 ignited at time 3324 seconds

&OBST ID='DESK47', XB=32.8,35.2,20.8,23.2,0.0,0.6, SURF_ID='DESK', RGB=240,230,140/
```

```
&DEVC ID='TIMER47', XYZ=32.8,20.8,1.6, QUANTITY='TIME', SETPOINT=3324 / top
&VENT XB=32.8,35.2,20.8,23.2,0.6,0.6,  SURF_ID='BURN', DEVC_ID='TIMER47', RGB=240,230,140 /

##### DESK 48 ignited at time 3601 seconds

&OBST ID='DESK48', XB=36.8,39.2,20.8,23.2,0.0,0.6, SURF_ID='DESK', RGB=240,230,140/

&DEVC ID='TIMER48', XYZ=36.8,20.8,1.6, QUANTITY='TIME', SETPOINT=3601 / top
&VENT XB=36.8,39.2,20.8,23.2,0.6,0.6,  SURF_ID='BURN', DEVC_ID='TIMER48',RGB=240,230,140  /

############## vertical slices #############
#### Temperature measurements to generate the color map using MATLAB

&DEVC ID='T1', XYZ=2,2,0.25, QUANTITY='TEMPERATURE'/
&DEVC ID='T3', XYZ=6,2,0.25, QUANTITY='TEMPERATURE'/
&DEVC ID='T7', XYZ=10,2,0.25, QUANTITY='TEMPERATURE'/
&DEVC ID='T10', XYZ=14,2,0.25, QUANTITY='TEMPERATURE'/
&DEVC ID='T13', XYZ=18,2,0.25, QUANTITY='TEMPERATURE'/
&DEVC ID='T19', XYZ=22,2,0.25, QUANTITY='TEMPERATURE'/
&DEVC ID='T22', XYZ=26,2,0.25, QUANTITY='TEMPERATURE'/
&DEVC ID='T28', XYZ=30,2,0.25, QUANTITY='TEMPERATURE'/
&DEVC ID='T30', XYZ=34,2,0.25, QUANTITY='TEMPERATURE'/
&DEVC ID='T36', XYZ=38,2,0.25, QUANTITY='TEMPERATURE'/

&DEVC ID='T1_1', XYZ=2,2,0.75, QUANTITY='TEMPERATURE'/
&DEVC ID='T3_1', XYZ=6,2,0.75, QUANTITY='TEMPERATURE'/
&DEVC ID='T7_1', XYZ=10,2,0.75, QUANTITY='TEMPERATURE'/
&DEVC ID='T10_1', XYZ=14,2,0.75, QUANTITY='TEMPERATURE'/
&DEVC ID='T13_1', XYZ=18,2,0.75, QUANTITY='TEMPERATURE'/
&DEVC ID='T19_1', XYZ=22,2,0.75, QUANTITY='TEMPERATURE'/
&DEVC ID='T22_1', XYZ=26,2,0.75, QUANTITY='TEMPERATURE'/
&DEVC ID='T28_1', XYZ=30,2,0.75, QUANTITY='TEMPERATURE'/
&DEVC ID='T30_1', XYZ=34,2,0.75, QUANTITY='TEMPERATURE'/
&DEVC ID='T36_1', XYZ=38,2,0.75, QUANTITY='TEMPERATURE'/

&DEVC ID='T1_2', XYZ=2,2,1.25, QUANTITY='TEMPERATURE'/
&DEVC ID='T3_2', XYZ=6,2,1.25, QUANTITY='TEMPERATURE'/
&DEVC ID='T7_2', XYZ=10,2,1.25, QUANTITY='TEMPERATURE'/
&DEVC ID='T10_2', XYZ=14,2,1.25, QUANTITY='TEMPERATURE'/
&DEVC ID='T13_2', XYZ=18,2,1.25, QUANTITY='TEMPERATURE'/
&DEVC ID='T19_2', XYZ=22,2,1.25, QUANTITY='TEMPERATURE'/
&DEVC ID='T22_2', XYZ=26,2,1.25, QUANTITY='TEMPERATURE'/
&DEVC ID='T28_2', XYZ=30,2,1.25, QUANTITY='TEMPERATURE'/
&DEVC ID='T30_2', XYZ=34,2,1.25, QUANTITY='TEMPERATURE'/
&DEVC ID='T36_2', XYZ=38,2,1.25, QUANTITY='TEMPERATURE'/
&DEVC ID='T1_3', XYZ=2,2,1.75, QUANTITY='TEMPERATURE'/
&DEVC ID='T3_3', XYZ=6,2,1.75, QUANTITY='TEMPERATURE'/
```

```
&DEVC ID='T7_3', XYZ=10,2,1.75, QUANTITY='TEMPERATURE'/
&DEVC ID='T10_3', XYZ=14,2,1.75, QUANTITY='TEMPERATURE'/
&DEVC ID='T13_3', XYZ=18,2,1.75, QUANTITY='TEMPERATURE'/
&DEVC ID='T19_3', XYZ=22,2,1.75, QUANTITY='TEMPERATURE'/
&DEVC ID='T22_3', XYZ=26,2,1.75, QUANTITY='TEMPERATURE'/
&DEVC ID='T28_3', XYZ=30,2,1.75, QUANTITY='TEMPERATURE'/
&DEVC ID='T30_3', XYZ=34,2,1.75, QUANTITY='TEMPERATURE'/
&DEVC ID='T36_3', XYZ=38,2,1.75, QUANTITY='TEMPERATURE'/

&DEVC ID='T1_4', XYZ=2,2,2.25,QUANTITY='TEMPERATURE'/
&DEVC ID='T3_4', XYZ=6,2,2.25, QUANTITY='TEMPERATURE'/
&DEVC ID='T7_4', XYZ=10,2,2.25, QUANTITY='TEMPERATURE'/
&DEVC ID='T10_4', XYZ=14,2,2.25, QUANTITY='TEMPERATURE'/
&DEVC ID='T13_4', XYZ=18,2,2.25, QUANTITY='TEMPERATURE'/
&DEVC ID='T19_4', XYZ=22,2,2.25, QUANTITY='TEMPERATURE'/
&DEVC ID='T22_4', XYZ=26,2,2.25, QUANTITY='TEMPERATURE'/
&DEVC ID='T28_4', XYZ=30,2,2.25, QUANTITY='TEMPERATURE'/
&DEVC ID='T30_4', XYZ=34,2,2.25, QUANTITY='TEMPERATURE'/
&DEVC ID='T36_4', XYZ=38,2,2.25, QUANTITY='TEMPERATURE'/

&DEVC ID='T1_5', XYZ=2,2,2.75, QUANTITY='TEMPERATURE'/
&DEVC ID='T3_5', XYZ=6,2,2.75, QUANTITY='TEMPERATURE'/
&DEVC ID='T7_5', XYZ=10,2,2.75, QUANTITY='TEMPERATURE'/
&DEVC ID='T10_5', XYZ=14,2,2.75, QUANTITY='TEMPERATURE'/
&DEVC ID='T13_5', XYZ=18,2,2.75, QUANTITY='TEMPERATURE'/
&DEVC ID='T19_5', XYZ=22,2,2.75, QUANTITY='TEMPERATURE'/
&DEVC ID='T22_5', XYZ=26,2,2.75, QUANTITY='TEMPERATURE'/
&DEVC ID='T28_5', XYZ=30,2,2.75, QUANTITY='TEMPERATURE'/
&DEVC ID='T30_5', XYZ=34,2,2.75, QUANTITY='TEMPERATURE'/
&DEVC ID='T36_5', XYZ=38,2,2.75, QUANTITY='TEMPERATURE'/

&DEVC ID='T5', XYZ=2,10,0.25, QUANTITY='TEMPERATURE'/
&DEVC ID='T6', XYZ=6,10,0.25, QUANTITY='TEMPERATURE'/
&DEVC ID='TA', XYZ=10,10,0.25, QUANTITY='TEMPERATURE'/
&DEVC ID='TB', XYZ=14,10,0.25, QUANTITY='TEMPERATURE'/
&DEVC ID='TC', XYZ=18,10,0.25, QUANTITY='TEMPERATURE'/
&DEVC ID='TD', XYZ=22,10,0.25, QUANTITY='TEMPERATURE'/
&DEVC ID='TE', XYZ=26,10,0.25, QUANTITY='TEMPERATURE'/
&DEVC ID='TF', XYZ=30,10,0.25, QUANTITY='TEMPERATURE'/
&DEVC ID='T41', XYZ=34,10,0.25, QUANTITY='TEMPERATURE'/
&DEVC ID='T42', XYZ=38,10,0.25, QUANTITY='TEMPERATURE'/

&DEVC ID='T5_1', XYZ=2,10,0.75, QUANTITY='TEMPERATURE'/
&DEVC ID='T6_1', XYZ=6,10,0.75, QUANTITY='TEMPERATURE'/
&DEVC ID='TA_1', XYZ=10,10,0.75, QUANTITY='TEMPERATURE'/
&DEVC ID='TB_1', XYZ=14,10,0.75, QUANTITY='TEMPERATURE'/
```

```
&DEVC ID='TC_1', XYZ=18,10,0.75, QUANTITY='TEMPERATURE'/
&DEVC ID='TD_1', XYZ=22,10,0.75, QUANTITY='TEMPERATURE'/
&DEVC ID='TE_1', XYZ=26,10,0.75, QUANTITY='TEMPERATURE'/
&DEVC ID='TF_1', XYZ=30,10,0.75, QUANTITY='TEMPERATURE'/
&DEVC ID='T41_1', XYZ=34,10,0.75, QUANTITY='TEMPERATURE'/
&DEVC ID='T42_1', XYZ=38,10,0.75, QUANTITY='TEMPERATURE'/

&DEVC ID='T5_2', XYZ=2,10,1.25, QUANTITY='TEMPERATURE'/
&DEVC ID='T6_2', XYZ=6,10,1.25, QUANTITY='TEMPERATURE'/
&DEVC ID='TA_2', XYZ=10,10,1.25, QUANTITY='TEMPERATURE'/
&DEVC ID='TB_2', XYZ=14,10,1.25, QUANTITY='TEMPERATURE'/
&DEVC ID='TC_2', XYZ=18,10,1.25, QUANTITY='TEMPERATURE'/
&DEVC ID='TD_2', XYZ=22,10,1.25, QUANTITY='TEMPERATURE'/
&DEVC ID='TE_2', XYZ=26,10,1.25, QUANTITY='TEMPERATURE'/
&DEVC ID='TF_2', XYZ=30,10,1.25, QUANTITY='TEMPERATURE'/
&DEVC ID='T41_2', XYZ=34,10,1.25, QUANTITY='TEMPERATURE'/
&DEVC ID='T42_2', XYZ=38,10,1.25, QUANTITY='TEMPERATURE'/

&DEVC ID='T5_3', XYZ=2,10,1.75, QUANTITY='TEMPERATURE'/
&DEVC ID='T6_3', XYZ=6,10,1.75, QUANTITY='TEMPERATURE'/
&DEVC ID='TA_3', XYZ=10,10,1.75, QUANTITY='TEMPERATURE'/
&DEVC ID='TB_3', XYZ=14,10,1.75, QUANTITY='TEMPERATURE'/
&DEVC ID='TC_3', XYZ=18,10,1.75, QUANTITY='TEMPERATURE'/
&DEVC ID='TD_3', XYZ=22,10,1.75, QUANTITY='TEMPERATURE'/
&DEVC ID='TE_3', XYZ=26,10,1.75, QUANTITY='TEMPERATURE'/
&DEVC ID='TF_3', XYZ=30,10,1.75, QUANTITY='TEMPERATURE'/
&DEVC ID='T41_3', XYZ=34,10,1.75, QUANTITY='TEMPERATURE'/
&DEVC ID='T42_3', XYZ=38,10,1.75, QUANTITY='TEMPERATURE'/

&DEVC ID='T5_4', XYZ=2,10,2.25, QUANTITY='TEMPERATURE'/
&DEVC ID='T6_4', XYZ=6,10,2.25, QUANTITY='TEMPERATURE'/
&DEVC ID='TA_4', XYZ=10,10,2.25, QUANTITY='TEMPERATURE'/
&DEVC ID='TB_4', XYZ=14,10,2.25, QUANTITY='TEMPERATURE'/
&DEVC ID='TC_4', XYZ=18,10,2.25, QUANTITY='TEMPERATURE'/
&DEVC ID='TD_4', XYZ=22,10,2.25, QUANTITY='TEMPERATURE'/
&DEVC ID='TE_4', XYZ=26,10,2.25, QUANTITY='TEMPERATURE'/
&DEVC ID='TF_4', XYZ=30,10,2.25, QUANTITY='TEMPERATURE'/
&DEVC ID='T41_4', XYZ=34,10,2.25, QUANTITY='TEMPERATURE'/
&DEVC ID='T42_4', XYZ=38,10,2.25, QUANTITY='TEMPERATURE'/

&DEVC ID='T5_5', XYZ=2,10,2.75, QUANTITY='TEMPERATURE'/
&DEVC ID='T6_5', XYZ=6,10,2.75, QUANTITY='TEMPERATURE'/
&DEVC ID='TA_5', XYZ=10,10,2.75, QUANTITY='TEMPERATURE'/
&DEVC ID='TB_5', XYZ=14,10,2.75, QUANTITY='TEMPERATURE'/
&DEVC ID='TC_5', XYZ=18,10,2.75, QUANTITY='TEMPERATURE'/
&DEVC ID='TD_5', XYZ=22,10,2.75, QUANTITY='TEMPERATURE'/
```

```
&DEVC ID='TE_5', XYZ=26,10,2.75, QUANTITY='TEMPERATURE'/
&DEVC ID='TF_5', XYZ=30,10,2.75, QUANTITY='TEMPERATURE'/
&DEVC ID='T41_5', XYZ=34,10,2.75, QUANTITY='TEMPERATURE'/
&DEVC ID='T42_5', XYZ=38,10,2.75, QUANTITY='TEMPERATURE'/

&DEVC ID='T17', XYZ=2,22,0.25, QUANTITY='TEMPERATURE'/
&DEVC ID='T18', XYZ=6,22,0.25, QUANTITY='TEMPERATURE'/
&DEVC ID='T23', XYZ=10,22,0.25, QUANTITY='TEMPERATURE'/
&DEVC ID='T26', XYZ=14,22,0.25, QUANTITY='TEMPERATURE'/
&DEVC ID='T31', XYZ=18,22,0.25, QUANTITY='TEMPERATURE'/
&DEVC ID='T33', XYZ=22,22,0.25, QUANTITY='TEMPERATURE'/
&DEVC ID='T37', XYZ=26,22,0.25, QUANTITY='TEMPERATURE'/
&DEVC ID='T39', XYZ=30,22,0.25, QUANTITY='TEMPERATURE'/
&DEVC ID='T47', XYZ=34,22,0.25, QUANTITY='TEMPERATURE'/
&DEVC ID='T48', XYZ=38,22,0.25, QUANTITY='TEMPERATURE'/

&DEVC ID='T17_1', XYZ=2,22,0.75, QUANTITY='TEMPERATURE'/
&DEVC ID='T18_1', XYZ=6,22,0.75, QUANTITY='TEMPERATURE'/
&DEVC ID='T23_1', XYZ=10,22,0.75, QUANTITY='TEMPERATURE'/
&DEVC ID='T26_1', XYZ=14,22,0.75, QUANTITY='TEMPERATURE'/
&DEVC ID='T31_1', XYZ=18,22,0.75, QUANTITY='TEMPERATURE'/
&DEVC ID='T33_1', XYZ=22,22,0.75, QUANTITY='TEMPERATURE'/
&DEVC ID='T37_1', XYZ=26,22,0.75, QUANTITY='TEMPERATURE'/
&DEVC ID='T39_1', XYZ=30,22,0.75, QUANTITY='TEMPERATURE'/
&DEVC ID='T47_1', XYZ=34,22,0.75, QUANTITY='TEMPERATURE'/
&DEVC ID='T48_1', XYZ=38,22,0.75, QUANTITY='TEMPERATURE'/

&DEVC ID='T17_2', XYZ=2,22,1.25, QUANTITY='TEMPERATURE'/
&DEVC ID='T18_2', XYZ=6,22,1.25, QUANTITY='TEMPERATURE'/
&DEVC ID='T23_2', XYZ=10,22,1.25, QUANTITY='TEMPERATURE'/
&DEVC ID='T26_2', XYZ=14,22,1.25, QUANTITY='TEMPERATURE'/
&DEVC ID='T31_2', XYZ=18,22,1.25, QUANTITY='TEMPERATURE'/
&DEVC ID='T33_2', XYZ=22,22,1.25, QUANTITY='TEMPERATURE'/
&DEVC ID='T37_2', XYZ=26,22,1.25, QUANTITY='TEMPERATURE'/
&DEVC ID='T39_2', XYZ=30,22,1.25, QUANTITY='TEMPERATURE'/
&DEVC ID='T47_2', XYZ=34,22,1.25, QUANTITY='TEMPERATURE'/
&DEVC ID='T48_2', XYZ=38,22,1.25, QUANTITY='TEMPERATURE'/

&DEVC ID='T17_3', XYZ=2,22,1.75, QUANTITY='TEMPERATURE'/
&DEVC ID='T18_3', XYZ=6,22,1.75, QUANTITY='TEMPERATURE'/
&DEVC ID='T23_3', XYZ=10,22,1.75, QUANTITY='TEMPERATURE'/
&DEVC ID='T26_3', XYZ=14,22,1.75, QUANTITY='TEMPERATURE'/
&DEVC ID='T31_3', XYZ=18,22,1.75, QUANTITY='TEMPERATURE'/
&DEVC ID='T33_3', XYZ=22,22,1.75, QUANTITY='TEMPERATURE'/
&DEVC ID='T37_3', XYZ=26,22,1.75, QUANTITY='TEMPERATURE'/
&DEVC ID='T39_3', XYZ=30,22,1.75, QUANTITY='TEMPERATURE'/
```

```
&DEVC ID='T47_3', XYZ=34,22,1.75, QUANTITY='TEMPERATURE'/
&DEVC ID='T48_3', XYZ=38,22,1.75, QUANTITY='TEMPERATURE'/

&DEVC ID='T17_4', XYZ=2,22,2.25, QUANTITY='TEMPERATURE'/
&DEVC ID='T18_4', XYZ=6,22,2.25, QUANTITY='TEMPERATURE'/
&DEVC ID='T23_4', XYZ=10,22,2.25, QUANTITY='TEMPERATURE'/
&DEVC ID='T26_4', XYZ=14,22,2.25, QUANTITY='TEMPERATURE'/
&DEVC ID='T31_4', XYZ=18,22,2.25, QUANTITY='TEMPERATURE'/
&DEVC ID='T33_4', XYZ=22,22,2.25, QUANTITY='TEMPERATURE'/
&DEVC ID='T37_4', XYZ=26,22,2.25, QUANTITY='TEMPERATURE'/
&DEVC ID='T39_4', XYZ=30,22,2.25, QUANTITY='TEMPERATURE'/
&DEVC ID='T47_4', XYZ=34,22,2.25, QUANTITY='TEMPERATURE'/
&DEVC ID='T48_4', XYZ=38,22,2.25, QUANTITY='TEMPERATURE'/

&DEVC ID='T17_5', XYZ=2,22,2.75, QUANTITY='TEMPERATURE'/
&DEVC ID='T18_5', XYZ=6,22,2.75, QUANTITY='TEMPERATURE'/
&DEVC ID='T23_5', XYZ=10,22,2.75, QUANTITY='TEMPERATURE'/
&DEVC ID='T26_5', XYZ=14,22,2.75, QUANTITY='TEMPERATURE'/
&DEVC ID='T31_5', XYZ=18,22,2.75, QUANTITY='TEMPERATURE'/
&DEVC ID='T33_5', XYZ=22,22,2.75, QUANTITY='TEMPERATURE'/
&DEVC ID='T37_5', XYZ=26,22,2.75, QUANTITY='TEMPERATURE'/
&DEVC ID='T39_5', XYZ=30,22,2.75, QUANTITY='TEMPERATURE'/
&DEVC ID='T47_5', XYZ=34,22,2.75, QUANTITY='TEMPERATURE'/
&DEVC ID='T48_5', XYZ=38,22,2.75, QUANTITY='TEMPERATURE'/

############ horizontal slices ##############
# Temperature measurements to generate the color map in MATLAB

&DEVC ID='T1_6', XYZ=2,2,2.75,  QUANTITY='TEMPERATURE'/
&DEVC ID='T3_6', XYZ=6,2,2.75,  QUANTITY='TEMPERATURE'/
&DEVC ID='T7_6', XYZ=10,2,2.75, QUANTITY='TEMPERATURE'/
&DEVC ID='T10_6', XYZ=14,2,2.75, QUANTITY='TEMPERATURE'/
&DEVC ID='T13_6', XYZ=18,2,2.75, QUANTITY='TEMPERATURE'/
&DEVC ID='T19_6', XYZ=22,2,2.75, QUANTITY='TEMPERATURE'/
&DEVC ID='T22_6', XYZ=26,2,2.75, QUANTITY='TEMPERATURE'/
&DEVC ID='T28_6', XYZ=30,2,2.75, QUANTITY='TEMPERATURE'/
&DEVC ID='T30_6', XYZ=34,2,2.75, QUANTITY='TEMPERATURE'/
&DEVC ID='T36_6', XYZ=38,2,2.75, QUANTITY='TEMPERATURE'/

&DEVC ID='T2_6', XYZ=2,4,2.75,  QUANTITY='TEMPERATURE'/
&DEVC ID='T4_6', XYZ=6,6,2.75,  QUANTITY='TEMPERATURE'/
&DEVC ID='T8_6', XYZ=10,6,2.75, QUANTITY='TEMPERATURE'/
&DEVC ID='T9_6', XYZ=14,6,2.75, QUANTITY='TEMPERATURE'/
&DEVC ID='T14_6', XYZ=18,6,2.75, QUANTITY='TEMPERATURE'/
&DEVC ID='T20_6', XYZ=22,6,2.75, QUANTITY='TEMPERATURE'/
&DEVC ID='T21_6', XYZ=26,6,2.75, QUANTITY='TEMPERATURE'/
```

```
&DEVC ID='T27_6', XYZ=30,6,2.75, QUANTITY='TEMPERATURE'/
&DEVC ID='T29_6', XYZ=34,6,2.75, QUANTITY='TEMPERATURE'/
&DEVC ID='T35_6', XYZ=38,6,2.75, QUANTITY='TEMPERATURE'/

&DEVC ID='T5_6', XYZ=2,10,2.75,  QUANTITY='TEMPERATURE'/
&DEVC ID='T6_6', XYZ=6,10,2.75,  QUANTITY='TEMPERATURE'/
&DEVC ID='TA_6', XYZ=10,10,2.75, QUANTITY='TEMPERATURE'/
&DEVC ID='TB_6', XYZ=14,10,2.75, QUANTITY='TEMPERATURE'/
&DEVC ID='TC_6', XYZ=18,10,2.75, QUANTITY='TEMPERATURE'/
&DEVC ID='TD_6', XYZ=22,10,2.75, QUANTITY='TEMPERATURE'/
&DEVC ID='TE_6', XYZ=26,10,2.75, QUANTITY='TEMPERATURE'/
&DEVC ID='TF_6', XYZ=30,10,2.75, QUANTITY='TEMPERATURE'/
&DEVC ID='T41_6', XYZ=34,10,2.75, QUANTITY='TEMPERATURE'/
&DEVC ID='T42_6', XYZ=38,10,2.75, QUANTITY='TEMPERATURE'/

&DEVC ID='T11_6', XYZ=2,14,2.75, QUANTITY='TEMPERATURE'/
&DEVC ID='T12_6', XYZ=6,14,2.75, QUANTITY='TEMPERATURE'/
&DEVC ID='TG_6',XYZ=10,14,2.75, QUANTITY='TEMPERATURE'/
&DEVC ID='TH_6', XYZ=14,14,2.75, QUANTITY='TEMPERATURE'/
&DEVC ID='TI_6', XYZ=18,14,2.75, QUANTITY='TEMPERATURE'/
&DEVC ID='TL_6', XYZ=22,14,2.75, QUANTITY='TEMPERATURE'/
&DEVC ID='TM_6', XYZ=26,14,2.75, QUANTITY='TEMPERATURE'/
&DEVC ID='TN_6', XYZ=30,14,2.75, QUANTITY='TEMPERATURE'/
&DEVC ID='T43_6', XYZ=34,14,2.75, QUANTITY='TEMPERATURE'/
&DEVC ID='T44_6', XYZ=38,14,2.75, QUANTITY='TEMPERATURE'/

&DEVC ID='T15_6', XYZ=2,18,2.75, QUANTITY='TEMPERATURE'/
&DEVC ID='T16_6', XYZ=6,18,2.75, QUANTITY='TEMPERATURE'/
&DEVC ID='T24_6', XYZ=10,18,2.75, QUANTITY='TEMPERATURE'/
&DEVC ID='T25_6', XYZ=14,18,2.75, QUANTITY='TEMPERATURE'/
&DEVC ID='T32_6', XYZ=18,18,2.75, QUANTITY='TEMPERATURE'/
&DEVC ID='T34_6', XYZ=22,18,2.75, QUANTITY='TEMPERATURE'/
&DEVC ID='T38_6', XYZ=26,18,2.75, QUANTITY='TEMPERATURE'/
&DEVC ID='T40_6', XYZ=30,18,2.75, QUANTITY='TEMPERATURE'/
&DEVC ID='T45_6', XYZ=34,18,2.75, QUANTITY='TEMPERATURE'/
&DEVC ID='T46_6', XYZ=38,18,2.75, QUANTITY='TEMPERATURE'/

&DEVC ID='T17_6', XYZ=2,22,2.75, QUANTITY='TEMPERATURE'/
&DEVC ID='T18_6', XYZ=6,22,2.75, QUANTITY='TEMPERATURE'/
&DEVC ID='T23_6', XYZ=10,22,2.75, QUANTITY='TEMPERATURE'/
&DEVC ID='T26_6', XYZ=14,22,2.75, QUANTITY='TEMPERATURE'/
&DEVC ID='T31_6', XYZ=18,22,2.75, QUANTITY='TEMPERATURE'/
&DEVC ID='T33_6', XYZ=22,22,2.75, QUANTITY='TEMPERATURE'/
&DEVC ID='T37_6', XYZ=26,22,2.75, QUANTITY='TEMPERATURE'/
&DEVC ID='T39_6', XYZ=30,22,2.75, QUANTITY='TEMPERATURE'/
&DEVC ID='T47_6', XYZ=34,22,2.75, QUANTITY='TEMPERATURE'/
```

```
&DEVC ID='T48_6', XYZ=38,22,2.75, QUANTITY='TEMPERATURE'/

############## Visibility #############

&DEVC ID='V1', XYZ=6,10,0.25,  QUANTITY='VISIBILITY'/
&DEVC ID='V2', XYZ=6,10,0.75,  QUANTITY='VISIBILITY'/
&DEVC ID='V3', XYZ=6,10,1.25,  QUANTITY='VISIBILITY'/
&DEVC ID='V4', XYZ=6,10,1.75,  QUANTITY='VISIBILITY'/
&DEVC ID='V5', XYZ=6,10,2.25,  QUANTITY='VISIBILITY'/
&DEVC ID='V6', XYZ=6,10,2.75,  QUANTITY='VISIBILITY'/
&DEVC ID='V7', XYZ=34,10,0.25, QUANTITY='VISIBILITY'/
&DEVC ID='V8', XYZ=34,10,0.75, QUANTITY='VISIBILITY'/
&DEVC ID='V9', XYZ=34,10,1.25, QUANTITY='VISIBILITY'/
&DEVC ID='V10', XYZ=34,10,1.75, QUANTITY='VISIBILITY'/
&DEVC ID='V11', XYZ=34,10,2.25, QUANTITY='VISIBILITY'/
&DEVC ID='V12', XYZ=34,10,2.75, QUANTITY='VISIBILITY'/

&DEVC ID='beam6_1_v', XB=6.0,6.0,8.0,12.0,0.25,0.25, QUANTITY='PATH OBSCURATION',
SETPOINT=33.0/
&DEVC ID='beam6_2_v', XB=6.0,6.0,8.0,12.0,0.75,0.75, QUANTITY='PATH OBSCURATION',
SETPOINT=33.0/
&DEVC ID='beam6_3_v', XB=6.0,6.0,8.0,12.0,1.25,1.25, QUANTITY='PATH OBSCURATION',
SETPOINT=33.0/
&DEVC ID='beam6_4_v', XB=6.0,6.0,8.0,12.0,1.75,1.75, QUANTITY='PATH OBSCURATION',
SETPOINT=33.0/
&DEVC ID='beam6_5_v', XB=6.0,6.0,8.0,12.0,2.25,2.25, QUANTITY='PATH OBSCURATION',
SETPOINT=33.0/
&DEVC ID='beam6_6_v', XB=6.0,6.0,8.0,12.0,2.75,2.75, QUANTITY='PATH OBSCURATION',
SETPOINT=33.0/
&DEVC ID='beam41_1_v', XB=34.0,34.0,8.0,12.0,0.25,0.25, QUANTITY='PATH OBSCURATION',
SETPOINT=33.0/
&DEVC ID='beam41_2_v', XB=34.0,34.0,8.0,12.0,0.75,0.75, QUANTITY='PATH OBSCURATION',
SETPOINT=33.0/
&DEVC ID='beam41_3_v', XB=34.0,34.0,8.0,12.0,1.25,1.25, QUANTITY='PATH OBSCURATION',
SETPOINT=33.0/
&DEVC ID='beam41_4_v', XB=34.0,34.0,8.0,12.0,1.75,1.75, QUANTITY='PATH OBSCURATION',
SETPOINT=33.0/
&DEVC ID='beam41_5_v', XB=34.0,34.0,8.0,12.0,2.25,2.25, QUANTITY='PATH OBSCURATION',
SETPOINT=33.0/
&DEVC ID='beam41_6_v', XB=34.0,34.0,8.0,12.0,2.75,2.75, QUANTITY='PATH OBSCURATION',
SETPOINT=33.0/

############## SLICES #############

&SLCF PBY=2.0, QUANTITY='TEMPERATURE'/ south
&SLCF PBY=10.0, QUANTITY='TEMPERATURE'/ central
```

```
&SLCF PBY=22.0, QUANTITY='TEMPERATURE'/ north
&SLCF PBZ=2.75, QUANTITY='TEMPERATURE'/ as in MZ fire model
&SLCF PBZ=2.0,QUANTITY='TEMPERATURE'/
&SLCF PBX=6.0,QUANTITY='VISIBILITY'/
&SLCF PBX=34.0, QUANTITY='VISIBILITY'/
&SLCF PBY=6.0, QUANTITY='VISIBILITY'/
&SLCF PBY=18.0, QUANTITY='VISIBILITY'/
&SLCF PBZ=2.0, QUANTITY='VISIBILITY'/

############ MASS FLOW #############

&DEVC ID='MF_out_LW', XB=0.1,0.1,4.0,20.0,0.0,1.0, QUANTITY='MASS FLOW +'/
&DEVC ID='MF_in_LW', XB=0.1,0.1,4.0,20.0,0.0,1.0, QUANTITY='MASS FLOW -'/
&DEVC ID='MF_out_RW', XB=40.1,40.1,4.0,20.0,0.0,1.0, QUANTITY='MASS FLOW +'/
&DEVC ID='MF_in_RW', XB=40.1,40.1,4.0,20.0,0.0,1.0, QUANTITY='MASS FLOW -'/
&DEVC ID='MF_out_UW', XB=4.0,8.0,24.1,24.1,0.0,1.0, QUANTITY='MASS FLOW +'/
&DEVC ID='MF_in_UW', XB=4.0,8.0,24.1,24.1,0.0,1.0, QUANTITY='MASS FLOW -'/
&DEVC ID='MF_out_UW1', XB=8.0,12.0,24.1,24.1,0.0,1.0, QUANTITY='MASS FLOW +'/
&DEVC ID='MF_in_UW1', XB=8.0,12.0,24.1,24.1,0.0,1.0, QUANTITY='MASS FLOW -'/
&DEVC ID='MF_out_UW2', XB=12.0,16.0,24.1,24.1,0.0,1.0, QUANTITY='MASS FLOW +'/
&DEVC ID='MF_in_UW2', XB=12.0,16.0,24.1,24.1,0.0,1.0, QUANTITY='MASS FLOW -'/
&DEVC ID='MF_out_UW3', XB=16.0,18.0,24.1,24.1,0.0,1.0, QUANTITY='MASS FLOW +'/
&DEVC ID='MF_in_UW3', XB=16.0,18.0,24.1,24.1,0.0,1.0, QUANTITY='MASS FLOW -'/
&DEVC ID='MF_out_UW4', XB=18.0,20.0,24.1,24.1,0.0,1.0, QUANTITY='MASS FLOW +'/
&DEVC ID='MF_in_UW4', XB=18.0,20.0,24.1,24.1,0.0,1.0, QUANTITY='MASS FLOW -'/
&DEVC ID='MF_out_UW5', XB=20.0,24.0,24.1,24.1,0.0,1.0, QUANTITY='MASS FLOW +'/
&DEVC ID='MF_in_UW5', XB=20.0,24.0,24.1,24.1,0.0,1.0, QUANTITY='MASS FLOW -'/
&DEVC ID='MF_out_UW6', XB=24.0,28.0,24.1,24.1,0.0,1.0, QUANTITY='MASS FLOW +'/
&DEVC ID='MF_in_UW6', XB=24.0,28.0,24.1,24.1,0.0,1.0, QUANTITY='MASS FLOW -'/
&DEVC ID='MF_out_UW7', XB=28.0,32.0,24.1,24.1,0.0,1.0, QUANTITY='MASS FLOW +'/
&DEVC ID='MF_in_UW7',XB=28.0,32.0,24.1,24.1,0.0,1.0, QUANTITY='MASS FLOW -'/
&DEVC ID='MF_out_UW8', XB=32.0,36.0,24.1,24.1,0.0,1.0, QUANTITY='MASS FLOW +'/
&DEVC ID='MF_in_UW8', XB=32.0,36.0,24.1,24.1,0.0,1.0, QUANTITY='MASS FLOW -'/

&DEVC ID='MF_out_LLW', XB=4.0,8.0,0.1,0.1,0.0,1.0, QUANTITY='MASS FLOW +'/
&DEVC ID='MF_in_LLW', XB=4.0,8.0,0.1,0.1,0.0,1.0, QUANTITY='MASS FLOW -'/
&DEVC ID='MF_out_LLW1', XB=8.0,12.0,0.1,0.1,0.0,1.0, QUANTITY='MASS FLOW +'/
&DEVC ID='MF_in_LLW1', XB=8.0,12.0,0.1,0.1,0.0,1.0, QUANTITY='MASS FLOW -'/
&DEVC ID='MF_out_LLW2', XB=12.0,16.0,0.1,0.1,0.0,1.0, QUANTITY='MASS FLOW +'/
&DEVC ID='MF_in_LLW2', XB=12.0,16.0,0.1,0.1,0.0,1.0, QUANTITY='MASS FLOW -'/
&DEVC ID='MF_out_LLW3', XB=16.0,20.0,0.1,0.1,0.0,1.0, QUANTITY='MASS FLOW +'/
&DEVC ID='MF_in_LLW3', XB=16.0,20.0,0.1,0.1,0.0,1.0, QUANTITY='MASS FLOW -'/
&DEVC ID='MF_out_LLW4', XB=20.0,24.0,0.1,0.1,0.0,1.0, QUANTITY='MASS FLOW +'/
&DEVC ID='MF_in_LLW4', XB=20.0,24.0,0.1,0.1,0.0,1.0, QUANTITY='MASS FLOW -'/
&DEVC ID='MF_out_LLW5', XB=24.0,28.0,0.1,0.1,0.0,1.0, QUANTITY='MASS FLOW +'/
&DEVC ID='MF_in_LLW5', XB=24.0,28.0,0.1,0.1,0.0,1.0, QUANTITY='MASS FLOW -'/
```

```
&DEVC ID='MF_out_LLW6', XB=28.0,32.0,0.1,0.1,0.0,1.0, QUANTITY='MASS FLOW +'/
&DEVC ID='MF_in_LLW6', XB=28.0,32.0,0.1,0.1,0.0,1.0, QUANTITY='MASS FLOW -'/
&DEVC ID='MF_out_LLW7', XB=32.0,36.0,0.1,0.1,0.0,1.0, QUANTITY='MASS FLOW +'/
&DEVC ID='MF_in_LLW7', XB=32.0,36.0,0.1,0.1,0.0,1.0, QUANTITY='MASS FLOW -'/
&DEVC ID='MF_out_LLW8', XB=36.0,40.0,0.1,0.1,0.0,1.0, QUANTITY='MASS FLOW +'/
&DEVC ID='MF_in_LLW8', XB=36.0,40.0,0.1,0.1,0.0,1.0, QUANTITY='MASS FLOW -'/

&TAIL/
```

Appendix H: Office scenario code: MZ fire model (time ignition)

```
&MESH IJK=10, 6, 6,  XB=0,40,0,24,0,3/
&TIME T_END=4712/
&MISC TMPA=20/

&FIRE  XB=0.8,3.2,0.8,3.2,0.6,0.6,alfa_t2=0.012,HRRPUA=279,t_begin=0,t_stop=1110,
RADI=0.35, SOOT_YIELD=0.015, HEAT_OF_COMBUSTION=18000/  1
&FIRE  XB=0.8,3.2,4.8,7.2,0.6,0.6,alfa_t2=0.012, HRRPUA=279,t_begin=277,t_stop=1387,
RADI=0.35, SOOT_YIELD=0.015, HEAT_OF_COMBUSTION=18000/  2
&FIRE  XB=4.8,7.2,0.8,3.2,0.6,0.6,alfa_t2=0.012,HRRPUA=279,t_begin=277,t_stop=1387,
RADI=0.35, SOOT_YIELD=0.015, HEAT_OF_COMBUSTION=18000/  3
&FIRE  XB=4.8,7.2,4.8,7.2,0.6,0.6, alfa_t2=0.012, HRRPUA=279,t_begin=277,t_stop=1387,
RADI=0.35, SOOT_YIELD=0.015, HEAT_OF_COMBUSTION=18000/  4
&FIRE  XB=0.8,3.2,8.8,11.2,0.6,0.6, alfa_t2=0.012, HRRPUA=279, t_begin=554,t_stop=1664,
RADI=0.35, SOOT_YIELD=0.015, HEAT_OF_COMBUSTION=18000/  5
&FIRE  XB=4.8,7.2,8.8,11.2,0.6,0.6, alfa_t2=0.012, HRRPUA=279, t_begin=554, t_stop=1664,
RADI=0.35, SOOT_YIELD=0.015, HEAT_OF_COMBUSTION=18000/  6
&FIRE  XB=8.8,11.2,0.8,3.2,0.6,0.6, alfa_t2=0.012, HRRPUA=279, t_begin=554, t_stop=1664,
RADI=0.35, SOOT_YIELD=0.015, HEAT_OF_COMBUSTION=18000/  7
&FIRE  XB=8.8,11.2,4.8,7.2,0.6,0.6, alfa_t2=0.012, HRRPUA=279, t_begin=554, t_stop=1664,
RADI=0.35, SOOT_YIELD=0.015, HEAT_OF_COMBUSTION=18000/  8
&FIRE  XB=12.8,15.2,4.8,7.2,0.6,0.6, alfa_t2=0.012, HRRPUA=279, t_begin=831, t_stop=1941,
RADI=0.35, SOOT_YIELD=0.015, HEAT_OF_COMBUSTION=18000/  9
&FIRE  XB=12.8,15.2,0.8,3.2,0.6,0.6, alfa_t2=0.012, HRRPUA=279, t_begin=831, t_stop=1941,
RADI=0.35, SOOT_YIELD=0.015, HEAT_OF_COMBUSTION=18000/  10
&FIRE  XB=0.8,3.2,12.8,15.2,0.6,0.6, alfa_t2=0.012, HRRPUA=279, t_begin=831, t_stop=1941,
RADI=0.35, SOOT_YIELD=0.015, HEAT_OF_COMBUSTION=18000/  11
&FIRE  XB=4.8,7.2,12.8,15.2,0.6,0.6, alfa_t2=0.012, HRRPUA=279, t_begin=831, t_stop=1941,
RADI=0.35, SOOT_YIELD=0.015, HEAT_OF_COMBUSTION=18000/  12
&FIRE  XB=16.8,19.2,0.8,3.2,0.6,0.6, alfa_t2=0.012, HRRPUA=279, t_begin=1108, t_stop=2218,
RADI=0.35, SOOT_YIELD=0.015, HEAT_OF_COMBUSTION=18000/  13
&FIRE  XB=16.8,19.2,4.8,7.2,0.6,0.6, alfa_t2=0.012, HRRPUA=279, t_begin=1108, t_stop=2218,
RADI=0.35, SOOT_YIELD=0.015, HEAT_OF_COMBUSTION=18000/  14
&FIRE  XB=0.8,3.2,16.8,19.2,0.6,0.6, alfa_t2=0.012, HRRPUA=279, t_begin=1108, t_stop=2218,
RADI=0.35, SOOT_YIELD=0.015, HEAT_OF_COMBUSTION=18000/  15
&FIRE  XB=4.8,7.2,16.8,19.2,0.6,0.6, alfa_t2=0.012, HRRPUA=279, t_begin=1108, t_stop=2218,
RADI=0.35, SOOT_YIELD=0.015, HEAT_OF_COMBUSTION=18000/  16
&FIRE  XB=0.8,3.2,20.8,23.2,0.6,0.6, alfa_t2=0.012, HRRPUA=279, t_begin=1385, t_stop=2495,
RADI=0.35, SOOT_YIELD=0.015, HEAT_OF_COMBUSTION=18000/  17
&FIRE  XB=4.8,7.2,20.8.0,23.2,0.6,0.6, alfa_t2=0.012, HRRPUA=279, t_begin=1385, t_stop=2495,
RADI=0.35, SOOT_YIELD=0.015, HEAT_OF_COMBUSTION=18000/  18
&FIRE  XB=20.8,23.2,0.8,3.2,0.6,0.6, alfa_t2=0.012, HRRPUA=279, t_begin=1385, t_stop=2495,
RADI=0.35, SOOT_YIELD=0.015, HEAT_OF_COMBUSTION=18000/  19
&FIRE  XB=20.8,23.2,4.8,7.2,0.6,0.6, alfa_t2=0.012, HRRPUA=279, t_begin=1385, t_stop=2495,
RADI=0.35, SOOT_YIELD=0.015, HEAT_OF_COMBUSTION=18000/  20
&FIRE  XB=24.8,27.2,4.8,7.2,0.6,0.6, alfa_t2=0.012, HRRPUA=279, t_begin=1662, t_stop=2772,
RADI=0.35, SOOT_YIELD=0.015, HEAT_OF_COMBUSTION=18000/  21
```

```
&FIRE  XB=12.8,15.2,20.8,23.2,0.6,0.6, alfa_t2=0.012, HRRPUA=279, t_begin=1939, t_stop=3049,
RADI=0.35, SOOT_YIELD=0.015, HEAT_OF_COMBUSTION=18000/  26
&FIRE  XB=28.8,31.2,4.8,7.2,0.6,0.6, alfa_t2=0.012, HRRPUA=279, t_begin=1939, t_stop=3049,
RADI=0.35, SOOT_YIELD=0.015, HEAT_OF_COMBUSTION=18000/  27
&FIRE  XB=28.8,31.2,0.8,3.2,0.6,0.6, alfa_t2=0.012, HRRPUA=279, t_begin=1939, t_stop=3049,
RADI=0.35, SOOT_YIELD=0.015, HEAT_OF_COMBUSTION=18000/  28
&FIRE  XB=32.8,35.2,4.8,7.2,0.6,0.6, alfa_t2=0.012, HRRPUA=279, t_begin=2216, t_stop=3326,
RADI=0.35, SOOT_YIELD=0.015, HEAT_OF_COMBUSTION=18000/  29
&FIRE  XB=32.8,35.2,0.8,3.2,0.6,0.6, alfa_t2=0.012, HRRPUA=279, t_begin=2216, t_stop=3326,
RADI=0.35, SOOT_YIELD=0.015, HEAT_OF_COMBUSTION=18000/  30
&FIRE  XB=16.8,19.2,20.8,23.2,0.6,0.6, alfa_t2=0.012, HRRPUA=279, t_begin=2216, t_stop=3326,
RADI=0.35, SOOT_YIELD=0.015, HEAT_OF_COMBUSTION=18000/  31
&FIRE  XB=16.8,19.2,16.8,19.2,0.6,0.6, alfa_t2=0.012, HRRPUA=279, t_begin=1939, t_stop=3049,
RADI=0.35, SOOT_YIELD=0.015, HEAT_OF_COMBUSTION=18000/  32
&FIRE  XB=20.8,23.2,20.8,23.2,0.6,0.6, alfa_t2=0.012, HRRPUA=279, t_begin=2493, t_stop=3903,
RADI=0.35, SOOT_YIELD=0.015, HEAT_OF_COMBUSTION=18000/  33
&FIRE  XB=20.8,23.2,16.8,19.2,0.6,0.6, alfa_t2=0.012, HRRPUA=279, t_begin=2216, t_stop=3326,
RADI=0.35, SOOT_YIELD=0.015, HEAT_OF_COMBUSTION=18000/  34
&FIRE  XB=36.8,39.2,4.8,7.2,0.6,0.6, alfa_t2=0.012, HRRPUA=279, t_begin=2493, t_stop=3603,
RADI=0.35, SOOT_YIELD=0.015, HEAT_OF_COMBUSTION=18000/  35
&FIRE  XB=36.8,39.2,0.8,3.2,0.6,0.6, alfa_t2=0.012, HRRPUA=279, t_begin=2493, t_stop=3603,
RADI=0.35, SOOT_YIELD=0.015, HEAT_OF_COMBUSTION=18000/  36
&FIRE  XB=24.8,27.2,20.8,23.2,0.6,0.6, alfa_t2=0.012, HRRPUA=279, t_begin=2770, t_stop=3380,
RADI=0.35, SOOT_YIELD=0.015, HEAT_OF_COMBUSTION=18000/  37
&FIRE  XB=24.8,27.2,16.8,19.2,0.6,0.6, alfa_t2=0.012, HRRPUA=279, t_begin=2493, t_stop=3603,
RADI=0.35, SOOT_YIELD=0.015, HEAT_OF_COMBUSTION=18000/  38
&FIRE  XB=28.8,31.2,20.8,23.2,0.6,0.6, alfa_t2=0.012, HRRPUA=279, t_begin=3047, t_stop=4157,
RADI=0.35, SOOT_YIELD=0.015, HEAT_OF_COMBUSTION=18000/  39
&FIRE  XB=28.8,31.2,16.8,19.2,0.6,0.6, alfa_t2=0.012, HRRPUA=279, t_begin=2770, t_stop=3380,
RADI=0.35, SOOT_YIELD=0.015, HEAT_OF_COMBUSTION=18000/  40
&FIRE  XB=32.8,35.2,8.8,11.2,0.6,0.6, alfa_t2=0.012, HRRPUA=279, t_begin=2493, t_stop=3603,
RADI=0.35, SOOT_YIELD=0.015, HEAT_OF_COMBUSTION=18000/  41
&FIRE  XB=36.8,39.2,8.8,11.2,0.6,0.6, alfa_t2=0.012, HRRPUA=279, t_begin=2770, t_stop=3380,
RADI=0.35, SOOT_YIELD=0.015, HEAT_OF_COMBUSTION=18000/  42
&FIRE  XB=32.8,35.2,12.8,15.2,0.6,0.6, alfa_t2=0.012, HRRPUA=279, t_begin=2770, t_stop=3380,
RADI=0.35, SOOT_YIELD=0.015, HEAT_OF_COMBUSTION=18000/  43
&FIRE  XB=36.8,39.2,12.8,15.2,0.6,0.6, alfa_t2=0.012, HRRPUA=279, t_begin=3047, t_stop=4157,
RADI=0.35, SOOT_YIELD=0.015, HEAT_OF_COMBUSTION=18000/  44
&FIRE  XB=32.8,35.2,16.8,19.2,0.6,0.6, alfa_t2=0.012, HRRPUA=279, t_begin=3047, t_stop=4157,
RADI=0.35, SOOT_YIELD=0.015, HEAT_OF_COMBUSTION=18000/  45
&FIRE  XB=36.8,39.2,16.8,19.2,0.6,0.6, alfa_t2=0.012, HRRPUA=279, t_begin=3324, t_stop=4434,
RADI=0.35, SOOT_YIELD=0.015, HEAT_OF_COMBUSTION=18000/  46
&FIRE  XB=32.8,35.2,20.8,23.2,0.6,0.6, alfa_t2=0.012, HRRPUA=279, t_begin=3324, t_stop=4434,
RADI=0.35, SOOT_YIELD=0.015, HEAT_OF_COMBUSTION=18000/  47
&FIRE  XB=36.8,39.2,20.8,23.2,0.6,0.6, alfa_t2=0.012, HRRPUA=279, t_begin=3601, t_stop=4711,
RADI=0.35, SOOT_YIELD=0.015, HEAT_OF_COMBUSTION=18000/  48

&MATL ID=1, CONDUCTIVITY=1.1, SPECIFIC_HEAT=880, DENSITY=2100, THICKNESS=0.2, EMISSIVITY=0.9/

&VENT XB=0,0,4.0,20,0,1.0/ opening left wall
&VENT XB=40,40,4.0,20,0,1.0/ opening right wall
&VENT XB=4,36,0.0,0.0,0,1.0/ opening lower wall
&VENT XB=4,36,24.0,24.0,0,1.0/ opening upper wall
```

```
&OBST  XB=0.0,0.0,0.0,24.0,0.0,3.0,  MATL_ID=1/ left wall
&OBST  XB=40.0,40.0,0.0,24.0,0.0,3.0, MATL_ID=1/ right wall
&OBST  XB=0.0,40.0,24.0,24.0,0.0,3.0, MATL_ID=1/ north wall
&OBST  XB=0.0,40.0,0.0,0.0,0.0,3.0, MATL_ID=1/ south wall
&OBST  XB=0.0,40.0,0.0,24.0,0.0,0.0, MATL_ID=1/
&OBST  XB=0.0,40.0,0.0,24.0,3.0,3.0, MATL_ID=1/

&OBST  XB=8.0,32.0,8.0,8.0,0.0,3.0, MATL_ID=1/ concrete core south
&OBST  XB=8.0,32.0,16.0,16.0,0.0,3.0, MATL_ID=1/ concrete core north
&OBST  XB=8.0,8.0,8.0,16.0,0.0,3.0, MATL_ID=1/ concrete core left
&OBST  XB=32.0,32.0,8.0,16.0,0.0,3.0, MATL_ID=1/ concrete core right

&DEVC XYZ=2,2,0.25, QUANTITY='TEMPERATURE' / TC1
&DEVC XYZ=6,2,0.25, QUANTITY='TEMPERATURE' / TC3
&DEVC XYZ=10,2,0.25, QUANTITY='TEMPERATURE'/ TC7
&DEVC XYZ=14,2,0.25, QUANTITY='TEMPERATURE'/ TC10
&DEVC XYZ=18,2,0.25, QUANTITY='TEMPERATURE'/ TC13
&DEVC XYZ=22,2,0.25, QUANTITY='TEMPERATURE'/ TC19
&DEVC XYZ=26,2,0.25, QUANTITY='TEMPERATURE'/ TC22
&DEVC XYZ=30,2,0.25, QUANTITY='TEMPERATURE'/ TC28
&DEVC XYZ=34,2,0.25, QUANTITY='TEMPERATURE'/ TC30
&DEVC XYZ=38,2,0.25, QUANTITY='TEMPERATURE'/ TC36

&DEVC XYZ=2,2,0.75, QUANTITY='TEMPERATURE' / TC1
&DEVC XYZ=6,2,0.75, QUANTITY='TEMPERATURE' / TC3
&DEVC XYZ=10,2,0.75, QUANTITY='TEMPERATURE'/ TC7
&DEVC XYZ=14,2,0.75, QUANTITY='TEMPERATURE'/ TC10
&DEVC XYZ=18,2,0.75, QUANTITY='TEMPERATURE'/ TC13
&DEVC XYZ=22,2,0.75, QUANTITY='TEMPERATURE'/ TC19
&DEVC XYZ=26,2,0.75, QUANTITY='TEMPERATURE'/ TC22
&DEVC XYZ=30,2,0.75, QUANTITY='TEMPERATURE'/ TC28
&DEVC XYZ=34,2,0.75, QUANTITY='TEMPERATURE'/ TC30
&DEVC XYZ=38,2,0.75, QUANTITY='TEMPERATURE'/ TC36

&DEVC XYZ=2,2,1.25, QUANTITY='TEMPERATURE' / TC1
&DEVC XYZ=6,2,1.25, QUANTITY='TEMPERATURE' / TC3
&DEVC XYZ=10,2,1.25, QUANTITY='TEMPERATURE'/ TC7
&DEVC XYZ=14,2,1.25, QUANTITY='TEMPERATURE'/ TC10
&DEVC XYZ=18,2,1.25, QUANTITY='TEMPERATURE'/ TC13
&DEVC XYZ=22,2,1.25, QUANTITY='TEMPERATURE'/ TC19
&DEVC XYZ=26,2,1.25, QUANTITY='TEMPERATURE'/ TC22
&DEVC XYZ=30,2,1.25, QUANTITY='TEMPERATURE'/ TC28
&DEVC XYZ=34,2,1.25, QUANTITY='TEMPERATURE'/ TC30
&DEVC XYZ=38,2,1.25, QUANTITY='TEMPERATURE'/ TC36

&DEVC XYZ=2,2,1.75, QUANTITY='TEMPERATURE' / TC1
&DEVC XYZ=6,2,1.75, QUANTITY='TEMPERATURE' / TC3
&DEVC XYZ=10,2,1.75, QUANTITY='TEMPERATURE'/ TC7
&DEVC XYZ=14,2,1.75, QUANTITY='TEMPERATURE'/ TC10
&DEVC XYZ=18,2,1.75, QUANTITY='TEMPERATURE'/ TC13
&DEVC XYZ=22,2,1.75, QUANTITY='TEMPERATURE'/ TC19
&DEVC XYZ=26,2,1.75, QUANTITY='TEMPERATURE'/ TC22
&DEVC XYZ=30,2,1.75, QUANTITY='TEMPERATURE'/ TC28
&DEVC XYZ=34,2,1.75, QUANTITY='TEMPERATURE'/ TC30
```

```
&DEVC XYZ=38,2,1.75, QUANTITY='TEMPERATURE'/ TC36

&DEVC XYZ=2,2,2.25, QUANTITY='TEMPERATURE' / TC1
&DEVC XYZ=6,2,2.25, QUANTITY='TEMPERATURE' / TC3
&DEVC XYZ=10,2,2.25, QUANTITY='TEMPERATURE'/ TC7
&DEVC XYZ=14,2,2.25, QUANTITY='TEMPERATURE'/ TC10
&DEVC XYZ=18,2,2.25, QUANTITY='TEMPERATURE'/ TC13
&DEVC XYZ=22,2,2.25, QUANTITY='TEMPERATURE'/ TC19
&DEVC XYZ=26,2,2.25, QUANTITY='TEMPERATURE'/ TC22
&DEVC XYZ=30,2,2.25, QUANTITY='TEMPERATURE'/ TC28
&DEVC XYZ=34,2,2.25, QUANTITY='TEMPERATURE'/ TC30
&DEVC XYZ=38,2,2.25, QUANTITY='TEMPERATURE'/ TC36

&DEVC XYZ=2,2,2.75, QUANTITY='TEMPERATURE' / TC1
&DEVC XYZ=6,2,2.75, QUANTITY='TEMPERATURE' / TC3
&DEVC XYZ=10,2,2.75, QUANTITY='TEMPERATURE'/ TC7
&DEVC XYZ=14,2,2.75, QUANTITY='TEMPERATURE'/ TC10
&DEVC XYZ=18,2,2.75, QUANTITY='TEMPERATURE'/ TC13
&DEVC XYZ=22,2,2.75, QUANTITY='TEMPERATURE'/ TC19
&DEVC XYZ=26,2,2.75, QUANTITY='TEMPERATURE'/ TC22
&DEVC XYZ=30,2,2.75, QUANTITY='TEMPERATURE'/ TC28
&DEVC XYZ=34,2,2.75, QUANTITY='TEMPERATURE'/ TC30
&DEVC XYZ=38,2,2.75, QUANTITY='TEMPERATURE'/ TC36

&DEVC XYZ=2,10,0.25, QUANTITY='TEMPERATURE'/ TC5
&DEVC XYZ=6,10,0.25, QUANTITY='TEMPERATURE'/ TC6
&DEVC XYZ=10,10,0.25, QUANTITY='TEMPERATURE'/ TCA
&DEVC XYZ=14,10,0.25, QUANTITY='TEMPERATURE'/ TCB
&DEVC XYZ=18,10,0.25, QUANTITY='TEMPERATURE'/ TCC
&DEVC XYZ=22,10,0.25, QUANTITY='TEMPERATURE'/ TCD
&DEVC XYZ=26,10,0.25, QUANTITY='TEMPERATURE'/ TCE
&DEVC XYZ=30,10,0.25, QUANTITY='TEMPERATURE'/ TCF
&DEVC XYZ=34,10,0.25, QUANTITY='TEMPERATURE'/ TC41
&DEVC XYZ=38,10,0.25, QUANTITY='TEMPERATURE'/ TC42

&DEVC XYZ=2,10,0.75, QUANTITY='TEMPERATURE'/ TC5
&DEVC XYZ=6,10,0.75, QUANTITY='TEMPERATURE'/ TC6
&DEVC XYZ=10,10,0.75, QUANTITY='TEMPERATURE'/ TCA
&DEVC XYZ=14,10,0.75, QUANTITY='TEMPERATURE'/ TCB
&DEVC XYZ=18,10,0.75, QUANTITY='TEMPERATURE'/ TCC
&DEVC XYZ=22,10,0.75, QUANTITY='TEMPERATURE'/ TCD
&DEVC XYZ=26,10,0.75, QUANTITY='TEMPERATURE'/ TCE
&DEVC XYZ=30,10,0.75, QUANTITY='TEMPERATURE'/ TCF
&DEVC XYZ=34,10,0.75, QUANTITY='TEMPERATURE'/ TC41
&DEVC XYZ=38,10,0.75, QUANTITY='TEMPERATURE'/ TC42

&DEVC XYZ=2,10,1.25, QUANTITY='TEMPERATURE'/ TC5
&DEVC XYZ=6,10,1.25, QUANTITY='TEMPERATURE'/ TC6
&DEVC XYZ=10,10,1.25, QUANTITY='TEMPERATURE'/ TCA
&DEVC XYZ=14,10,1.25, QUANTITY='TEMPERATURE'/ TCB
&DEVC XYZ=18,10,1.25, QUANTITY='TEMPERATURE'/ TCC
&DEVC XYZ=22,10,1.25, QUANTITY='TEMPERATURE'/ TCD
&DEVC XYZ=26,10,1.25, QUANTITY='TEMPERATURE'/ TCE
&DEVC XYZ=30,10,1.25, QUANTITY='TEMPERATURE'/ TCF
```

```
&DEVC XYZ=34,10,1.25, QUANTITY='TEMPERATURE'/ TC41
&DEVC XYZ=38,10,1.25, QUANTITY='TEMPERATURE'/ TC42

&DEVC XYZ=2,10,1.75, QUANTITY='TEMPERATURE'/ TC5
&DEVC XYZ=6,10,1.75, QUANTITY='TEMPERATURE'/ TC6
&DEVC XYZ=10,10,1.75, QUANTITY='TEMPERATURE'/ TCA
&DEVC XYZ=14,10,1.75, QUANTITY='TEMPERATURE'/ TCB
&DEVC XYZ=18,10,1.75, QUANTITY='TEMPERATURE'/ TCC
&DEVC XYZ=22,10,1.75, QUANTITY='TEMPERATURE'/ TCD
&DEVC XYZ=26,10,1.75, QUANTITY='TEMPERATURE'/ TCE
&DEVC XYZ=30,10,1.75, QUANTITY='TEMPERATURE'/ TCF
&DEVC XYZ=34,10,1.75, QUANTITY='TEMPERATURE'/ TC41
&DEVC XYZ=38,10,1.75, QUANTITY='TEMPERATURE'/ TC42

&DEVC XYZ=2,10,2.25, QUANTITY='TEMPERATURE'/ TC5
&DEVC XYZ=6,10,2.25, QUANTITY='TEMPERATURE'/ TC6
&DEVC XYZ=10,10,2.25, QUANTITY='TEMPERATURE'/ TCA
&DEVC XYZ=14,10,2.25, QUANTITY='TEMPERATURE'/ TCB
&DEVC XYZ=18,10,2.25, QUANTITY='TEMPERATURE'/ TCC
&DEVC XYZ=22,10,2.25, QUANTITY='TEMPERATURE'/ TCD
&DEVC XYZ=26,10,2.25, QUANTITY='TEMPERATURE'/ TCE
&DEVC XYZ=30,10,2.25, QUANTITY='TEMPERATURE'/ TCF
&DEVC XYZ=34,10,2.25, QUANTITY='TEMPERATURE'/ TC41
&DEVC XYZ=38,10,2.25, QUANTITY='TEMPERATURE'/ TC42

&DEVC XYZ=2,10,2.75, QUANTITY='TEMPERATURE'/ TC5
&DEVC XYZ=6,10,2.75, QUANTITY='TEMPERATURE'/ TC6
&DEVC XYZ=10,10,2.75, QUANTITY='TEMPERATURE'/ TCA
&DEVC XYZ=14,10,2.75, QUANTITY='TEMPERATURE'/ TCB
&DEVC XYZ=18,10,2.75, QUANTITY='TEMPERATURE'/ TCC
&DEVC XYZ=22,10,2.75, QUANTITY='TEMPERATURE'/ TCD
&DEVC XYZ=26,10,2.75, QUANTITY='TEMPERATURE'/ TCE
&DEVC XYZ=30,10,2.75, QUANTITY='TEMPERATURE'/ TCF
&DEVC XYZ=34,14,2.75, QUANTITY='TEMPERATURE'/ TC41
&DEVC XYZ=38,14,2.75, QUANTITY='TEMPERATURE'/ TC42

&DEVC XYZ=2,22,0.25, QUANTITY='TEMPERATURE'/ TC17
&DEVC XYZ=6,22,0.25, QUANTITY='TEMPERATURE'/ TC18
&DEVC XYZ=10,22,0.25, QUANTITY='TEMPERATURE'/ TC23
&DEVC XYZ=14,22,0.25, QUANTITY='TEMPERATURE'/ TC26
&DEVC XYZ=18,22,0.25, QUANTITY='TEMPERATURE'/ TC31
&DEVC XYZ=22,22,0.25, QUANTITY='TEMPERATURE'/ TC33
&DEVC XYZ=26,22,0.25, QUANTITY='TEMPERATURE'/ TC37
&DEVC XYZ=30,22,0.25, QUANTITY='TEMPERATURE'/ TC39
&DEVC XYZ=34,22,0.25, QUANTITY='TEMPERATURE'/ TC47
&DEVC XYZ=38,22,0.25, QUANTITY='TEMPERATURE'/ TC48

&DEVC XYZ=2,22,0.75, QUANTITY='TEMPERATURE'/ TC17
&DEVC XYZ=6,22,0.75, QUANTITY='TEMPERATURE'/ TC18
&DEVC XYZ=10,22,0.75, QUANTITY='TEMPERATURE'/ TC23
&DEVC XYZ=14,22,0.75, QUANTITY='TEMPERATURE'/ TC26
&DEVC XYZ=18,22,0.75, QUANTITY='TEMPERATURE'/ TC31
&DEVC XYZ=22,22,0.75, QUANTITY='TEMPERATURE'/ TC33
&DEVC XYZ=26,22,0.75, QUANTITY='TEMPERATURE'/ TC37
```

```
&DEVC XYZ=30,22,0.75, QUANTITY='TEMPERATURE'/ TC39
&DEVC XYZ=34,22,0.75, QUANTITY='TEMPERATURE'/ TC47
&DEVC XYZ=38,22,0.75, QUANTITY='TEMPERATURE'/ TC48

&DEVC XYZ=2,22,1.25, QUANTITY='TEMPERATURE'/ TC17
&DEVC XYZ=6,22,1.25, QUANTITY='TEMPERATURE'/ TC18
&DEVC XYZ=10,22,1.25, QUANTITY='TEMPERATURE'/ TC23
&DEVC XYZ=14,22,1.25, QUANTITY='TEMPERATURE'/ TC26
&DEVC XYZ=18,22,1.25, QUANTITY='TEMPERATURE'/ TC31
&DEVC XYZ=22,22,1.25, QUANTITY='TEMPERATURE'/ TC33
&DEVC XYZ=26,22,1.25, QUANTITY='TEMPERATURE'/ TC37
&DEVC XYZ=30,22,1.25, QUANTITY='TEMPERATURE'/ TC39
&DEVC XYZ=34,22,1.25, QUANTITY='TEMPERATURE'/ TC47
&DEVC XYZ=38,22,1.25, QUANTITY='TEMPERATURE'/ TC48

&DEVC XYZ=2,22,1.75, QUANTITY='TEMPERATURE'/ TC17
&DEVC XYZ=6,22,1.75, QUANTITY='TEMPERATURE'/ TC18
&DEVC XYZ=10,22,1.75, QUANTITY='TEMPERATURE'/ TC23
&DEVC XYZ=14,22,1.75, QUANTITY='TEMPERATURE'/ TC26
&DEVC XYZ=18,22,1.75, QUANTITY='TEMPERATURE'/ TC31
&DEVC XYZ=22,22,1.75, QUANTITY='TEMPERATURE'/ TC33
&DEVC XYZ=26,22,1.75, QUANTITY='TEMPERATURE'/ TC37
&DEVC XYZ=30,22,1.75, QUANTITY='TEMPERATURE'/ TC39
&DEVC XYZ=34,22,1.75, QUANTITY='TEMPERATURE'/ TC47
&DEVC XYZ=38,22,1.75, QUANTITY='TEMPERATURE'/ TC48

&DEVC XYZ=2,22,2.25, QUANTITY='TEMPERATURE'/ TC17
&DEVC XYZ=6,22,2.25, QUANTITY='TEMPERATURE'/ TC18
&DEVC XYZ=10,22,2.25, QUANTITY='TEMPERATURE'/ TC23
&DEVC XYZ=14,22,2.25, QUANTITY='TEMPERATURE'/ TC26
&DEVC XYZ=18,22,2.25, QUANTITY='TEMPERATURE'/ TC31
&DEVC XYZ=22,22,2.25, QUANTITY='TEMPERATURE'/ TC33
&DEVC XYZ=26,22,2.25, QUANTITY='TEMPERATURE'/ TC37
&DEVC XYZ=30,22,2.25, QUANTITY='TEMPERATURE'/ TC39
&DEVC XYZ=34,22,2.25, QUANTITY='TEMPERATURE'/ TC47
&DEVC XYZ=38,22,2.25, QUANTITY='TEMPERATURE'/ TC48

&DEVC XYZ=2,22,2.75, QUANTITY='TEMPERATURE'/ TC17
&DEVC XYZ=6,22,2.75, QUANTITY='TEMPERATURE'/ TC18
&DEVC XYZ=10,22,2.75, QUANTITY='TEMPERATURE'/ TC23
&DEVC XYZ=14,22,2.75, QUANTITY='TEMPERATURE'/ TC26
&DEVC XYZ=18,22,2.75, QUANTITY='TEMPERATURE'/ TC31
&DEVC XYZ=22,22,2.75, QUANTITY='TEMPERATURE'/ TC33
&DEVC XYZ=26,22,2.75, QUANTITY='TEMPERATURE'/ TC37
&DEVC XYZ=30,22,2.75, QUANTITY='TEMPERATURE'/ TC39
&DEVC XYZ=34,22,2.75, QUANTITY='TEMPERATURE'/ TC47
&DEVC XYZ=38,22,2.75, QUANTITY='TEMPERATURE'/ TC48

&DEVC XYZ=6,10,0.25, QUANTITY='OBSCURATION'/ TC6
&DEVC XYZ=6,10,0.75, QUANTITY='OBSCURATION'/ TC6
&DEVC XYZ=6,10,1.25, QUANTITY='OBSCURATION'/ TC6
&DEVC XYZ=6,10,1.75, QUANTITY='OBSCURATION'/ TC6
&DEVC XYZ=6,10,2.25, QUANTITY='OBSCURATION'/ TC6
&DEVC XYZ=6,10,2.75, QUANTITY='OBSCURATION'/ TC6
```

```
&DEVC XYZ=34,10,0.25, QUANTITY='OBSCURATION'/ TC41
&DEVC XYZ=34,10,0.75, QUANTITY='OBSCURATION'/ TC41
&DEVC XYZ=34,10,1.25, QUANTITY='OBSCURATION'/ TC41
&DEVC XYZ=34,10,1.75, QUANTITY='OBSCURATION'/ TC41
&DEVC XYZ=34,10,2.25, QUANTITY='OBSCURATION'/ TC41
&DEVC XYZ=34,10,2.75, QUANTITY='OBSCURATION'/ TC41

&DEVC XYZ=2,2,2.75,  QUANTITY='TEMPERATURE'/ TC1
&DEVC XYZ=6,2,2.75,  QUANTITY='TEMPERATURE'/ TC3
&DEVC XYZ=10,2,2.75, QUANTITY='TEMPERATURE'/ TC7
&DEVC XYZ=14,2,2.75, QUANTITY='TEMPERATURE'/ TC10
&DEVC XYZ=18,2,2.75, QUANTITY='TEMPERATURE'/ TC13
&DEVC XYZ=22,2,2.75, QUANTITY='TEMPERATURE'/ TC19
&DEVC XYZ=26,2,2.75, QUANTITY='TEMPERATURE'/ TC22
&DEVC XYZ=30,2,2.75, QUANTITY='TEMPERATURE'/ TC28
&DEVC XYZ=34,2,2.75, QUANTITY='TEMPERATURE'/ TC30
&DEVC XYZ=38,2,2.75, QUANTITY='TEMPERATURE'/ TC36

&DEVC XYZ=2,4,2.75,  QUANTITY='TEMPERATURE'/ TC2
&DEVC XYZ=6,6,2.75,  QUANTITY='TEMPERATURE'/ TC4
&DEVC XYZ=10,6,2.75, QUANTITY='TEMPERATURE'/ TC8
&DEVC XYZ=14,6,2.75, QUANTITY='TEMPERATURE'/ TC9
&DEVC XYZ=18,6,2.75, QUANTITY='TEMPERATURE'/ TC14
&DEVC XYZ=22,6,2.75, QUANTITY='TEMPERATURE'/ TC20
&DEVC XYZ=26,6,2.75, QUANTITY='TEMPERATURE'/ TC21
&DEVC XYZ=30,6,2.75, QUANTITY='TEMPERATURE'/ TC27
&DEVC XYZ=34,6,2.75, QUANTITY='TEMPERATURE'/ TC29
&DEVC XYZ=38,6,2.75, QUANTITY='TEMPERATURE'/ TC35

&DEVC XYZ=2,10,2.75,  QUANTITY='TEMPERATURE'/ TC5
&DEVC XYZ=6,10,2.75,  QUANTITY='TEMPERATURE'/ TC6
&DEVC XYZ=10,10,2.75, QUANTITY='TEMPERATURE'/ TCA
&DEVC XYZ=14,10,2.75, QUANTITY='TEMPERATURE'/ TCB
&DEVC XYZ=18,10,2.75, QUANTITY='TEMPERATURE'/ TCC
&DEVC XYZ=22,10,2.75, QUANTITY='TEMPERATURE'/ TCD
&DEVC XYZ=26,10,2.75, QUANTITY='TEMPERATURE'/ TCE
&DEVC XYZ=30,10,2.75, QUANTITY='TEMPERATURE'/ TCF
&DEVC XYZ=34,10,2.75, QUANTITY='TEMPERATURE'/ TC41
&DEVC XYZ=38,10,2.75, QUANTITY='TEMPERATURE'/ TC42

&DEVC XYZ=2,14,2.75, QUANTITY='TEMPERATURE'/ TC11
&DEVC XYZ=6,14,2.75, QUANTITY='TEMPERATURE'/ TC12
&DEVC XYZ=10,14,2.75, QUANTITY='TEMPERATURE'/ TCG
&DEVC XYZ=14,14,2.75, QUANTITY='TEMPERATURE'/ TCH
&DEVC XYZ=18,14,2.75, QUANTITY='TEMPERATURE'/ TCI
&DEVC XYZ=22,14,2.75, QUANTITY='TEMPERATURE'/ TCL
&DEVC XYZ=26,14,2.75, QUANTITY='TEMPERATURE'/ TCM
&DEVC XYZ=30,14,2.75, QUANTITY='TEMPERATURE'/ TCN
&DEVC XYZ=34,14,2.75, QUANTITY='TEMPERATURE'/ TC43
&DEVC XYZ=38,14,2.75, QUANTITY='TEMPERATURE'/ TC44

&DEVC XYZ=2,18,2.75, QUANTITY='TEMPERATURE'/ TC15
&DEVC XYZ=6,18,2.75, QUANTITY='TEMPERATURE'/ TC16
```

```
&DEVC XYZ=10,18,2.75, QUANTITY='TEMPERATURE'/ TC24
&DEVC XYZ=14,18,2.75, QUANTITY='TEMPERATURE'/ TC25
&DEVC XYZ=18,18,2.75, QUANTITY='TEMPERATURE'/ TC32
&DEVC XYZ=22,18,2.75, QUANTITY='TEMPERATURE'/ TC34
&DEVC XYZ=26,18,2.75, QUANTITY='TEMPERATURE'/ TC38
&DEVC XYZ=30,18,2.75, QUANTITY='TEMPERATURE'/ TC40
&DEVC XYZ=34,18,2.75, QUANTITY='TEMPERATURE'/ TC45
&DEVC XYZ=38,18,2.75, QUANTITY='TEMPERATURE'/ TC46

&DEVC XYZ=2,22,2.75, QUANTITY='TEMPERATURE'/ TC17
&DEVC XYZ=6,22,2.75, QUANTITY='TEMPERATURE'/ TC18
&DEVC XYZ=10,22,2.75, QUANTITY='TEMPERATURE'/ TC23
&DEVC XYZ=14,22,2.75, QUANTITY='TEMPERATURE'/ TC26
&DEVC XYZ=18,22,2.75, QUANTITY='TEMPERATURE'/ TC31
&DEVC XYZ=22,22,2.75, QUANTITY='TEMPERATURE'/ TC33
&DEVC XYZ=26,22,2.75, QUANTITY='TEMPERATURE'/ TC37
&DEVC XYZ=30,22,2.75, QUANTITY='TEMPERATURE'/ TC39
&DEVC XYZ=34,22,2.75, QUANTITY='TEMPERATURE'/ TC47
&DEVC XYZ=38,22,2.75, QUANTITY='TEMPERATURE'/ TC48

&TAIL/
```

Appendix I: HRR comparison

Heat release rate for each fire scenario were compared after the codes were run, to make sure that the prescribed scenarios were modelled as intended. Below, are the graphs that compare the HRR curves for all scenarios considered in this study.

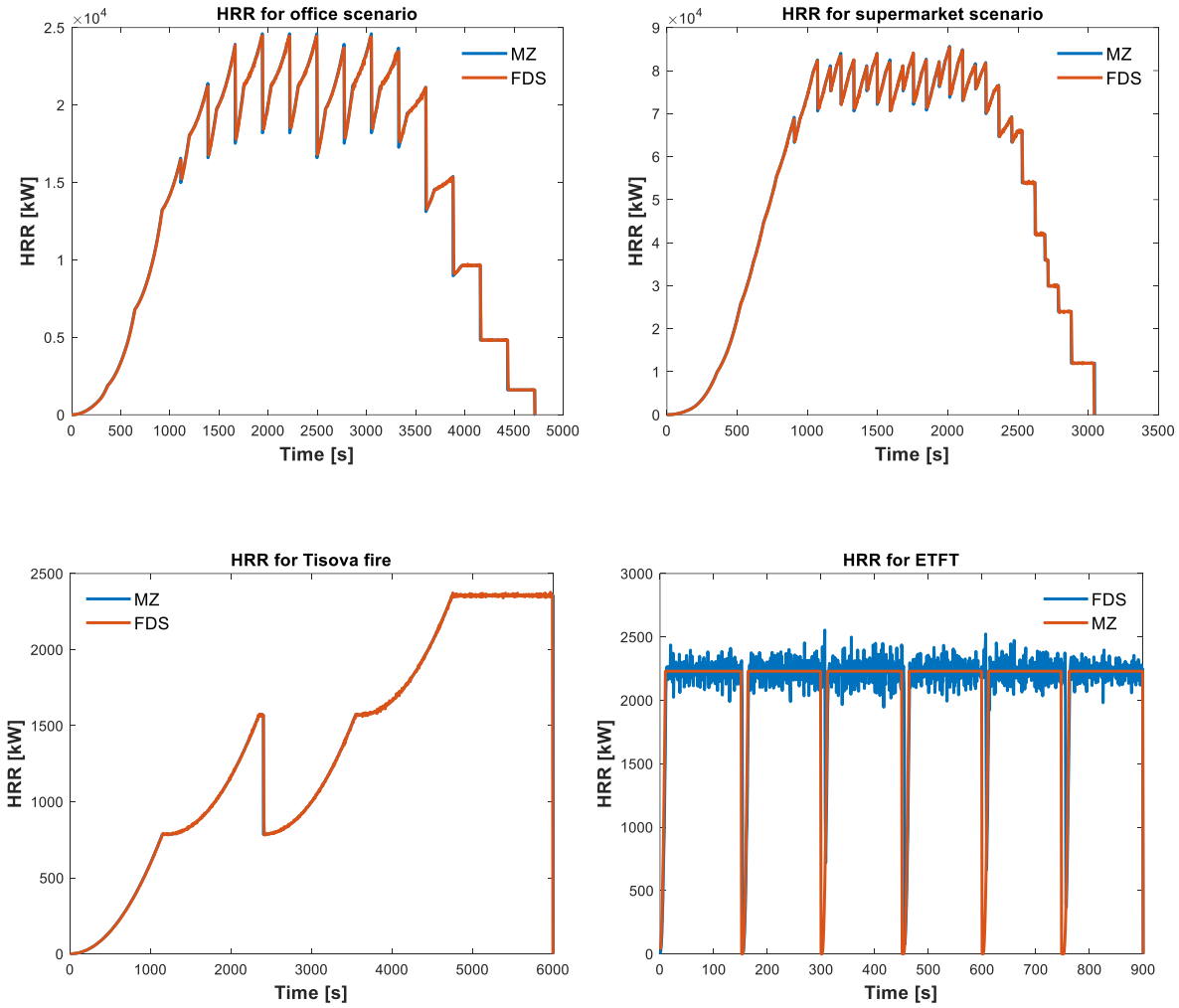

Figure 51 Comparison of HRR curves for each fire scenario.

Appendix J: MZ fire model with extended domain

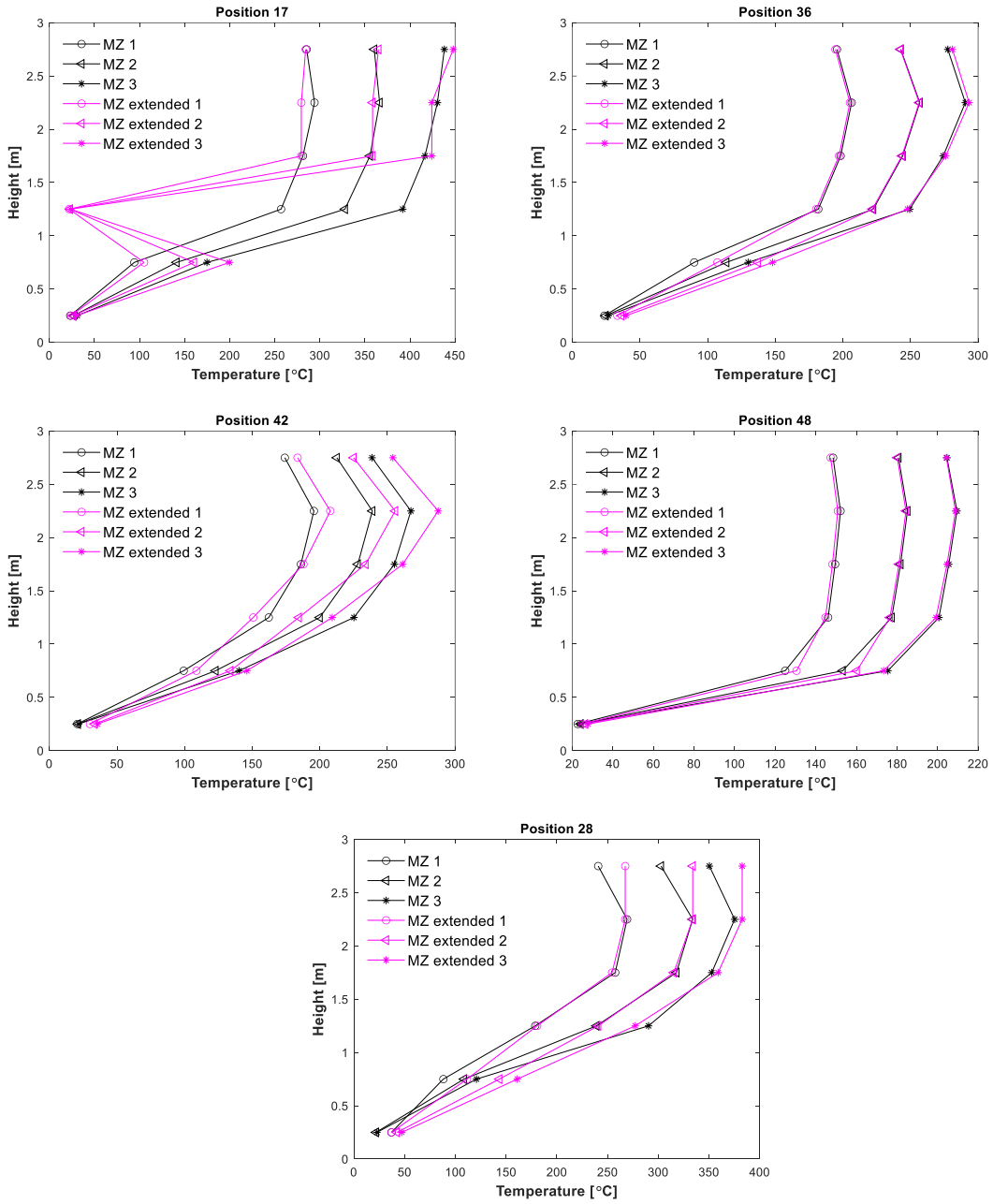

Figure 52 Office scenario results in MZ fire model with an extended domain of one cell outside the openings (magenta) compared to a simulation without extension.

Appendix K: Tisova fire test results with changes in height

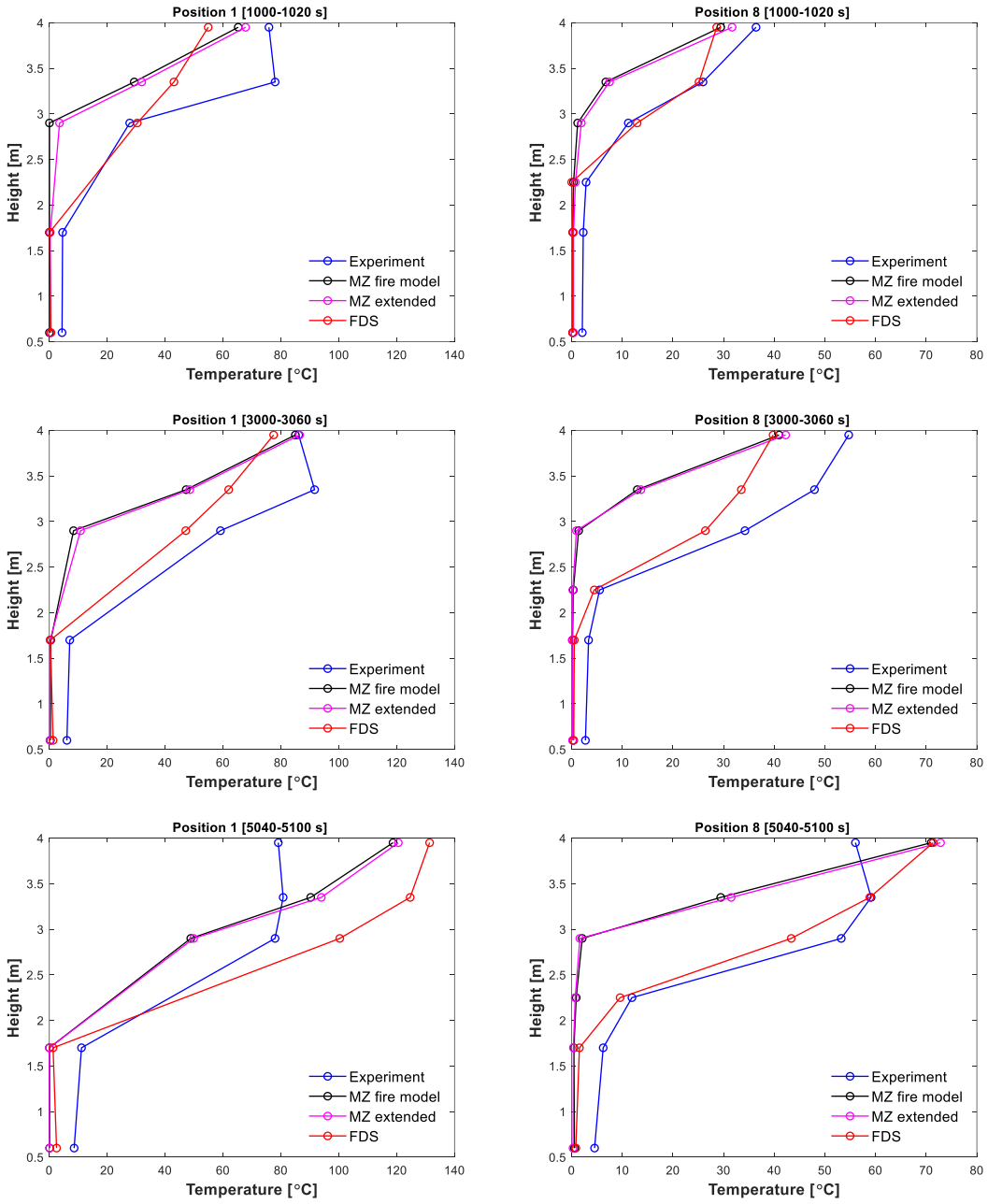

Figure 53 The Tisova fire test temperature profiles, MZ fire model with (magenta) and without (black) extended domain.

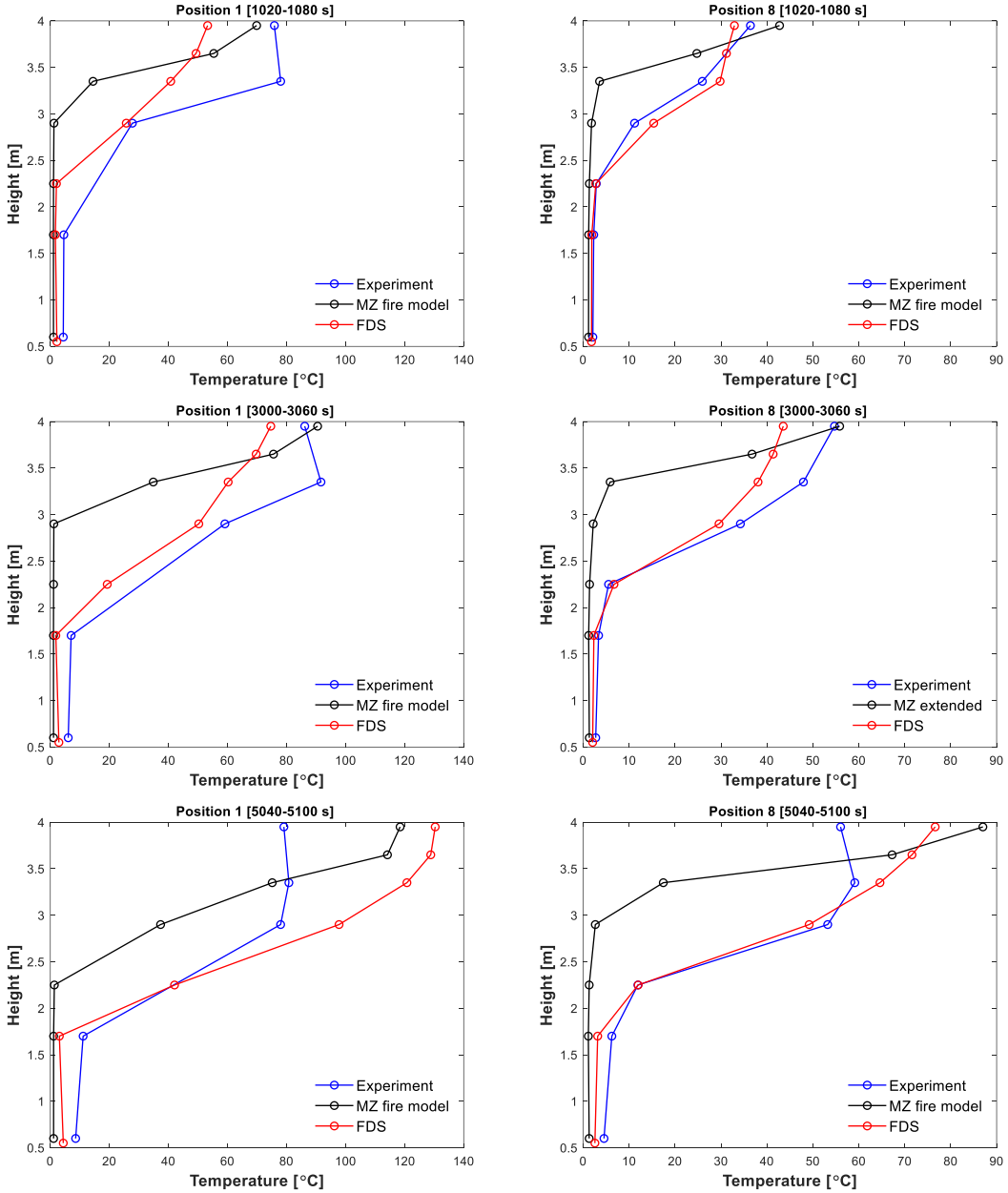

Figure 54 Average temperatures over hight for the Tisova fire test for compartment with height 4.2 m, positions 1 and 8.

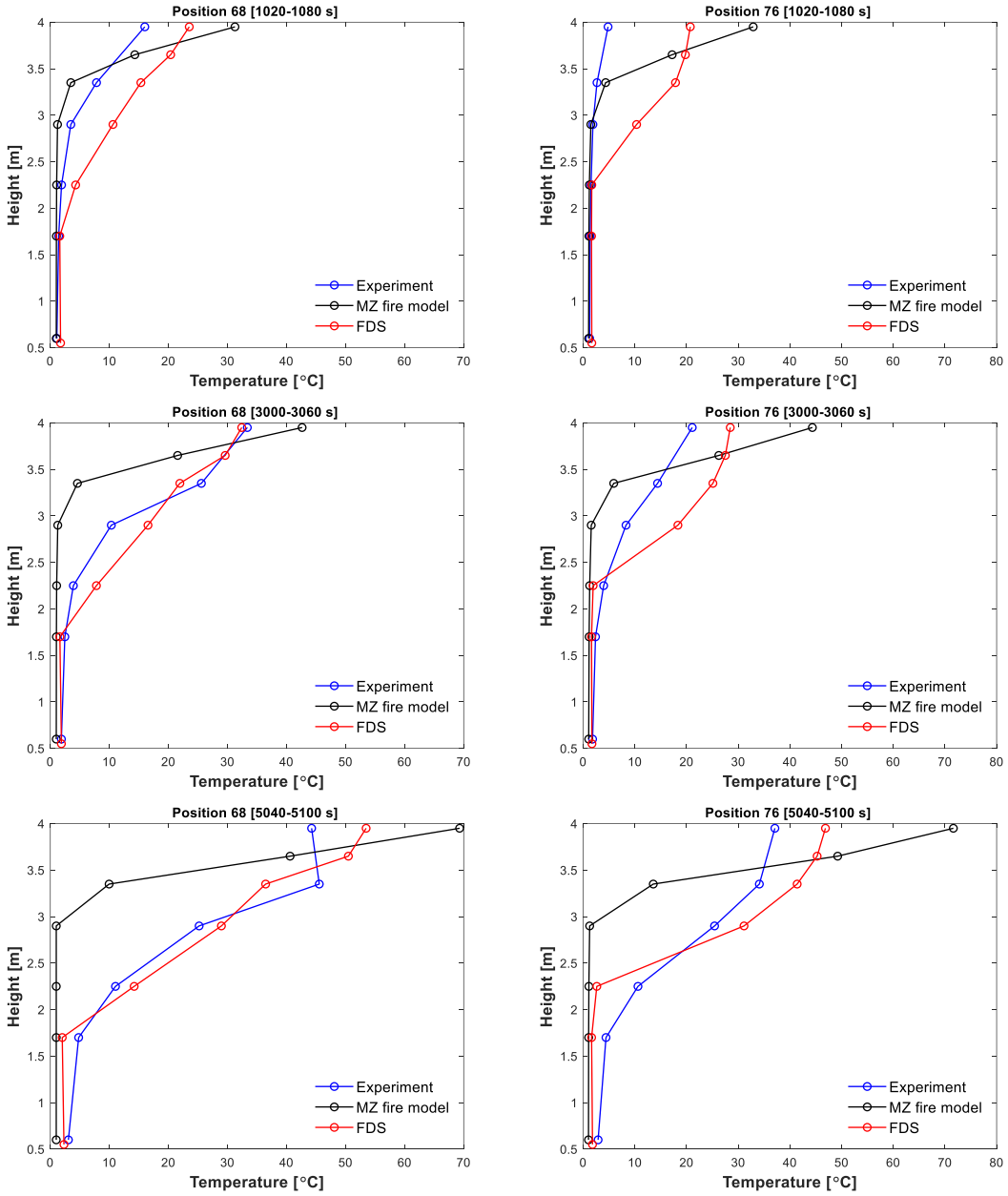

Figure 55 Average temperatures over hight for the Tisova fire test for compartment with height 4.2 m, positions 68 and 76.

Appendix L: Office scenario with higher resolution in z-direction(30 cm cell size)

This appendix presents the results for the office scenario with higher number of cells in MZ fire model in z-direction (30 cm cell size). The previous results (Figure 20) are reported for 6 cells in z-direction.

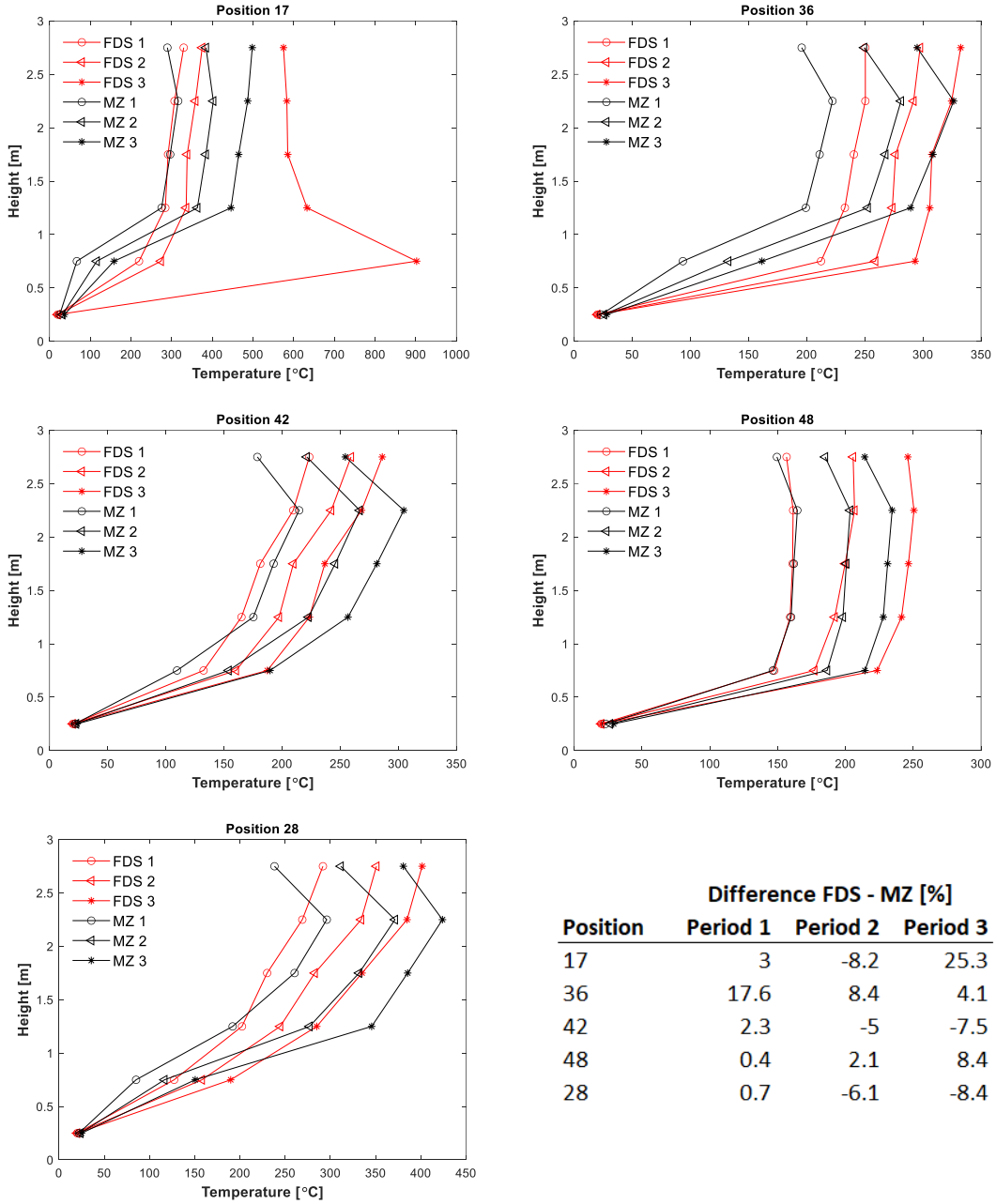

Difference FDS - MZ [%]			
Position	Period 1	Period 2	Period 3
17	3	-8.2	25.3
36	17.6	8.4	4.1
42	2.3	-5	-7.5
48	0.4	2.1	8.4
28	0.7	-6.1	-8.4

Figure 56 Temperature profiles for office scenario with higher number of zones (10) in MZ fire model. The table shows the average temperature results for FDS compared to MZ fire model averaged from 1.25 m height.